Université de Lille 1 Sciences et Technologies
École Doctorale Sciences Pour l'Ingénieur
Laboratoire Génie Civil et géo-Environnement

THÈSE

Pour l'obtention du grade de

DOCTEUR DE L'UNIVERSITÉ DE LILLE

Discipline : Génie Civil

Par

Dina RAMMAL

THERMO-MECHANICAL BEHAVIOUR OF GEOTHERMAL STRUCTURES: NUMERICAL MODELLING AND RECOMMENDATIONS

Soutenu le 12 Décembre 2017

Devant le jury composé de

MROUEH Hussein	Professeur, Université de Lille 1	Directeur
EMEREIAULT Fabrice	Professeur, Université Grenoble Alpes	Rapporteur
TANG Anh Minh	Directeur de recherche, Ecole des Ponts Paris Tech	Rapporteur
DEMONGODIN Lionel	Docteur, chef de projet EGIS France	Examinateur
DI DONNA Alice	MCF, Université Grenoble Alpes	Examinateur
BURLON Sébastien	HDR, Ingénieur de recherche IFSTTAR Paris	Examinateur
HABERT Julien	Ingénieur de recherche CEREMA, Lille	Invité

This PhD thesis is dedicated to my beloved parents, and loving sisters.

Thank you for all your sacrifices, trust, and support.

Acknowledgement

The work conducted in this thesis has been carried out at the Laboratory of Civil and Geo-Environmental Engineering LGCgE at Polytech'Lille, University of Lille 1 under the supervision of Professor Hussein MROUEH and the assistance of Dr. Sébastien BURLON. This PhD thesis has been funded by the Ministry of High and National Education, and Research in France.

Foremost, I would like to express my sincere gratitude to my supervisor, Professor Hussein MROUEH for his trust, continuous support, patience, and guidance all along those three years. My gratefulness goes also to Doctor Sébastien BURLON for sharing his knowledge with me, for his precious advices and for the fruitful discussions, all these contributed to improve this work.

I would like to thank my PhD committee for accepting to be a part of this achievement by reading, examining, and reporting my work. Thanks to Prof. Anh Minh TANG, Prof. Fabrice EMERIAULT, Dr. Alice DI DONNA, Dr. Lionel DIMONGODIN, and Eng. Julien HABERT.

I would like to thank also the Laboratory of Civil and Geo-Environmental Engineering represented by its director Prof. Isam SHAHROUR. My further thanks go to all my friends and colleagues in the LGCgE, in Lille, and in Lebanon. Thanks to your encouragement and motivations.

Last but not least, I would like to express my deep gratitude to my father Mohammad, my mother Mariam, and for my sisters Jana, Doha, and Zeina. I would like to thank them for their care, love, support, confidence, and continuous motivation. Without being by my side at every instant, I would not have been here today. Thank you and I love you!

Abstract

Calorific needs for heating and cooling the buildings account for the majority of their energy demands. To fulfill the thermal needs of constructions without increasing the energy bill and the pollution levels, a solution is to use renewable energy sources that guarantee all these. In this context, geothermal structures represent a promising solution that could satisfy the environmental and the economical necessities at the long term.

Geothermal structures act as heat exchanger elements in addition to their major role as bearing structures. Thus, they are subjected to thermal solicitations as well as to mechanical loading. However, their design methods are not clearly defined yet. This work is divided into two main parts that cover the thermal and mechanical design of thermo-active piles and diaphragm walls.

Regarding the thermal performance of geothermal structures, the impact of groundwater flow on the heat exchange phenomena between them and the soil is indeed a complex issue. For this reason, in this thesis, two strategies are introduced that are capable to evaluate the allowable exchanged conductive and advective energies. They help to distinguish between different forms of exchanged energies and show how they may vary under cyclic thermal loading. Two and three dimensional hydro-thermal numerical models of geothermal piles and diaphragm walls have been conducted and their thermal performance has been evaluated based on the two presented approaches.

On the other hand, regarding the mechanical design, this work covers the issues related to the choice of the thermal solicitation that the designer has to consider for the mechanical design of geothermal structures such as the number of cycles, cyclic thermal amplitude, and influence of

the thermal loading order. This work deals with these issues with the aim to facilitate the design of geothermal structures. Adding to this, it considers the factors that may affect their mechanical behaviour. Recommendations are given for the mechanical design of both thermo-active piles and diaphragm walls based on the results obtained from the thermo-mechanical numerical analyses.

Résumé

Les besoins calorifiques pour le chauffage et le refroidissement des bâtiments représentent la majorité des leurs exigences énergétiques. Pour répondre à ces besoins sans augmenter la facture d'énergie et les niveaux de pollution, une solution est d'utiliser des sources d'énergie renouvelables qui garantissent cela. Dans ce contexte, les structures géothermiques, représentent une solution prometteuse qui pourrait satisfaire les besoins environnementaux et économiques à long terme.

Les structures géothermiques agissent comme éléments échangeurs de chaleur en plus de leur rôle majeur en tant que structures porteuses. De ce fait, ils sont soumis à des sollicitations thermiques en plus des charges mécaniques. Cependant, leurs méthodes de dimensionnement ne sont pas encore clairement définies. Ce travail est divisé en deux parties principales qui couvrent le dimensionnement thermique et mécanique des pieux géothermiques et des parois moulées.

En ce qui concerne les performances thermiques des structures géothermiques, l'impact du flux d'eau souterraine sur les phénomènes d'échange de chaleur entre les fondations et le sol est en effet un problème complexe. Pour cette raison, dans cette thèse, deux stratégies sont introduites qui sont capables d'évaluer les énergies conductives et advectives échangées admissibles. Ils permettent de distinguer différentes formes d'énergies échangées et montrent comment elles peuvent varier en cas de chargement thermique cyclique. Des modèles numériques couples thermo-hydraulique bidimensionnels et tridimensionnels de pieux géothermiques et de parois moulées ont été réalisés et leur performance thermique a été évaluée en fonction des deux approches présentées.

D'autre part, en ce qui concerne le dimensionnement mécanique, ce travail couvre les problèmes liés au choix de la sollicitation thermique que le concepteur doit considérer pour la conception mécanique des structures géothermiques telles que le nombre de cycles, l'amplitude thermique cyclique et l'influence de l'ordre de chargement thermique. Ce travail traite ces problèmes dans le but de faciliter la conception des structures géothermiques. De plus, il considère les facteurs qui peuvent affecter leur comportement mécanique. Des recommandations sont données pour la conception mécanique des pieux géothermiques et des parois moulées basées sur les résultats obtenus à partir des analyses numériques thermo-mécanique.

Table of contents

Table of contents i
List of figures vi
List of tables xii
Nomenclature xiii
General introduction 1
CHAPTER 1 : Mechanisms related to the thermal transfer and mechanical behaviour of energy geo-structures 6
1.1 Introduction 6
1.2 Overview on energy geo-structures 9
1.2.1 Energy piles 9
1.2.2 Energy diaphragm walls 10
1.3 Heat transfer mechanisms 11
1.3.1 Heat transfer in soil 11
1.3.2 Heat transfer in energy geo-structures 14
1.4 Assessment of the exchanged heat between geothermal structures and the surrounding media 16
1.4.1 Principles 16
1.4.2 Factors impacting the heat transfer phenomena between energy-geo structure and soil 20

1.5 Main issues concerning the thermo-mechanical behaviour of soil and energy geo-structures 22

1.5.1 Thermo-mechanical behaviour of saturated soil 22

1.5.2 Thermo-mechanical behaviour of thermo-active piles.....25

1.5.3 Thermo-mechanical behaviour of thermo-active diaphragm walls.....27

1.6 Main issues and methodology 28

CHAPTER 2 : Possible strategies for the evaluation of the thermal exchanged power 31

2.1 Introduction 31

2.2 Available studies dealing with the assessment of the energy exchange between energy structures and the surrounding media.....32

2.2.1 Studies carried on energy diaphragm walls.....32

2.2.2 Studies carried on energy piles.....37

2.3 Strategies for the assessment of exchanged thermal power 37

2.3.3 Approach 1 38

Power transferred by conduction.....38

Power transferred by advection.....40

Total transferred power 41

2.3.4 Approach 2 41

2.4 Conclusion.....44

2.5 Appendix: Calculation of the conductive and advective powers and energies 44

CHAPTER 3 : Assessment of the exchanged energy between geothermal structures and soil 48

3.1 Introduction 48

3.2 Materials' properties 49

3.3 Two-dimensional energy diaphragm walls 49

3.3.1 Model geometry and boundary conditions 49

3.3.2 Approach 1 52

Influence of groundwater flow on the temperature profile 52

Temporal and spatial variation of the allowable exchanged power 52

Impact of groundwater flow on the exchanged thermal power 54

Impact of cyclic thermal loading on the allowable exchanged thermal power 55

Impact of the active length of the diaphragm wall 59

3.3.3 Approach 2 60

Distribution of the divergence in the soil 61

Evolution of the total exchanged power during the winter season 62

Cyclic variation of the total exchanged power 65

3.3.4 Comparison between approach 1 and 2 68

3.3.5 Influence of the applied thermal load 69

3.4 Three dimensional energy diaphragm wall model 74

3.5 Three dimensional energy pile model 79

3.5.1 Cyclic thermal loading of 3-D energy pile 81

3.5.2 Comparison between 3-D energy diaphragm walls and energy piles 83

3.6 Conclusion 84

CHAPTER 4 : Thermo-mechanical behaviour of energy piles: Impact of imposed thermal loads 85

4.1 Introduction 85

4.2 Numerical model 86

4.3 Thermal solicitations under consideration 89

4.4 Thermal volumetric strain: TS0 91

4.4.1 Pile head displacement 91

4.4.2 Normal force distribution 92

4.5 Constant pile temperature: TS1 and TS2 94

4.5.1 Pile head displacement 94

4.5.2 Normal force distribution 96

4.5.3 Comparison between TS0, TS1, and TS2 99

4.6 Continuous sinusoidal pile temperature: TS3 100

4.6.1 Pile head displacement 100

4.6.2 Normal force distribution 101

4.7 Comparison between the four thermal solicitations 103

4.8 Impact of pile head fixity 104

4.8.1 Case TS0R 105

4.8.2 TS1R and TS2R 106

4.8.3 TS3R 109

4.8.4 Comparison between different pile head fixities under variable thermal loads 110

4.9 Influence of soil thermal and thermo-mechanical properties 111

4.9.1 Pile head displacement 112
4.9.2 Normal force distribution 114
4.10 Recommendations for the energy pile design 115
4.11 Conclusion 116
CHAPTER 5 : Thermo-mechanical behaviour of energy diaphragm walls 118
5.1 Introduction 118
5.2 Numerical modelling 119
5.3 Impact of thermal loading type on the mechanical behaviour of energy diaphragm walls 121
5.3.1 Normal forces distribution 122
5.3.2 Shear forces 124
5.3.3 Bending moment 125
5.4 Impact of soil thermal properties on the mechanical behaviour of energy diaphragm walls 126
5.5 Impact of the soil thermo-mechanical property on the mechanical behaviour of energy diaphragm walls 127
5.6 Accounting for the soil hardening 128
5.7 Comparison between the studied cases 133
5.8 Recommendations 134
5.9 Conclusion 135
Conclusion and recommendations for further research 136
References 141

List of figures

Figure 1. Comparison of worldwide direct-use geothermal energy in TJ/year from 1995, 2000, 2005, 2010, and 2015 (Lund & Boyd, 2016). ……2

Figure 1.1 Installation and carbon dioxide savings in UK by the end of 2015 (GI Energy 2017).10

Figure 1.2 Heat transfer paths in soil; 1 for particles conduction, 2 for air conduction, 3 for air radiation, 4 for pore air convection, 5 for vapour diffusion, 6 for liquid convection, 7 for liquid conduction (Alrtimi et al. 2016). 12

Figure 1.3 Thermal pile heat transfer concepts (a) plan of thermal pile components; (b) temperature differences and component resistances (Loveridge & Powrie 2012).....16

Figure 1.4 Thermal resistances in the case of energy diaphragm wall (upper part in contact with the excavation on one side). 18

Figure 1.5 Longitudinal distribution of normal and shear forces in a HEP according to thermo-elastic model (Arson et al. 2013). 25

Figure 1.6 Variation of the thermally induced strains, normal forces, and shear stresses for an energy pile partially restrained at its both ends (Amatya et al. 2012).....26

Figure 2.1 Representation of the energy geo-structure and the surrounding soil zones. 39

Figure 2.2. Resistive model for the energy geo-structure and the soil.....39

Figure 2.3 Flow chart for the calculation sequence of the conductive and advective powers. 44

Figure 2.4 Illustration of the divergence theorem (https://fr.wikipedia.org/wiki/Flux_électrique). 47

Figure 3.1 Geometry of the 2D model representing energy diaphragm walls constituting a metro station. 50

Figure 3.2 Temperature profile around the diaphragm walls-k_h=10^{-5} m/s - a) case 1 b) case 2 c) case 3. 52

Figure 3.3Variation of the allowable thermal exchanged power along *x*-direction for the right and left walls (Case 1, k_h=10^{-5} m/s). 53

Figure 3.4 Variation of the total allowable thermal exchanged power during winter season (case 1, k_h=10^{-5} m/s). 54

Figure 3.5 Variation of P_{total} with Péclet number. 54

Figure 3.6 Influence of groundwater flow on the exchanged powers P_c and P_v. 55

Figure 3.7 Temperature variations imposed into the diaphragm wall. 56

Figure 3.8 Variation of temperature during the loading cycles. 57

Figure 3.9 Variation of the exchanged power under cyclic loading (k_h=10^{-5} m/s). 59

Figure 3.10 The modelled diaphragm wall with the two considered configurations. 59

Figure 3.11 Ratio of the total thermal power between the configurations W1 and W2 (k_h=10^{-5} m/s). 60

Figure 3.12 Distribution of the total divergence in the domain in the case of pure conduction a) Winter b) Summer. 61

Figure 3.13 Evolution of the a) advective, b) conductive, and c) total divergences in the soil zones at the end of the winter season (cooling period). 62

Figure 3.14 Total power a) and advective power b) exchanged by the whole domain during the winter season for the three considered cases with k_h=10^{-5} m/s. 63

Figure 3.15 Evolution of the total, conductive, and advective powers of the whole domain with Péclet number. 63

Figure 3.16 Variation of the power exchanged by the soil surrounding the walls for a) case 1 b) case 2 c) case 3. 64
Figure 3.17 Total exchanged power a) for the whole domain b) for the zones surrounding the energy walls. 66
Figure 3.18 Exchanged conductive and advective powers, bold lines for conduction, and dotted lines for advection, a) for the whole domain b) for the zones surrounding the diaphragm walls. . 67
Figure 3.19 Energy supplied by the system during the three thermal cycles. 68
Figure 3.20 Variation of the sinusoidal temperature imposed into the wall. 69
Figure 3.21 Power exchanged by the whole domain for one year thermal loading under sinusoidal thermal solicitation. 70
Figure 3.22 Conductive and advective power exchanged by the whole domain. 71
Figure 3.23 Energy delivered by the energy diaphragm walls. 72
Figure 3.24 Variation of the thermal exchanged power for both types of thermal loading order. . 73
Figure 3.25 Thermal power exchanged in the whole domain and in the zones surrounding the energy walls. 74
Figure 3.26 Geometry of the 3D modeled metro stations with the energy diaphragm walls in green. 75
Figure 3.27 Distribution of the total divergence in the domain. 76
Figure 3.28 Exchanged power for the whole domain without the thermally activated elements. . 77
Figure 3.29 Exchanged power by the surrounding zones only. 77
Figure 3.30 Distribution of the conductive and advective powers in the surrounding zones. 78
Figure 3.31 Conductive power exchanged by the energy diaphragm walls. 79
Figure 3.32 Geometry of the three dimensional energy pile model. 80

Figure 3.33 Distribution of the total divergence in the zones around the pile at the end of the first a) heating phase b) cooling phase. 81

Figure 3.34 Power exchanged by the whole domain during three thermal cycles. 82

Figure 3.35 Power exchanged by the zones surrounding the energy pile only. 83

Figure 4.1 Model geometry, thermal and mechanical boundary conditions. 87

Figure 4.2 Load ratio-head displacement variation. 88

Figure 4.3 Variation of the pile temperature for the three types of thermal solicitations. 90

Figure 4.4 Variation of the thermally induced pile head displacement for a) TS0 b) TS0 with reversed heating and cooling phases. 92

Figure 4.5 Axially induced forces at the end of the first and tenth cycles a) TS0 b) TS0 with reversed heating and cooling phases. 93

Figure 4.6 Thermally induced axial force a) TS0 b) TS0 with reversed heating and cooling phases. 93

Figure 4.7 Variation of the pile head displacement for the cases of constant pile temperature; a) TS1 and TS2 b) TS1 and TS2 with reversed heating and cooling phases. 95

Figure 4.8 Variation of the axial force at the end of the first and tenth thermal cycles for the case of constant pile temperature a) TS1 b) TS2 c) TS1 with reversed order d) TS2 with reversed order. 97

Figure 4.9 Variation of the thermally induced axial force with time a) TS1 b) TS2 c) TS1 with reversed heating and cooling phases d) TS2 with reversed heating and cooling phases. 99

Figure 4.10 Variation of the thermally induced pile head displacement a) TS3 b) TS3 with reversed order of heating and cooling phases. 101

Figure 4.11 Variation of the axial force at the end of the first and tenth cycles a) TS3 b) TS3 with reversed order of heating and cooling phases. 102

Figure 4.12 Variation of the thermally induced axial force with time a) TS3 b) TS3 with reversed order of heating and cooling phases. 102

Figure 4.13 Variation of the axial stress for the fixed pile head a) TS0R b) TS0R with reversed order. 106

Figure 4.14 Variation of the thermal axial force with time for the fixed pile head a) TS0R b) TS0R with reversed order. 106

Figure 4.15 Variation of the axial stress for fixed pile head a) TS1R b) TS1R with reversed order c) TS2R d) TS2R with reversed order. 108

Figure 4.16 Thermally induced axial force for fixed pile head a) TS1R b) TS1R with reversed order c) TS2R d) TS2R with reversed order. 109

Figure 4.17 Variation of the axial stress for fixed pile head a) TS3R b) TS3R with reversed order. 110

Figure 4.18 Thermally induced axial force for fixed pile head a) TS3R b) TS3R with reversed order. 110

Figure 4.19 Variation of the pile head displacement for the four cases with respect to the reference case. 113

Figure 4.20 Vertical displacement (in m) at the end of the tenth cooling phase for a) reference case ($\alpha_T=5x10^{-6}{}^{\circ}C^{-1}$) b) case a ($\alpha_T=10x10^{-6}{}^{\circ}C^{-1}$). 113

Figure 4.21 Variation of the axial normal forces of the four cases and the reference case.....115

Figure 5.1 Geometry and the mesh of the model. 121

Figure 5.2 Different types of the considered thermal loads. 122

Figure 5.3 Variation of the axial normal forces along the diaphragm wall for a) TS2 b) TS2r...123

Figure 5.4 Axial normal force for case TS3. 124

Figure 5.5 Shear forces along the diaphragm wall for a) TS2 b) TS2r c) TS3. 125

Figure 5.6 Bending moment of the diaphragm wall for a) TS2 b) TS2r c) TS3. 126
Figure 5.7 Variation of the a) normal forces b) shear forces c) bending moment of the diaphragm wall for TS2 with new soil thermal properties. 127
Figure 5.8 Variation of the structural forces along the diaphragm wall for $\alpha=10x10^{-6}\,^{\circ}C^{-1}$.....128
Figure 5.9 Variation of the a) principal stress difference and axial strain b) volumetric strain and axial strain. 129
Figure 5.10 Deformed mesh and deformation contours for Mohr-Coulomb i and ii, and for Hardening soil model iii and iv. 130
Figure 5.11 Variation of the normal force N, shear force Q, and bending moment M along the wall at the end of the second excavation phase. 131
Figure 5.12 Distribution of the plastic zones in the soil for i) Mohr-Coulomb model ii) Hardening soil model. 131
Figure 5.13 Variation of the normal and shear forces and bending moment for both constitutive laws.....133

List of tables

Table 2.1 Influence parameters affecting the thermal performance of energy diaphragm walls examined by previous researchers. 36

Table 2.2 Thermal resistance values for energy piles (SIA 2005). 40

Table 3.1 Hydraulic and thermal parameters of soil and concrete. 49

Table 3.2 Temperature imposed in the diaphragm walls (Suryatriyastuti, 2013). 51

Table 3.3 Hydraulic boundary conditions and flow velocity. 52

Table 4.1 Mechanical parameters of the soil and the pile. 88

Table 4.2 Thermal parameters of the soil and the pile. 89

Table 4.3 Thermal parameters of the four studied cases. 112

Table 5.1 Mechanical parameters of concrete and soil. 119

Table 5.2 Thermal parameters of concrete and soil. 120

Table 5.3 Values of the considered mechanical parameters. 129

Nomenclature

Greek symbols:

α_T	thermal expansion coefficient	$^o C^{-1}$
ΔT	temperature gradient	$^o C$
Δx	center-to-center distance between two adjacent zones	m
ε	deformation	
λ	thermal conductivity	W/mK
ν	Poisson's coefficient	
ρ	density	Kg/m^3
σ	stress	Pa
φ	friction angle	^{o}
ψ	dilation angle	^{o}
ω	angular frequency	

Roman letters:

A_0	annual amplitude of soil temperature	$^o C$
B	width of rectangular pile	m
c	cohesion	kPa
c^T	specific heat extraction of solid material	$J/m^3.K$
C_v	volumetric heat capacity	J/kgK
C_p	specific heat capacity	J/kgK
d	damping depth	M

D_T	thermal diffusivity	m^2/s
E	elastic modulus	MPa
E_{50}^{ref}	reference triaxial loading stiffness	MPa
E_{oed}^{ref}	reference oedometric stiffness	MPa
E_{ur}^{ref}	reference unloading/reloading stiffness	MPa
E	exchanged energy	kWh
h	heat transfer coefficient	$W/m^2.K$
$\vec{j}$	vector representing heat exchange	
k_0^{nc}	coefficient of earth pressure at rest for normal consolidation	
kh	hydraulic conductivity	m/s
L	length	m
L_c	characteristic length	m
m	power for stress/level dependency of stiffness used in the hardening soil model	
m	mass flow rate	kg/sec
M	bending moment	kN.m/lm
n	porosity	
N	normal force	kN
Pc	conductive power	W/m
Pe	Péclet number	
Pv	advective power	W/m^2
q^T	diffusive heat flux	W/m^2
q_w	fluid specific discharge	m/s
q_v^T	volumetric heat source intensity	W/m^3
q	heat flux	W/m^2
Q	exchanged heat	W/m
Q	shear frictional force	kN/lm
R	thermal resistance	mK/W
S	degree of saturation	
t	time	s

T	temperature	º C
T_{ave}	annual mean ground temperature	º C
v	velocity	m/s
w	axial displacement	m
x	distance from the edge of the geothermal structure	m
z	depth	m

Subscripts:

adv	advective
c	concrete
cond	conductive
d	dry
d	day
es	energy geostructure
excavation,conv	convection at the excavation side
f	fluid
g	ground
h	hour
in	inlet
mech	due to mechanical load
out	outlet
pcond	conduction of the pipe wall
pconv	convection of the heat carrier fluid
pi	pipe
s	soil
th	due to thermal load
v	volumetric
w	water
y	year

General introduction

Pollution aggravation induced by large emissions of harmful gases, increases in the price of primary energy sources due to their quick run out caused by excessive demand, and the need to save more spaces; all these factors combined together have led planners and local authorities to encourage the usage of geothermal energy (Lofthouse et al. 2016, P.A. CoE 2010). Energy geo-structures that rely on geothermal heat pumps belong to the category of geothermal energy and serve as clean, renewable, and a long-term cost-saving energy source. Following Lund & Boyd (2016), energy savings from the usage of geothermal energy accounted for 352 million barrels of annually oil, and contributed in avoiding 46.1 million tons of carbon and 149.1 million tons of carbon dioxide emissions into the atmosphere.

The outcome of the COP 2015 that was held in Paris in December 2015; the Paris agreement has recommended to limit the global temperature rise to well less than 2°C, and has given the grave risk to strive for 1.5°C. To accomplish this goal, the usage of geothermal energy is highly recommended.

The concept of geothermal energy is being widely spread in many countries, and this is reflected by the increase in the installed direct-use geothermal capacity and annual utilization by the end of 2014 compared to the data available in 1995 (Lund & Boyd, 2016). Figure 1 represents the evolution of the utilization of direct-use geothermal energy since 1995 till 2015, and it is significant that geothermal heat pumps acquire the highest figures. According to Lund & Boyd

(2016), the five leading countries in terms of installed capacity of geothermal heat pumps are: USA, China, Sweden, Germany, and France.

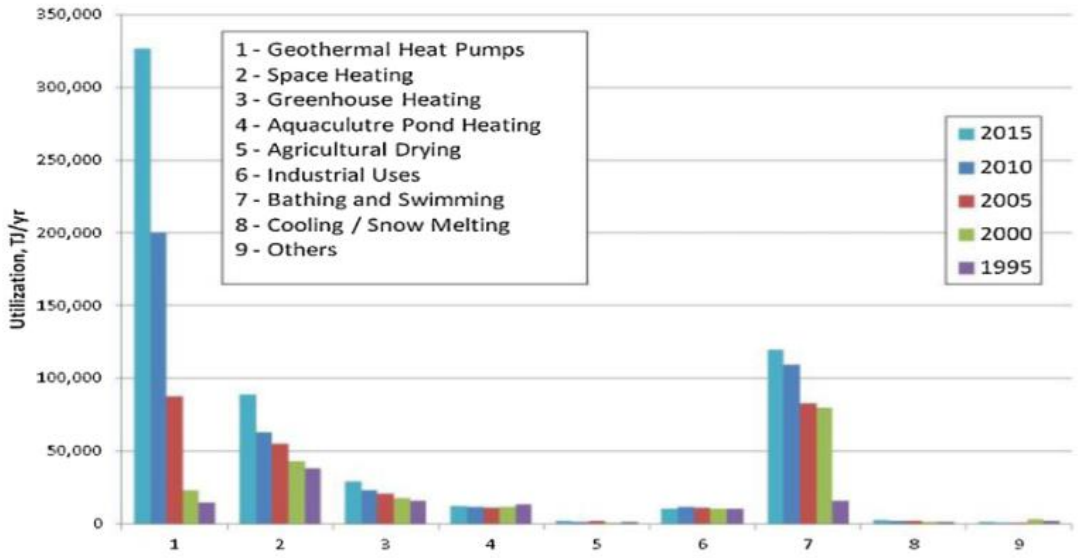

Figure 1. Comparison of worldwide direct-use geothermal energy in TJ/year from 1995, 2000, 2005, 2010, and 2015 (Lund & Boyd, 2016).

Geothermal structures present a promising technology in this field. Beside their major role as bearing elements for the constructions, they are gaining attention nowadays due to several reasons. Among these reasons, environmental aspects are prominent with the high need to reduce carbon dioxide emissions all over the world, and consequently alleviate pollution. Moreover, implementing geothermal structures limits the depletion of non-renewable energy sources. Adding to this, the increase of the energy bill required for heating and cooling of the buildings presents a critical issue that requires serious action steps. In this manner, geothermal structures present a promising example for clean and sustainable energy, which are considered as economical solutions at the long-term.

Energy piles and recently energy diaphragm walls are being highly installed in several newly developed projects, and thus they require deep studies to improve their design. Despite of the

wide installation of geothermal structures, the assessment of their sustainability is a tough issue, knowing that the sustainability is an important key factor that allows the evaluation of the thermal and mechanical performance of geothermal structures.

The work conducted in this thesis is divided into two main parts. The first part is advocated to study the thermal performance of energy diaphragm walls and energy piles. The impact of the presence of the underground water flow is studied according to two new presented approaches.

The second part focuses on the mechanical behaviour of energy piles and diaphragm walls. The influence of the thermal load that must be implemented in these structures at the design stage is studied. Several thermal loading types are considered to give feasible recommendations regarding the most appropriate thermal load to be imposed in geothermal structures. Adding to this, the effect of the thermal and thermo-mechanical parameters of the soil surrounding geothermal structures is evaluated.

The presented thesis consists of an introduction, four chapters describing the carried work, and a general conclusion and perspectives.

Chapter One is the introduction, it presents an overview on the implementation of energy piles and diaphragm walls around the world. Then, the general mechanisms of heat transfer in the soil and in energy geo-structures are described. Following the factors affecting the heat exchange processes are briefly presented. After that, the mechanical behaviour of the soil and energy geo-structures (piles and diaphragm walls) under the impact of thermal loading are presented. These are followed by the main issues that will be dealt with in the presented thesis regarding the energy exchange between energy piles and diaphragm walls, and the surrounding soil, and the mechanical behaviour of energy piles and energy diaphragm walls.

Chapter Two is advocated to present in details the two new and simplified approaches that will be used to assess the allowable exchanged energy between energy piles and diaphragm walls, and

the surrounding soil. Approach 1 is based on the main formulae for conduction and advection, and it calculates the power transferred between the energy geo-structures and the surrounding soil. It is concerned only with the energy exchanged in the soil zones surrounding these structures and are affected by the heat exchange phenomena. Approach 2 based on the energy balance equation tries to evaluate the exchanged power through the assessment of the conductive and advective divergences using the Ostrogradsky theorem.

Chapter Three deals with the sustainability of energy piles and diaphragm walls embedded in saturated sandy soil and subjected to cyclic thermal loading. It presents direct numerical applications for the two approaches explained in the preceding chapter using the finite difference code FLAC 3D. Two and three dimensional models are conducted for energy diaphragm walls and energy piles installed in saturated sandy soil. The impact of the presence of underground water flow and thus the advective term is studied as well as the influence of the thermal cyclic loading on the thermal performance of geothermal structures is discussed. Moreover, the effect of the type of the applied thermal load is evaluated.

Chapter Four discusses in details the impact of the thermal loads imposed into energy piles on their mechanical behaviour. Different types of thermal loads are considered to cover several climatic conditions and be able to determine the more appropriate thermal load that should be adopted for the design of energy piles. Moreover, the existence of strong super structure-pile connection requires the analysis of the behaviour of restrained pile head, therefore when thermal load is added; the behaviour of restrained piles varies and needs to be studied. Adding to this, the impact of the soil thermal and thermo-mechanical parameters are evaluated to illustrate the importance of assuming real field properties at the design stage. Recommendations are given at the end of this chapter regarding the mechanical design of energy piles.

Chapter Five is dedicated to study the impacts of the thermal loading types and the thermal and thermo-mechanical parameters of the soil on the mechanical behaviour of energy diaphragm walls. Finally, it gives some recommendations about the mechanical design of energy diaphragm walls.

CHAPTER 1 :

Mechanisms related to the thermal transfer and mechanical behaviour of energy geo-structures

---

1.1 Introduction

Geothermal structures may comprise base slabs, piles, diaphragm walls, and supporting elements for tunnels as linings and anchors. In addition to their traditional role as structural bearing elements, geothermal structures possess a double role as heat exchanger elements that are capable to totally or partially supply other structures with their thermal needs for heating and/or cooling. They are shallow geothermal closed systems, where thin high-density polyethylene plastic pipes are installed as loops within the concrete elements (Brandl 2006, Adam & Markiewicz 2009), these pipes will be connected to the reinforcement bars and a heat carrier fluid flows through them. By virtue of the thermal properties of concrete, the thermal exchange between the energy geo-structures and the surrounding ground is enhanced (Brandl, 2006).

Although the implementation of geothermal structures is increasing rapidly, but till now there are no specific design codes and methodologies that state the design methods for such structures, except for some recommendations and guidelines regarding their usage in some countries (VDI 2001, SIA 2005, NHBC 2010, GSHP 2012, French Recommendations 2017).

A lot of challenges are facing energy geo-structures as the presence of ground water flow near them, thermally induced behaviour of the surrounding soil and its impact on the structures, climatic conditions, presence of near-by existing buildings, and the interaction between heat exchanger elements and their interaction with the super structures. Thus, extensive work should account for all these issues in order to be capable to develop design codes for geothermal structures, with the aim to provide design engineers with simple tools that help them and facilitate the implementation of these structures.

Two main issues related to the performance of energy geo-structures need to be studied to better understand their behaviour and facilitate the development of design methods.

The first issue is related to the evaluation of the thermal efficiency of geothermal structures. In fact, the key point for assessing the efficiency of geothermal structures is evaluating their sustainability. Sustainability signifies the ability of the production system applied to sustain the production level over long times. Therefore, the sustainability secures the longevity of the resource at a lower production level (Raybach 2002). The thermal performance of energy geo-structures is an indicator of their sustainability, thus focusing on the factors that affect their performance is helpful and leads to efficient results. Being surrounded with soil having specific thermal and hydraulic properties, this absolutely affects the thermal exchange between energy geo-structures and the surrounding media (Di Donna & Barla 2016, Di Donna et al. 2016b, Gashti et al. 2015, Maragna & Rachez 2015, Bayandor et al. 2014, Ma & Grabe 2010).

Assessment of the exchanged heat is indeed a complex issue that needs correct tools for its evaluation and deep analysis to fully understand the heat exchange phenomena including conduction and advection when underground water flow is present.

Beside the assessment of the heat exchanged between geothermal structures and the surrounding media, the mechanical behaviour of geothermal structures is the second issue that requires further study. Even though it gains more interest from researchers than the first issue, but till now, taking into account when designing energy geo-structures, the thermal interaction with the soil and its impacts on the mechanical behaviour of the soil and the geothermal structures is not very clear. In this context, the choice of the thermal solicitation (its type, duration, amplitude) to be imposed into the geothermal structures is based on assumptions. Some studies impose a uniform constant temperature neglecting the presence of the U-tubes (Laloui et al. 2006, Suryatriyastuti 2013, Saggu et al. 2015), while others depend on the temperature values measured or obtained at the inlet and outlet tubes (Batini et al. 2015, Gashti et al. 2015, Cecinato & Loveridge 2015, Sterpi et al. 2016). But in fact, with the lack of sufficient in-situ data registration in many regions and climates, then the latter assumption may lead to conservative or may be inefficient results. Thus, defining the thermal solicitation in a proper way could solve such problems and facilitate the design of energy geo-structures.

This chapter will present an overview on geothermal structures specifically piles and diaphragm walls, then the heat transfer mechanisms that take place in the soil and in the geothermal structures are discussed, following the approaches that could be used to assess the energy exchanged between geothermal structures and soil are presented. Thereafter, the main issues related to the thermo-mechanical behaviour of soils and energy geo-structures are discussed.

Finally the main issues considered in this thesis regarding the thermal performance and thermo-mechanical behaviour of energy piles and diaphragm walls are listed.

1.2 Overview on energy geo-structures

1.2.1 **Energy piles**

Piles are deep foundations formed by a comparatively long and slender columns forced mechanically into the ground. They are used to transfer loads from the super structures to strong and stiff soil with the purpose to decrease the settlement of the super structures (Bazant 1979, Tomlinson & Woodward 2008). Piles foundations, once they are equipped with closed vertical heat exchanger tubes; they will act as heat exchanger elements in addition to their traditional role, thus forming energy piles. Since 1984, energy piles have begun to be used in Austria and Switzerland (Brandl 2006), and their implementation is spreading all around the world. The installation of energy piles is increasing worldwide, but there is lack in the data related to their installation number and the related carbon dioxide savings; Figure 1.1 represents these figures related to the UK experience in this domain.

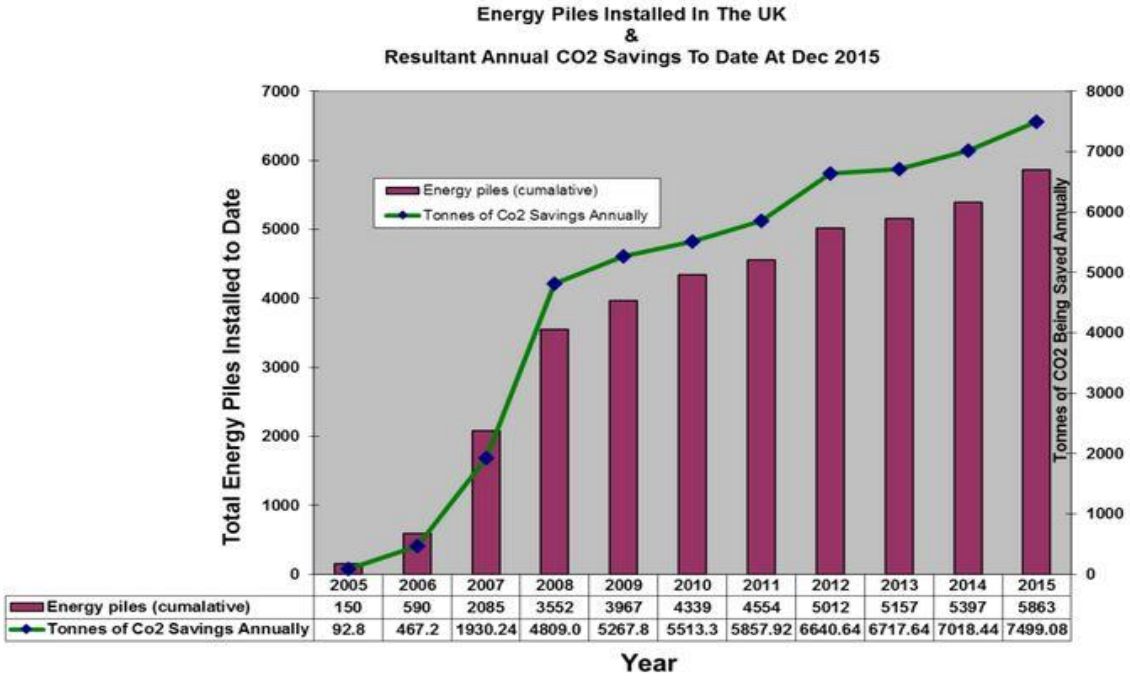

Figure 1.1 Installation and carbon dioxide savings in UK by the end of 2015 (GI Energy 2017).

1.2.2 **Energy diaphragm walls**

Diaphragm walls are considered as vertical cantilever and they are designed to provide structural support in addition to water tightness. They are widely used in urban excavations for building basements, parking and underground works realized by the cut-and-cover methods, and they are commonly designed as flexible retaining walls.

Diaphragm walls started to be equipped with heat exchanger tubes since 1996 (Brandl 2006) where some projects rely on energy diaphragm walls to support excavations or structures and deliver exchanged heat to other buildings. Compared to energy piles, energy diaphragm walls present a great interest through their larger exchange surface area. Mostly, energy diaphragm walls are being used in metro stations as in metro line U2, Vienna (Brandl 2006), Metro line 13 under Shanghai museum (Sun et al. 2013, Xia et al. 2012), Dean Street Station, London (Rui 2014), Tottenham Court Road Station and Moorgate Shaft, London (Di Donna et al. 2016b), Line

2 of Metro Torino (Cornelio et al. 2016), and Lines 14 and 12 of Paris Metro stations. Even though the spread of energy diaphragm walls remains scarce compared to energy piles, recently, researchers are interested in studying the thermal exchange between energy diaphragm walls and the soil (Di Donna et al. 2016b, Cornelio et al. 2016, Di Donna 2016, Bourne-Webb et al. 2016b), adding to their mechanical behaviour affected by applied thermal loads (Sterpi et al. 2016, Bourne-Webb et al. 2016b, Habert & Burlon 2015). Nevertheless, extensive research is needed to cover all the aspects related to the thermal exchange and mechanical behaviour of energy diaphragm walls as a result of thermally activating them.

1.3 Heat transfer mechanisms

Heat transfer takes place when spatial variations of temperature occur. There exist three main mechanisms for heat transfer: conduction, convection, and radiation.

1.3.1 **Heat transfer in soil**

In general, heat transfer in soil is affected by soil thermal properties as thermal conductivity, specific heat capacity, and thermal diffusivity, in addition to the soil hydraulic properties as hydraulic conductivity and flow velocity if groundwater flow of non-static regime exists. These properties depend on the type of soil, its geometry, mineral composition, water content, air content, and porosity.

Heat transfer in soils may take place through three main phenomena: conduction, convection and radiation as presented in Figure 1.2.

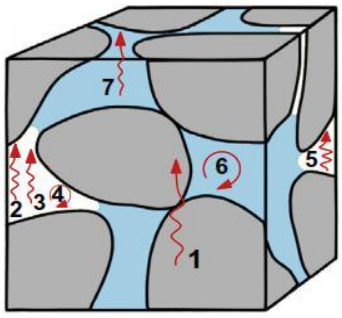

Figure 1.2 Heat transfer paths in soil; 1 for particles conduction, 2 for air conduction, 3 for air radiation, 4 for pore air convection, 5 for vapour diffusion, 6 for liquid convection, 7 for liquid conduction (Alrtimi et al. 2016).

- Conduction:

  It's the transfer of heat due to direct contact between two bodies derived by temperature difference between them, where these bodies are not moving relative to each other. Conduction is governed by Fourier's Law presented by the following equation:

  $$\vec{q}_{cond} = -\lambda.\nabla T \tag{1.1}$$

  where $\vec{q}$ is the heat flux, λ is the thermal conductivity coefficient, and T stands for the temperature.

  Equation 1.1 represents the first heat conduction law under steady-state conditions, but for non-steady or transient heat conduction we need another law analogous to Fick's second law of diffusion in order to obtain the second law of conduction that is given by the following equation:

  $$\rho C_p \frac{\partial T}{\partial t} = -\nabla.q \tag{1.2}$$

  where ρ is the density and C_p is the specific heat capacity.

  In soils, conduction takes place in the solid phase of the porous media and fluids, which are at rest. Since the soil grains are in contact with each other and the pores in between are

filled with a mixture of air and water, then heat conduction takes place. Once the soil is more saturated, this means that higher conductive heat transfer occurs. This is related to the dependence of the thermal conductivity on the water content. In addition, it varies with the composition of soil and its compacity, and with the mineralogical components and the chemical properties of the pore water (Brandl, 2006). According to Eslami 2014, the addition of sand to the studied soil samples had a positive impact through increasing their thermal conductivity.

As presented by equations 1.1 and 1.2, heat transfer by conduction depends on the thermal properties of the soil, its thermal conductivity, and specific heat capacity. In transient conditions, as C_p starts to play a role, then it is important to note that it increases also with the increase in water content.

- Convection:

  It's the movement of molecules within fluids and is considered as the major mode of heat and mass transfer based on differential movements, due to spatial variations in temperature or chemical concentration. Convection is the sum of advection (molecules are being carried) and diffusion (molecules are being dispersed). Thus, convection is considered as a special form of advection, where advection is a transport mechanism of a substance by a fluid, due to the fluid's bulk motion in a particular direction.

  In soils, the moving particles which transport heat are water molecules. Therefore, when groundwater flow exists, then one should account for advection that is represented by the following equation:

$$\vec{q}_{adv} = \rho_f C_f \vec{\upsilon}_f T \tag{1.3}$$

where ρ_f is the fluid density, C_f is the specific heat capacity of the fluid, v_f is the groundwater velocity in liquid phase. Convection in soils can be of two types; forced convection that can be associated with groundwater flow or free convection that can occur due to upward heat flow (Johansen, 1975).

To evaluate the relative importance of convective and diffusive heat transport in soils, it is good to introduce Péclet number:

$$P_e = \frac{\rho_f C_f \upsilon_f}{\lambda} \tag{1.4}$$

Once the Péclet number is greater than 1, then heat exchange is governed by advection, otherwise it is governed by conduction.

- Radiation:

  Radiation is the movement of energy through a medium or vacuum without the movement of molecules. In soils, higher temperature grains radiate more energy and thus energy is transferred by radiation to the lower temperature grains. Generally, in soils, radiation plays almost a negligible role for heat transfer.

According to the soil temperature and its permeability coefficient, one of the three presented mechanisms dominates. Conduction dominates for all ranges of temperature (Sundberg, 1988). However, for temperature above 0°C and in highly permeable soils, forced or/and natural convection will occur and may be significant (Dawson, 2008)

1.3.2 **Heat transfer in energy geo-structures**

Heat transfer in energy geo-structures is a complex phenomenon but can be simplified as presented in Figure 1.3 (for energy piles); it is governed by conduction and convection. Due to the particles' movement, conduction occurs in the concrete and in the pipe wall. On the other

hand, inside the pipes, heat transfer occurs by convection due to the internal flow of the heat carrier fluid. Convective heat transfer is considered forced since the fluid flow is forced by the heat pump, and it is represented in the following equation:

$$\vec{q}_{conv} = h.\left(T_{pi} - T_f\right) \tag{1.5}$$

where h is the heat transfer coefficient, T_{pi} and T_f are the temperature of the pipe wall and the fluid respectively.

To account for the heat exchange, thermal resistances are to be defined for each heat transfer mechanism taking place. The thermal conductivity is analogous to the Darcy hydraulic conductivity and to electrical conductance, thus thermal resistance can be defined as:

$$R = \frac{\Delta T}{|Q|} \tag{1.6}$$

where Q may represent either conductive or convective transferred heat in W/m depending on the heat transfer mechanism. For the thermal resistance R as presented in Figure 1.3, it is the sum of the resistances of heat carrier fluid R_{pconv}, of pipe wall R_{pcond}, of concrete R_c, and of ground R_g.

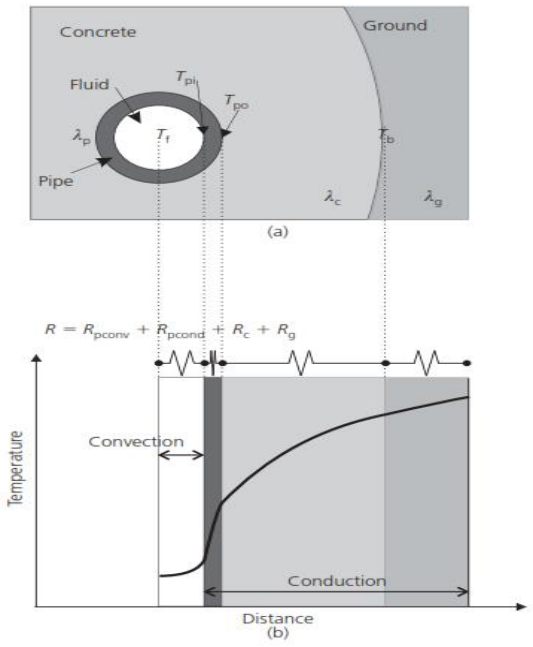

Figure 1.3 Thermal pile heat transfer concepts (a) plan of thermal pile components; (b) temperature differences and component resistances (Loveridge & Powrie 2012).

Heat transfer in energy geo-structures depends on the material properties of the concrete, pipe, and fluid, and especially on the thermal conductivity (Abuel-Naga et al. 2015). In addition, heat transfer relies on the heat transfer coefficient that depends on the pipe diameter, pipe length, flow velocity, viscosity, density and specific heat capacity, geometric dimensions, and length of heat transfer occurrence (Brandl 2006).

1.4 Assessment of the exchanged heat between geothermal structures and the surrounding media

1.4.1 **Principles**

The thermal exchange between energy geo-structures and the surrounding media differs from one type of structure to the other. In this manner, it is important to note that Figure 1.3 well represents the heat transfer for energy piles, where the pile is totally embedded in soil. For the soil,

conductive heat transfer always occurs and leads to symmetrical heat exchange, however when water flow is significant then advection takes place too (Chiasson et al. 2000), and then the ground resistivity will be composed of two parts; conductive and advective parts. On the other hand, for energy diaphragm walls; it is not exactly the same. In fact, for energy diaphragm walls, the upper part is in contact with the soil on one side and with the excavation on the other side, thus convection may occur also on the excavation side and depends on the heat transfer coefficient at the excavation side (Figure 1.4). In this figure, $R_{excavation,conv}$ stands for the thermal resistance representing the exchange at the excavation side. However, the lower part which is totally embedded in the soil transfers heat with the surrounding in the same way as presented in Figure 1.3.

$$R=R_g + R_c + R_{p,cond} + R_{p,conv} + R_{p,cond} + R_c + R_{p,cond} + R_{p,conv} + R_{p,cond} + R_c + R_{excavation,conv}$$

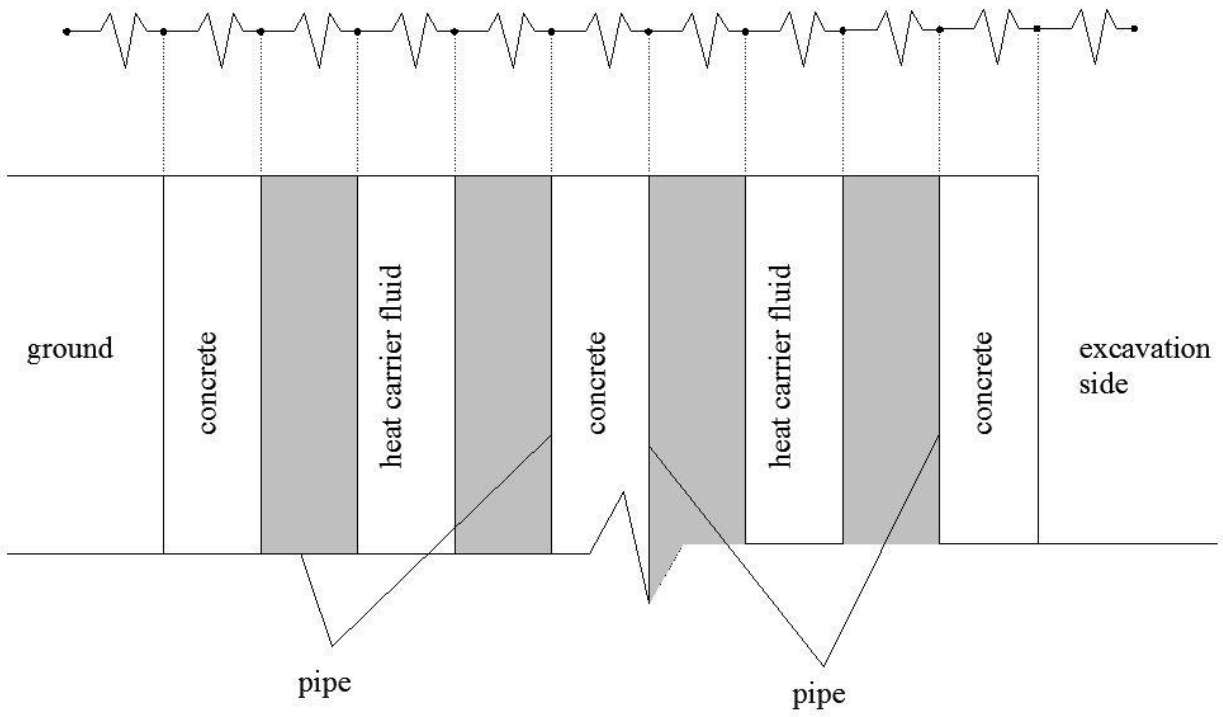

Figure 1.4 Thermal resistances in the case of energy diaphragm wall (upper part in contact with the excavation on one side).

Generally for a system where there is a convective-diffusive heat transfer, then the energy balance equation is as follows:

$$c^T \frac{\partial T}{\partial t} + \nabla q^T + \rho_w c_w q_w \nabla T - q_v^T = 0 \quad (1.7)$$

where q^T is the diffusive heat flux (W/m^2), q_w is the fluid specific discharge that stands here for the velocity of ground water flow (m/s), $q_v{}^T$ is the volumetric heat source intensity (W/m^3), and c^T is the effective specific heat (J/m^3/K).

The assessment of the energy exchanged between energy geo-structures and the surrounding media is a complicated issue especially at the design stage where no information about the inlet and outlet heat carrier fluid temperatures would be available. Thus, a more general approach

should be defined in order to guide the designers, and to avoid conservatism or over-designing of energy geo-structures.

Despite of the many applications on energy geo-structures, there is no common approach for the assessment of their thermal performance which depends largely on the thermal transfer between them and the surrounding media. Most of the existing studies estimate the total thermal transfer through Equation 1.8, by taking into account only the thermal and hydraulic properties of the heat carrier fluid (Gao et al. 2008, Bouazza et al. 2013).

$$Q_{total} = Q_{in} - Q_{out} = m_f .C_f .(T_{in} - T_{out}) \quad (1.8)$$

where Q_{in} and Q_{out} (W) are the inlet and outlet heat respectively, m_f and C_f are the mass flow rate (kg/s) and the specific heat capacity (J/kg/K) of the heat carrier fluid respectively, and T_{in} and T_{out} are the temperatures of the inlet and outlet tubes.

Through Equation 1.8, it is difficult to assess precisely the influence of ground conditions on the thermal exchanges: the soil thermal conductivity and its specific heat capacity, the presence of groundwater flow and its permeability. Thus, indeed defining general strategies for evaluating the heat exchange capable to take into account all heat transfer mechanisms is urgently needed to alleviate complexities and facilitate such calculations.

Several studies have been conducted on the heat transfer for borehole heat exchangers (Sigfusson & Uihlein, 2015; Diao et al. 2004; Tolooiyan & Hemmingway 2012; Choi et al. 2012), energy piles (Bouazza et al. 2013; Cecinato & Loveridge 2015; Cervera 2013; Ma & Grabe 2010; Zhang et al. 2015; Sedano et al. 2011), and for energy tunnels (Di Donna & Barla, 2016). Energy diaphragm walls present interesting benefits compared to energy piles, they possess a bigger exchange surface with the soil especially in the case of metro stations. They have begun to be studied recently (Di Donna 2016, Cornelio et al. 2016, Di Donna et al. 2016b, Bourne-Webb et

al. 2016b). All existing studies concerning the energy exchange between energy geo-structures and the surrounding media rely on Equation 1.8 to evaluate the possible exchanged power.

1.4.2 **Factors impacting the heat transfer phenomena between energy-geo structure and soil**

Generally, several factors affect the heat transfer between energy geo-structures and the surrounding media:

- Geometrical configuration of the heat exchanger pipes (Abuel-Naga et al. 2015, Sterpi et al. 2014; Gashti et al. 2014), whether they are single U-tubes, double U-tubes, or W-shaped tubes….
- Working heat carrier fluid properties and its flow conditions (Abdeen 2014, Sterpi & Angelotti 2013, Xia et al. 2012).
- Heat transfer at the excavation side in the case of energy diaphragm walls (Bourne-Webb et al. 2016b, Di Donna 2016).
- Thermal properties of soil and concrete (Abuel-Naga et al. 2015, Abdeen 2014). Higher thermal conductivity boosts conductive heat exchange and thus affects positively the total thermal exchange (Di Donna & Barla 2016; Bourne-Webb et al. 2016b).
- Groundwater flow properties (Abdeen 2014), its direction and magnitude especially in granular soils have a direct influence on the evolution of temperature around the structural elements and thus on the exchanged energy (Ma & Grabe 2010, Bayandor et al. 2014, Katzenbach et al. 2008, Di Donna & Barla 2016, Di Donna 2016, Maragna & Rachez 2015, Gashti et al. 2015, Zhang et al. 2015), since water flow enhances heat transfer by advection. All studies confirm the positive impact of the presence of water flow on the thermal performance on the system. Concerning the impact of the direction of water flow on the thermal exchange of group of energy piles, Katzenbach et al. 2008 found that

highest expansion of the temperature field occurs towards the direction of the groundwater steam due to stronger convective heat transfer processes compared to sections orthogonal to the groundwater flow.

The impact of groundwater flow on the thermal performance of the system depends also on the functioning mode of this system; whether it will be used for heating or cooling only or for both heating and cooling modes. It's noted that heat influx and extraction are necessary for buildings with no or with low flow of ground water, since they provide "active regeneration". In this manner, whenever the water flow exceeds 0.05 m/day, then heat storage requires protecting hydraulic screen (Van Meurs, 1986). In addition heat injection and extraction ensure that energy balance will occur during the whole year, also this confirms that individual systems don't short-circuit, that the natural recovery process can still occur at long term and prevents possible impacts on other nearby installations (Bouazza et al. 2011, Brandl 2006). However, if only cooling or heating is required then high soil permeability and high ground water flow velocity are required (Brandl, 2006). Briefly, since the soil temperature recovery ability is strengthened in the presence of water flow, then the steady-state heat transfer would arrive more quickly (Rui et al. 2007), thus affecting positively the thermal performance of the system.

Therefore, the presence of water table has a direct impact on the dimensioning of heat exchanger elements, since water movement can result in smaller ground heat exchangers, and thus decreases the costs dedicated to the heat exchanger tubes.

As mentioned before, Equation 1.8 depends on the properties of the heat carrier fluid and thus the interaction between the soil and the geothermal structure is not well presented. Moreover, in case where groundwater flow is significant, then advection could not be neglected anymore. It is

interesting then to be able to distinguish between the conductive and advective heat exchange contributions in the total heat exchange phenomenon, which is not possible through Equation 1.8. Thus, two new strategies based on the energy balance equation are introduced in this thesis that are capable to take into account the interference of the thermally affected soil, and distinguish between the exchanged advective and conductive energies and to show how they could influence the global thermal performance of the geothermal system.

1.5 Main issues concerning the thermo-mechanical behaviour of soil and energy geo-structures

Thermal exchange between energy geo-structures and the surrounding media affects absolutely the mechanical behaviour of the structure regarding axial displacements and distribution of forces, also the surrounding soil will be mechanically influenced depending on its type.

1.5.1 **Thermo-mechanical behaviour of saturated soil**

Once a cold or heat fluid passes into the structural elements, an exchange will occur with the surrounding soil. This exchange affects the soil and may influence its behaviour depending on the soil type and its degree of saturation.

- *Clayey soil*

When soil is heated, all of the constituents dilate. In the case of clayey soil, this dilation produces a decrease in the strength of the adsorbed layers and modification in the distance between the clayey particles (Fleureau, 1979). This leads to change in the equilibrium between the Van der Waals attractive forces and the electrostatic repulsive forces.

Thermally induced volume change behaviour in clays is attributed to temperature effects on the physico-chemical interactions between clay particles, which depend on the clay lattice

constitution, the chemical nature of the interstitial fluid and the interlayer distance (Cekerevac, 2003), and is related directly to the over consolidation ratio (OCR). Plasticity index (PI) also affects the magnitude of thermally induced axial strain (Abuel-Naga et al. 2015), where a linear trend is found between thermally induced strains and PI (Abuel-Naga et al. 2007c).

In normally consolidated conditions (NC) and under drained conditions, clay contracts when it's heated and a significant part of this deformation is irrecoverable upon cooling. Under heating, a NC clay sample will settle with a non-linear volume variation, and the volume increases (Laloui et al. 2013). The behaviour of NC clay over a whole cycle indicates the irreversibility of strain due to thermal loading, which is representative to thermal hardening, and can be interpreted as soil undergoing densification (Laloui et al. 2013).

For over consolidated clay (OC), under drained cyclic thermal loading they undergo reversible dilation. Slightly OC clays first produce dilation and then have a tendency towards contraction.

In general, the intensity of reversible/irreversible parts of deformation due to temperature cycling depends on the soil type, plasticity and the stress level indicated by the OCR (Laloui et al. 2013).

On the other hand, under undrained cyclic thermal loading, since water is not allowed to flow in or out of the sample, then the particle's density can't change without drainage, but pore water pressure and effective stresses will change. Upon heating under undrained conditions, no volume change is noted and the pore pressure increases causing failure of clays between 70-90 °C which leads to drop in the effective main stress attaining the critical state line (Suryatriyastuti, 2013).

- *Sandy soil*

Sandy soils are characterized by their high permeability, and then the ground water diffuses rapidly the imposed temperature through heat advection transfer phenomenon. They have a very small thermal gradient, and only the structure undergoes additional thermal volumetric

deformation, leading to unfavorable condition in which the additional stresses induced by temperature variation are concentrated in the concrete and soil-structure interface (Suryatriyastuti, 2013). It's important to note that soil with large groundwater flow (up to 35 m/year) can produce natural heat energy regeneration, thus heat extracted during winter doesn't depend on that injected during summer, then the ground temperature equilibrium is guaranteed and the surrounding soil is not affected by thermal volumetric variations (Suryatriyastuti, 2013).

Scare studies deal with the mechanical behaviour of sandy soil affected by heating and cooling cycles in comparison to clayey soil. Among these few researches, and with the aim to study the impact of heating and cooling cycles on the behaviour of saturated sandy soil surrounding energy geo-structures, Ng et al. (2016) performed temperature controlled experimental tests. Loose and medium dense sands showed a contractive behaviour upon heating from 23 to 35°C, whereas a dilative behaviour was found for heating from 35 till 50°C. The contractive behaviour is attributed to the thermal expansion of soil particles that adjusts soil force chains inducing plastic contraction and soil hardening. On the other hand, dense sand shows a dilative behaviour when heated from 23 to 50°C. After two thermal cycles, the behaviour of sand was found to be reversible regardless of its density. Concerning the impact of confinement, under higher confining stress, the sand behaves as loose sand and larger volumetric contractions occur after heating; this agrees with the results of Yavari et al. (2016) who studied the mechanical behaviour of Fontainebleau sand under heating till 40°C. In addition, Yavari et al. (2016) found that at low normal stresses, the studied Fontainebleau sand tends to dilate from the beginning of the test, and that the effect of temperature on the shear strength of sand was found to be negligible.

Regarding fine sands, Recordon (1993) found that, its deformation, initial compacity, and elastic modulus are not influenced by temperature varying between 2° and 40°C.

1.5.2 **Thermo-mechanical behaviour of thermo-active piles**

Energy piles experience modifications in their mechanical behaviour affected by the thermal loads imposed into the piles. This thermal load will affect also the surrounding soil which in return will influence the pile behaviour. The change in the pile behaviour is obvious through the variations that may happen in the pile head settlements, distribution of the normal axial forces, shaft and base resistances. The response of energy piles is highly affected by different ground conditions and degrees of end restraints (Laloui & Di Donna 2011, Amatya et al. 2012, Saggu et al. 2015), in addition to the pile characteristics as its geometry and the elastic modulus of concrete E beside its thermal expansion coefficient (Bourne-Webb et al. 2013), and absolutely the applied thermal load (Bourne-Webb, 2013).

When the pile is free to move (no restraints are present neither at the top nor at the bottom), then no stresses will be mobilized at its ends, it tends to settle during cooling and heave during heating freely; this may lead to possible movement of the building (Nicholson et al. 2013), whereas the normal and shear stresses will be mobilized as shown in Figure 1.5.

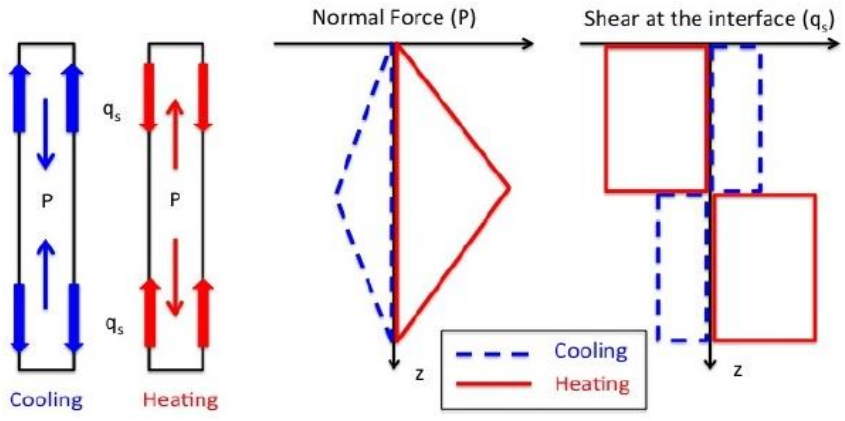

Figure 1.5 Longitudinal distribution of normal and shear forces in a HEP according to thermo-elastic model (Arson et al. 2013).

The thermally induced free strains and stresses are represented as follows:

$$\begin{cases} \varepsilon_{th,\,free} = \alpha_c . \Delta T \\ \sigma_{th,\,free} = 0 \end{cases} \quad (1.9)$$

where α_c is the concrete thermal expansion coefficient.

On the other hand, when an energy pile has a certain degree of fixity at its head, different behaviour will occur according to the imposed thermal loading (Laloui & Di Donna 2011, Tang et al. 2013, Bourne-Webb et al. 2009, Amatya et al. 2012, Suryatriyastuti 2013). Generally, the displacement will be blocked partially or totally and this in return generates high stresses. During heating, compressive stresses will appear at the ends due to heave being restrained, and mobilized shear stresses are reduced as presented in Figure 1.6, and the opposite occurs during cooling. Now, the measured thermal strains $\varepsilon_{th,meas}$ will be lower than the free thermal strains, and the generated thermal stress is expressed as follows:

$$\sigma_{th} = -E.(\varepsilon_{th,\,free} - \varepsilon_{th,meas}) \quad (1.10)$$

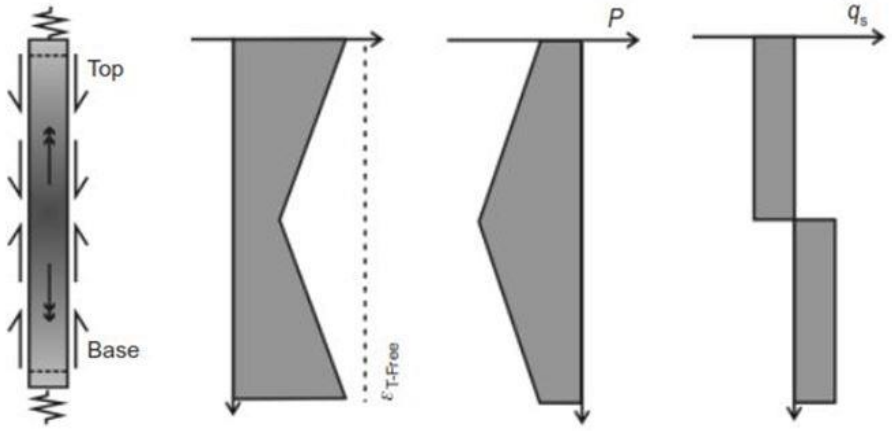

Figure 1.6 Variation of the thermally induced strains, normal forces, and shear stresses for an energy pile partially restrained at its both ends (Amatya et al. 2012).

In general, heating piles induces additional compression stresses in the pile and increases the mobilized shear stresses, whereas cooling leads to the development of tensile stresses in the pile (Abuel-Naga et al. 2015, Bourne-Webb et al. 2009).

The behaviour of energy piles is evaluated through different in-situ tests, experimental and numerical models. Among the full-scale in-situ tests on energy piles, Laloui et al. (2006) consider a thermal solicitation consisting of a heating period followed by a recovery period, where the temperature variation during heating was 21°C. Bourne-Webb et al. (2009) considered extreme conditions where the temperature varies between -6°C and 56°C.

In fact, for the design of energy piles, defining the thermal solicitation that best represents the real temperature fluctuations in the pile is a complex issue. This thermal solicitation imposed into the pile has a direct impact on its mechanical behaviour, thus our work highlights on the impact of the choice and type of thermal loading imposed into the pile on its mechanical behaviour. Many studies consider a constant temperature as a thermal load imposed into the pile while others depend on the inlet and outlet temperatures of the heat carrier fluid measured at the field. Several types of thermal loadings are examined and their impact on the mechanical behaviour of the piles is studied. In addition, the pile end restraints were varied in order to highlight on the importance of considering the pile-structure interaction. Moreover, the impact of various soil thermal and thermo-mechanical properties is evaluated and recommendations are given concerning energy piles design.

1.5.3 **Thermo-mechanical behaviour of thermo-active diaphragm walls**

The mechanical design of energy diaphragm walls is perhaps more complicated than that of energy piles as the constraints present in the walls may affect and lead their mechanical

behaviour. When subjected to thermal loads, their structural performance may be altered and thus requires to be studied in order to design energy diaphragm walls properly. Few studies exist dealing with the design and mechanical behaviour of energy diaphragm walls. Through conducted numerical models, Habert & Burlon (2015), and Sterpi et al. (2016) show that temperature variations imposed into the walls do not alter the geotechnical and structural safety of the system, but it is advisable to consider them at the design stage. On the other hand, the soil surrounding energy diaphragm walls and the thermal boundary conditions imposed at the interface with the excavation, both may have certain influence on the mechanical behaviour of energy diaphragm walls, and require special attention (Bourne-Webb et al. 2016b).

The literature lacks information about the type of the thermal load that should be applied into the energy diaphragm walls and its duration. Therefore, this work covers this topic; moreover, it deals with the soil properties that could influence the mechanical behaviour of energy diaphragm walls.

1.6 Main issues and methodology

This chapter presents an overview on the implementation of geothermal structures (piles and diaphragm walls) and their progress in the world. Then it depicts the recent work that deals with their thermal performance based on the assessment of the thermally exchanged heat between these structures and the surrounding soil. This chapter highlights also on the advantages behind studying the thermal performance of energy piles and diaphragm walls through distinguishing between the conductive and advective contributions and how this is related to the sustainability of energy geo-structures. Thereafter, the general mechanisms related to the mechanical behaviour of energy piles and diaphragm walls are presented.

Briefly, this thesis deals with two main topics which are the thermal performance of geothermal piles and diaphragm walls, and their mechanical behaviour.

Several issues related to the thermal energy assessment of energy geo-structures require detailed studies. The presented thesis discusses and deals with the following:

1- Issue: Simplification of the heat exchange phenomena through neglecting advective heat transfer.

   Proposal: Taking into account the impact of groundwater flow through varying the soil hydraulic conductivity and the imposed hydraulic flux.

2- Issue: Lack of studies capable to distinguish between the conductive and advective exchanged heat.

   Proposal: Introducing two new strategies based on the energy balance equation capable to assess separately the conductive and advective exchanged heat in order to know their relative importance on the thermal performance of the system.

3- Issue: Impact of water flow direction on the heat exchange in the case of energy diaphragm walls.

   Proposal: Three dimensional numerical model for energy diaphragm walls through which the impact of the direction of water flow can be evaluated.

On the other hand, there are several issues related to the mechanical aspects of energy piles and energy diaphragm walls:

1- Issue: Choice of the proper thermal solicitation to be imposed in the geothermal structures at the design stage.

Proposal: Modelling several thermal solicitation types through which different climatic conditions are taken into consideration. This is done through varying the thermal loading type, the order of the thermal phases, and the number of thermal cycles.

2- Issue: Influence of the soil thermal and thermo-mechanical parameters on the structural behaviour of geothermal structures.

   Proposal: Parametric study considering various soil parameters to determine the most influential ones.

3- Issue: Influence of pile-structure interaction on the design of energy piles.

   Proposal: Modelling energy piles with head end-restraints to account for the presence of the super structures.

4- Issue: Does the assumption of a simple constitutive law for the soil guarantee the proper design of geothermal structures.

   Proposal: Considering constitutive law that accounts for shear and volumetric hardening, and evaluate how this may affect the mechanical behaviour of energy diaphragm walls.

All these issues are treated through conducting two and three dimensional numerical models for energy piles and energy diaphragm walls embedded in saturated sandy soils.

CHAPTER 2 :

Possible strategies for the evaluation of the thermal exchanged power

2.1 Introduction

Geothermal structures exchange heat with the surrounding media by virtue of the seasonal temperature that is imposed into these structures. The thermal exchange provides the supported buildings and other constructions in some cases, with the thermal needs for heating and/or cooling. This exchange is influenced by several parameters and gives an indication about the thermal performance and thus the sustainability of geothermal structures. Therefore, implementing heat exchanger tubes in geothermal structures and the heat transfer processes that occur between the structures and the surrounding soil; how these may affect the design and the thermal performance of geothermal structures, these are critical issues that require extensive work and research to assure the durability and sustainability of such structures.

In general, the energy performance of geothermal structures relies on three main parameters. The first parameter is the structure itself, its geometry, thermal properties, and thermal boundary conditions (exposed to air/soil on one side or totally embedded in soil); where all affect the system's performance. In addition, the hydro-geological conditions and thermal properties of the soil surrounding the structure play an important role. Finally, the climatic conditions of the

studied zone and the heating/cooling demands of the building have a direct impact on the efficiency of the geothermal system.

The assessment of the possible exchanged energy between geothermal structures and the surrounding soil is a key indicator of their efficiency and sustainability. Thus, accounting for the presence of groundwater flow when it really exists; its intensity and direction, is vital. Almost all existing studies are capable to evaluate the total exchanged power without distinguishing between the conductive and advection energies especially when groundwater flow is present. For this, defining simple methods that are able to calculate the conductive and advective exchanged heat is necessary in order to understand the role of each heat transfer phenomenon and how it could affect the total thermal performance of the geothermal structures.

In the present chapter, two different approaches for the assessment of the thermal performance of geothermal structures are presented to evaluate the conductive and advective transferred heat that could be exchanged between the energy geo-structure and the soil.

2.2 Available studies dealing with the assessment of the energy exchange between energy structures and the surrounding media

Few studies exist dealing with the thermal performance of energy diaphragm walls compared to those dealing with energy piles; this is related to the wide implementation of energy piles around the world. Following are the present studies that consider the thermal performance of energy diaphragm walls and energy piles.

2.2.1 **Studies carried on energy diaphragm walls**

The literature is deficient regarding the design methods for energy diaphragm walls. Among the analytical models, Sun et al. 2013 established two-dimensional heat transfer models and

developed a design method to calculate the hourly heat exchange capacity of diaphragm wall heat exchangers (over and under the excavation). The proposed models are limited since they are based on several assumptions as the constant soil temperature at any depth and the thermal contact resistance is assumed to be null between the heat exchanger tubes and the walls, and between the wall and the soil. For this, more general design methods are in need to be proposed in order to safely design energy diaphragm walls.

On the other hand, conducted numerical studies allow defining the parameters that affect the thermal performance of energy diaphragm walls through evaluating the heat exchange rate between them and the surrounding soil. The influencing parameters according to the carried studies are listed in Table 2.1.

The heat exchanger layout is one of the affecting parameters, it is found that the best layout is the one that optimizes the heat flux and thus limits the occurrence of high temperature gradients between different portions of the pipe itself (Sterpi & Angelotti 2013, Sterpi et al. 2014). In addition, enlarging the distance of branch tubes near the soilward face improves the heat transfer performance (Xia et al. 2012). Moreover, increasing the number of pipes has a positive impact on the energy performance (Xia et al. 2012).

The velocity of the heat carrier fluid proves to have a direct influence on the heat transfer capacity of energy diaphragm walls. The value of the velocity should be chosen in a way to provide the best heat transfer rate depending on the heat exchangers layout.

The position of the U-tubes; installed along the face near the excavation or near the soil, or even in case where they are installed on both sides, this would affect the heat transfer capacity of energy diaphragm walls (Amis et al. 2010, Bourne-Webb et al. 2016b). In this manner, installing

exchanger tubes on both sides enhances the heat exchange process (Bourne-Webb et al. 2016b, Di Donna et al. 2016b).

Regarding the wall geometry including its depth, embedment depth, and panel width and length; they prove to have almost a negligible impact (Di Donna et al. 2016b).

Concrete thermal conductivity is one of the most influential parameters that affect directly the thermal performance of energy diaphragm walls; increasing the thermal conductivity enhances the thermal transfer (Di Donna et al. 2016b, Bourne-Webb et al. 2016b). Regarding the soil's thermal conductivity, also it has a similar impact (Bourne-Webb et al. 2016b).

The presence of groundwater flow has an enhancing effect on the thermal performance of energy walls leading to increase the exchanged heat (Di Donna 2016).

Regarding the operation mode, there are two types. Type 1 is related to the mode of operation whether the system is single needed for either heating or cooling, or it is dual needed for both types of thermal loading. Type 2 is related to the duration of operation, whether it is intermittent or continuous. Both types of operation modes influence the overall performance of the system. The impact of type 1 depends also on the presence of water flow; its direction and intensity (Sterpi & Angelotti 2013, Sterpi et al. 2014). For type 2, having an intermittent mode proved to be more beneficial (Xia et al. 2012).

The thermal boundary conditions along the excavation side, affect absolutely the heat transfer processes. Assuming adiabatic conditions leads to the most conservative results (Di Donna 2016). On the other hand, imposing a constant temperature along the excavation face gives the largest heat exchange values (Di Donna et al. 2016b). Depending on the air movements and the method of usage of the excavation, different boundary conditions could be imposed. Convective boundary condition with very small convective heat transfer coefficient leads to the lowest heat

transfer capability (Bourne-Webb et al. 2016b). Thus, specifying the appropriate thermal boundary condition is indispensable for the proper assessment of the heat exchange rate.

Table 2.1 Influence parameters affecting the thermal performance of energy diaphragm walls examined by previous researchers.

	Xia et al. 2012	Sterpi & Angelotti 2013	Sterpi et al. 2014	Di Donna 2016	Di Donna et al. 2016b	Bourne-Webb et al. 2016b
Shape of heat exchangers	X	X	X			
Length of heat exchangers	X	X	X			
Layout of heat exchangers	X	X	X		X	
Heat carrier fluid velocity	X	X	X		X	
Inlet water temperature	X					
Position of the tubes						X
Concrete cover to pipes					X	
Geometry of the wall (panel width, embedment ratio…)					X	
Thermal conductivity of concrete					X	X
Thermal conductivity of soil						X
Groundwater flow				X		
Operation mode (single or dual)		X	X			
Operation mode (continuous or intermittent)	X					
Thermal boundary conditions				X		X
Difference in temperature between excavation and soil					X	

2.2.2 **Studies carried on energy piles**

The literature is rich in studies related to the energy performance of geothermal piles, either regarding analytical models that are capable to assume the pile temperature or their heat transfer capacity, or numerical models and real case studies that are conducted to study the evolution of temperature inside and around an energy pile, and also to evaluate its heat exchange rate. As for energy diaphragm walls, heat transferred by energy piles is governed by various parameters and mechanisms. These influencing parameters can be divided into three major categories; the energy pile, the surrounding soil, and the thermal operation mode. For the geothermal pile; the pile geometry (Batini et al. 2015, Loveridge 2012), layout of the heat exchanger tubes (Luo et al. 2016, Zarrella et al. 2013, Hamada et al. 2007) and characteristics of the heat carrier fluid (Ghasemi-Fare & Basu 2013, Cui & Zhu 2016), thermal properties of concrete including its thermal conductivity (Loveridge et al. 2012, Ghasemi-Fare & Basu 2013) and its thermal expansion coefficient; all these influence directly the heat exchange. For the surrounding soil; its thermal and hydraulic properties including the soil thermal conductivity (Loveridge et al. 2012, Ghasemi-Fare & Basu 2013)and specific heat capacity and the presence of groundwater flow; its intensity (Ma & Grabe 2010, Gashti et al. 2015, Akrouch et al. 2015, Zhang et al. 2015) and flow direction (Zhang et al. 2015). For the operation mode, cyclic heat injection and extraction increases the thermal transfer performance of energy piles (Ghasemi-Fare & Basu 2013, Park et al. 2012).

2.3 Strategies for the assessment of exchanged thermal power

The energy exchanged by geothermal structures is evaluated almost by all existing studies depending on the thermal and hydraulic properties of the heat carrier fluid circulating in the exchanger tubes, and on their inlet and outlet temperatures using Equation 1.8 presented in chapter one. This equation does not allow the assessment of the exchanged conductive and

advective heat separately, and thus it cannot give an idea about how the various parameters and conditions could affect each term. Knowing that examining the sustainability of geothermal structures requires evaluating their thermal efficiency, thus it is necessary to define strategies that are capable to assess clearly the heat exchange rate of geothermal structures. For this, the two following approaches are introduced:

- Approach 1: It delivers a simple tool for the calculation of the power that could be exchanged between energy geo-structures and the surrounding soil, and it is useful for the evaluation of the impact of groundwater flow on the heat exchange phenomena.
- Approach 2: Is based on the energy balance equation and on the flux-divergence theorem. The main aim of this approach is to define the divergences of the advective and conductive terms, and then use them to assess the possible exchanged thermal energy.

2.3.3 **Approach 1**

Power transferred by conduction

In all ground conditions, conductive heat transfer exists when there is a temperature difference between two media independently of the water flow conditions. By an analogy to a resistive model, the power transferred by conduction can be expressed as follows (Fromentin et al. 1997):

$$P_c(X,t) = \frac{T_s(X,t) - T_s(x,t)}{R_s + R_{es}} \tag{2.1}$$

$$T_{es} = \frac{T_{in} + T_{out}}{2} \tag{2.2}$$

where the exchanged power $P_c(X,t)$ is the thermal power transferred by conduction between two adjacent zones at time *t.* It is calculated at distance X from the edge of the structure, where $X=x+\Delta x$. $T_s(x,t)$ is either the temperature of the geo-structure or the temperature of the soil zones at time t that are situated at a certain distance from the edge of the energy geo-structure. Figure 2.1 represents the zones where the zone numbered 0 stands for the energy geo-structure.

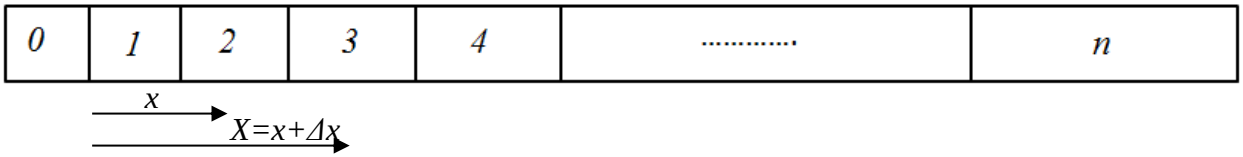

Figure 2.1 Representation of the energy geo-structure and the surrounding soil zones.

In a simplified manner, $T_s(x,t)$ varies as follows:

$$\begin{cases} T_s(x,t)=T_{es} \quad for \ \ x=0 \\ T_s(x,t)=temperature\ of\ the\ soil\ zones\ (1,\ 2,\ ....,\ n) \qquad for\ x>0 \end{cases} \tag{2.3}$$

In this manner, T_{es} is the temperature of the energy geo-structure which is considered as the average heat carrier fluid temperature for each season and is represented in equation 2.2.

In this approach, the soil and the energy geo-structure are considered as two resistors connected in series (Figure 2.2). The equivalent thermal resistance is the sum of the thermal resistances of the energy geo-structure R_{es} and the soil R_s.

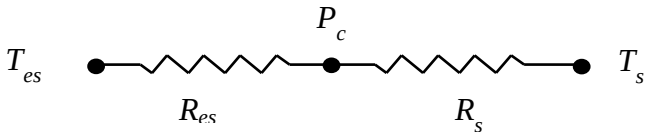

Figure 2.2. Resistive model for the energy geo-structure and the soil.

The thermal resistances used for the calculation of the allowable power transmitted by conduction are determined according to two approaches. For the soil, the thermal resistance can be considered as the inverse of its thermal conductivity (λ_s): $R_s=1/\lambda_s$. Numerous theoretical and experimental studies have shown the relationship between the soil thermal conductivity and its nature, granulometry, compacity, and water content. In this study, the following correlation is chosen to describe the thermal conductivity of the studied sandy soil (Kersten, 1949):

$$\frac{1}{R_s} = \lambda_s = 0.1442(0.7\log w + 0.4).10^{0.6243\rho_d} \quad (2.4)$$

where w is the water content of the soil and ρ_d (kg/m^3) is its dry density.

For the energy geo-structure, the values indicated by the Swiss Society of Architects and Engineers can be considered (Table 2.2).

Table 2.2 Thermal resistance values for energy piles (SIA 2005).

Pile type		Pile diameter (m)	Total thermal resistance (m.K/W)
Driven tube with double U-tube		0.3-1.5	0.15
Precast or cast in situ	Double U-tube*	0.3-1.5	0.10-0.11
	Triple U-tube*	0.3-1.5	0.07-0.08
	Quadruple U-tube*	0.3-1.5	0.06

* U-tube attached to reinforcement

Power transferred by advection

In the case of groundwater flow with a significant Darcy velocity, there may be advection in addition to conduction. Advection refers to the transfer of a certain quantity by the fluid motion; such as the transfer of heat through water flowing between the soil particles. In a given direction, the thermal power transferred by advection between the energy geo-structure and the soil is given by the following relation:

$$P_v(X,t) = v \cdot \rho_w \cdot c_w \cdot (T_s(X,t) - T_s(x,t)) \quad (2.5)$$

where $P_v(X,t)$ is the thermal power transferred by advection between two adjacent zones at time t. It is calculated at the point situated at distance X from the edge of the structure. ρ_w (kg/m^3) is the density of groundwater, c_w (J/kg/K) is the specific heat capacity of groundwater, and v (m/s) is the Darcy velocity in the given direction, T_s is the same as that used in Equation 2.3.

In order to analyze precisely the effect of groundwater flow, the dimensionless parameter Péclet number P_e is introduced, defined as the ratio of heat transferred by convection to the heat transferred by conduction:

$$P_e = \frac{\rho_w c_w}{\lambda_s} \cdot v \cdot L_c \tag{2.6}$$

where L_c (m) is the characteristic length. The characteristic length depends on the type of the problem but can be considered as the ratio of the soil volume to the surface area exchanging heat.

Total transferred power

In order to analyze the heat exchange in details, the total average allowable thermal power P_{total} between the energy geo-structure and the soil is defined as follows:

$$P_{total} = \overline{P}(X,t) \text{ and } P(X,t) = \frac{P_c(X,t)}{L_c} + P_v(X,t) \tag{2.7a}$$

$$\begin{cases} P(X,t) = \dfrac{T_s(X,t) - T_s(x,t)}{L_c(R_s + R_{es})} + v\rho_w c_w (T_s(X,t) - T_s(x,t)) \\ P(X,t) = (T_s(X,t) - T_s(x,t)) \left(\dfrac{1}{L_c(R_s + R_{es})} + v\rho_w c_w \right) \end{cases} \tag{2.7b}$$

where $\overline{P}$ is the average of the allowable thermal exchanged power *P(X,t),* and *P(X,t)* corresponds to the sum of the power exchanged by conduction and by advection between the energy geo-structure and the soil situated at distance *X* from the energy geo-structure and at time *t* during the loading season. The characteristic length L_c, in this case is equal to 1 m; the thickness of the studied model.

2.3.4 **Approach 2**

The flux-divergence theorem relates the power to its divergence; it is represented by the following equation:

$$\iiint_{\Omega} div(\vec{j}).d\Omega = \oiint_{\partial\Omega} \vec{j}.d\vec{S} \tag{2.8}$$

where Ω is the volume of a body that is subjected to vector *j* and *S* is the body surface. This equation is used to calculate the advective and conductive powers after calculating their divergences.

Generally, for a convective-diffusive heat transfer condition, the energy balance equation is:

$$c^T \frac{\partial T}{\partial t} + \nabla q^T + \rho_w c_w q_w \nabla T - q_v^T = 0 \tag{2.9}$$

where q^T is the diffusive heat flux (W/m^2), q_w is the fluid specific discharge (stands here for the velocity of ground water), $q_v{}^T$ is the volumetric heat source or sink intensity (W/m^3), and c^T is the effective specific heat represented by the following formula:

$$c^T = \rho_d C_v + nS\rho_w c_w \tag{2.10}$$

where *S* is the degree of saturation, *n* is the porosity, and C_v is the volumetric heat capacity.

Equation 2.9 can be re-arranged as follows:

$$\begin{cases} c^T \dfrac{\partial T}{\partial t} + div(\vec{j}_{cond}) + div(\vec{j}_{adv}) - q_v^T = 0 & (2.11a) \\ \vec{j}_{cond} = \vec{q}^T & (2.11b) \\ \vec{j}_{adv} = \rho_w c_w \vec{q}_w T & (2.11c) \end{cases}$$

where $\vec{j}_{cond}$ and $\vec{j}_{adv}$ are the vectors representing the conductive and advective terms of heat exchange.

It is worth noting that the divergence of the advective term is divided into two parts as follows:

$$div\left(\vec{j}_{adv}\right) = \rho_w c_w \left((div(\vec{q}_w)).T + \vec{q}_w.\overrightarrow{grad T}\right) \tag{2.12}$$

Water particles in between the soil behave as incompressible fluid, and then the first term on the right side of Equation 2.12 is equal to zero. Therefore, Equation 2.12 becomes:

$$div\left(\vec{j}_{adv}\right) = \rho_w c_w \left(\vec{q}_w.\overrightarrow{grad T}\right) \tag{2.13}$$

In the case where no heat sinks or sources are found, then the last term of equation 2.11a will be eliminated. Therefore, it will be clear that the system would be considered sustainable when the temperature doesn't vary with time. This means that at a local scale the divergence of the conductive and advective terms will be equal but with opposite senses.

Concerning the thermal powers exchanged between the energy geo-structure and the soil, the following formulae represent this exchange:

$$\vec{P}_c = \vec{j}_{cond} = \vec{q}^T = -\lambda_s \overrightarrow{grad}T \tag{2.14}$$

$$\vec{P}_v = \vec{j}_{adv} = \rho_w.C_w.\vec{q}_w.T \tag{2.15}$$

These formulae depend directly on the thermal properties of the soil and its hydrological conditions (presence or absence of groundwater flow), and they are vector field parameters.

Knowing that the divergence calculation provides scalar quantities, then it can be said that calculating the divergence can give also an idea about the thermal exchange between the energy geo-structure and the surrounding soil. Thus, the divergence of each conductive and advective term must be calculated at each instant for every structural and soil zone.

The calculation sequence used to obtain the conductive and advective exchanged powers is presented in Figure 2.3 and explained in details in the Appendix following this chapter.

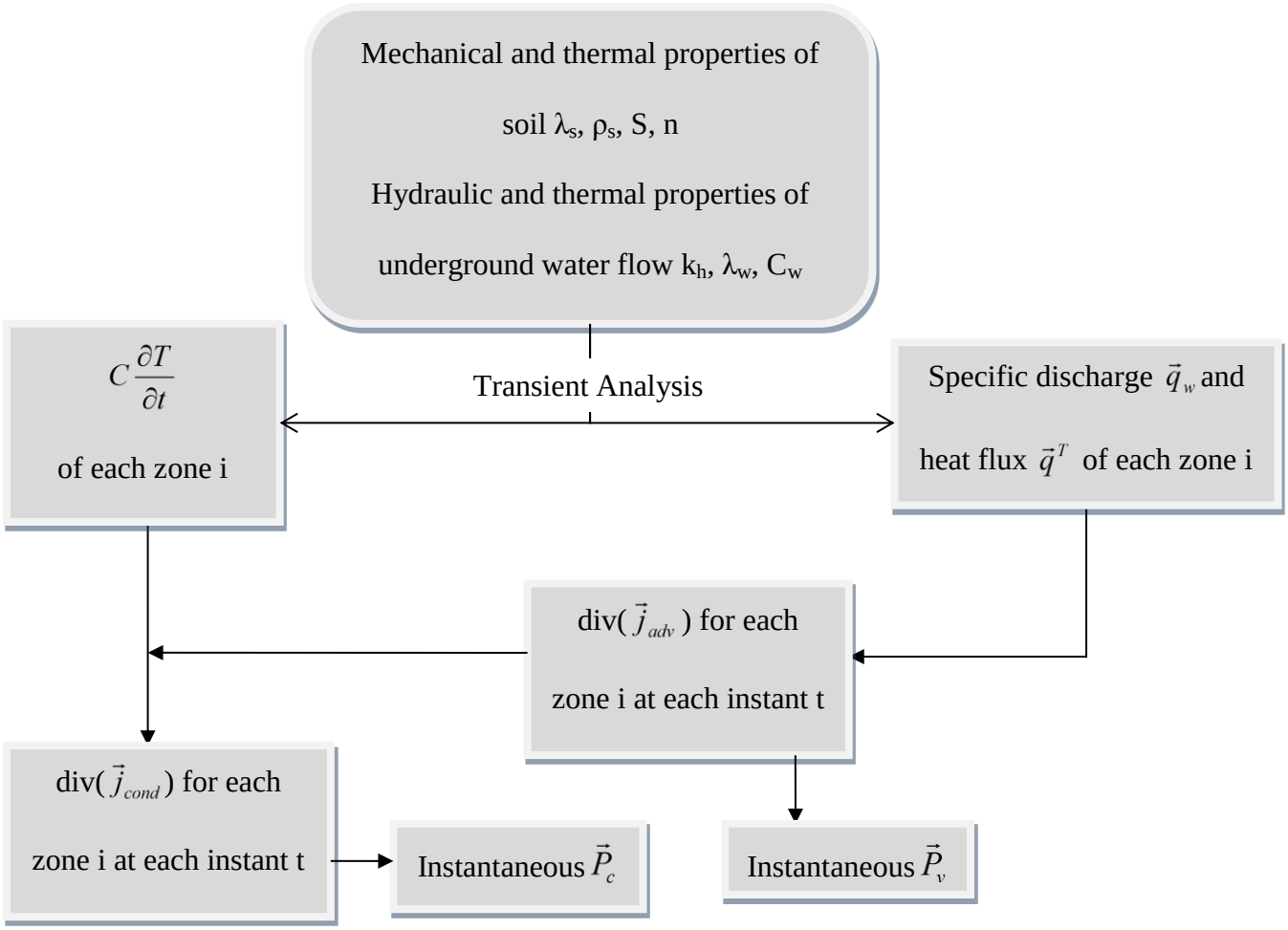

Figure 2.3 Flow chart for the calculation sequence of the conductive and advective powers.

2.4 Conclusion

This chapter presents two strategies that can be used to evaluate the conductive and advective exchanged heat by geothermal structures and the surrounding soil. The calculation of each term separately allows the assessment of the influencing parameters in a precise way. In the following chapter, energy diaphragm walls and energy piles are modelled numerically and the presented strategies are used to calculate their exchanged heat.

2.5 Appendix: Calculation of the conductive and advective powers and energies

This appendix is dedicated to explain in details the calculation sequence for Approach 2:

As presented in the flow chart (Figure 2.3 of Chapter 2), the steps for calculating the divergence and the power induced by conduction and advection are as follows:

1- Definition of the soil thermal, mechanical and hydraulic properties. Adding to this, the thermal properties of concrete are also needed.

2- For each time step in the transient calculation, the model is capable to calculate automatically the heat flux $\vec{q}^T$ and the specific discharge $\vec{q}_{w/f}$ for each zone *i* ($\vec{q}_{w/f}$ stands for the heat carrier fluid velocity or for the groundwater velocity).

3- The divergence of the advective term for each zone *i* and at each time step *t* could be calculated now:

$$div(\vec{j}_{adv}) = \rho_{w/f} c_{w/f} \vec{q}_{w/f} \nabla T \quad (1)$$

Where ∇ T is substituted by the heat flux term following Fourier's law:

$$\vec{q}^T = -\lambda . \nabla T \quad (2)$$

then the divergence of advection becomes:

$$div(\vec{j}_{adv}) = \frac{-\rho_{w/f} c_{w/f} \vec{q}_{w/f} \vec{q}^T}{\lambda} \quad (3)$$

where λ is either the thermal conductivity of the soil or of the structure in case heat exchanger tubes are modelled along the structural elements.

4- The instantaneous conductive and advective fluxes (powers) could be calculated now:

$$\vec{P}_c = \vec{q}^T \quad (4)$$

$$\vec{P}_v = \rho_{w/f} c_{w/f} \vec{q}_{w/f} T \quad (5)$$

where T is the zone (soil or structure) temperature at a given instant.

5- Since no heat source is considered then the divergence of the conductive term is:

$$div(\vec{j}_{cond}) = -\left[div(\vec{j}_{adv}) + c^T \frac{\partial T}{\partial t} \right] \quad (6)$$

It is important to note that no heat exchanger pipes are modeled in the energy geo-structure and it is impermeable, therefore, the divergence of the advective term for the structure is zero. Following, the conductive term depends only on the effective specific heat of concrete and the variation of temperature in the structure.

In fact, for both the structure and the soil, the total divergence could be expressed only in terms of effective specific heat and temperature variation as presented in the following formulae.

For the structure: $div(\vec{j}_{cond}) = -\left[c_w{}^T \frac{\partial T}{\partial t} \right]$ (7)

For the soil: $div(\vec{j}_{cond}) + div(\vec{j}_{adv}) = -\left[c_s^T \frac{\partial T}{\partial t} \right]$ (8)

The flux-divergence theorem also known as Ostrogradsky theorem states that the sum of all sources gives the net flux out of a region (Figure 2.4). The exchanged advective or conductive flux is equal to the total heat exchange in the considered volume Ω according to the following formula:

$$\iiint_{\Omega} div(\vec{j}).d\Omega = \oiint_{\partial\Omega} \vec{j}.d\vec{S} \quad (9)$$

As presented in the following figure, the net rate of change of the divergence of the flow rate divF (diffusive or advective) in a volume Ω equals the flux F (of the flow rate) flowing through surface dΩ.

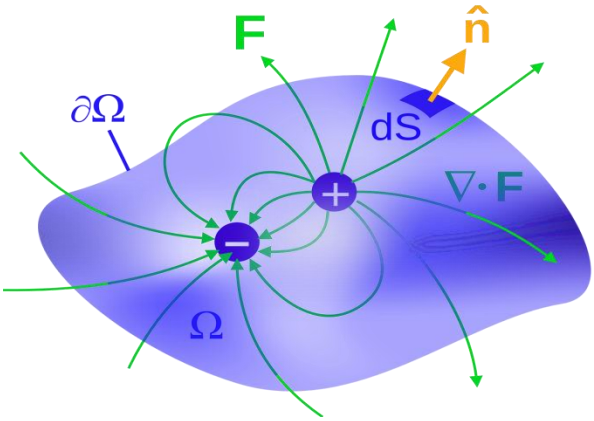

Figure 2.4 Illustration of the divergence theorem (https://fr.wikipedia.org/wiki/Flux_électrique).

The above two formulae 7 and 8 give us the volumetric power exchanged in each soil or structure zone, thus the total volumetric power exchanged by the soil or the structure, and based on Equation 9, it becomes:

$$P = \sum_{zone} \int_{\Omega} \left(-c^T \frac{\partial T}{\partial t} \right) d\Omega \tag{10}$$

where Ω is either the volume of the soil or the structure zone.

The above formula is used to compute the instantaneous power exchanged by the structure and the soil, thus defining the energy term could be useful also. Energy produced during each season for the structure and the soil will be calculated as follows:

$$E = \sum_{zone} \int_{\Omega} \left(\int_{0}^{t} c \frac{\partial T}{\partial t} dt \right) d\Omega \tag{11}$$

where t stands for the duration of a season (90 days).

CHAPTER 3 :

Assessment of the exchanged energy between geothermal structures and soil

3.1 Introduction

This chapter presents numerical applications on approaches 1 and 2 presented in details in Chapter 2 as these approaches allow the evaluation of the heat exchanged between geothermal structures and the surrounding soils. Energy diaphragm walls are modeled in two-dimensional models through approaches 1 and 2, allowing the comparison between both approaches. Then, approach 2 is adapted to conduct three dimensional models for energy diaphragm walls and energy piles. The aim of the obtained results is to give insights about the possible heat exchange between energy geo-structures and the surrounding media, and how do they contribute in delivering the buildings thermal needs. Moreover, our objective is to highlight on the importance of the ability to distinguish between conductive and advective exchanged heat, and to show how the thermal and hydraulic parameters could affect the heat transfer processes.

3.2 Materials' properties

Energy diaphragm walls and energy piles embedded in sandy soils are studied in this chapter. The modelled materials are concrete and sandy soil for the geothermal structures and the surrounding media respectively. The values of the thermal and hydraulic parameters of both materials are listed in Table 3.1, where the values of hydraulic conductivity falls in the range of values given by Chiasson et al. 2000 for sandy soil.

Table 3.1 Hydraulic and thermal parameters of soil and concrete.

	Soil	Concrete
Hydraulic conductivity (m/s)	variable	-
Porosity	0.4	0.15
Specific heat capacity (J/kg/K)	1000	880
Thermal conductivity (W/m.K)	2	1.8

3.3 Two-dimensional energy diaphragm walls

Approaches 1 and 2 are used to model energy diaphragm walls. The aim of this section is the assessment of the possible exchanged heat and thus the comparison between both approaches. Moreover, several parametric analyses are conducted regarding the impact of groundwater flow, active length of the diaphragm wall, cyclic thermal loading, and type of the imposed thermal solicitation.

3.3.1 **Model geometry and boundary conditions**

The numerical modeling of energy diaphragm walls used as structural bearing elements in metro stations is conducted using the finite difference software FLAC3D (ITASCA 2005, ITASCA 2012). The soil volume is modeled in three dimensions over one meter thickness and presents a vertical length of 50 m and a width of 60 m. These values are chosen on the base of a preliminary parametric study in a way to be able to assess the effect of the groundwater flow on the temperature profile near the wall. The dimensions of the diaphragm wall and the raft

foundation constituting the modeled metro station are inspired from the project "Grand Paris" (Fig. 3.1). Each diaphragm wall has 32.5 m length and 1.2 m thickness. The embedded parts are of 10.5 m length, and the raft foundation is of 21 m length and of 1.5 m thickness.

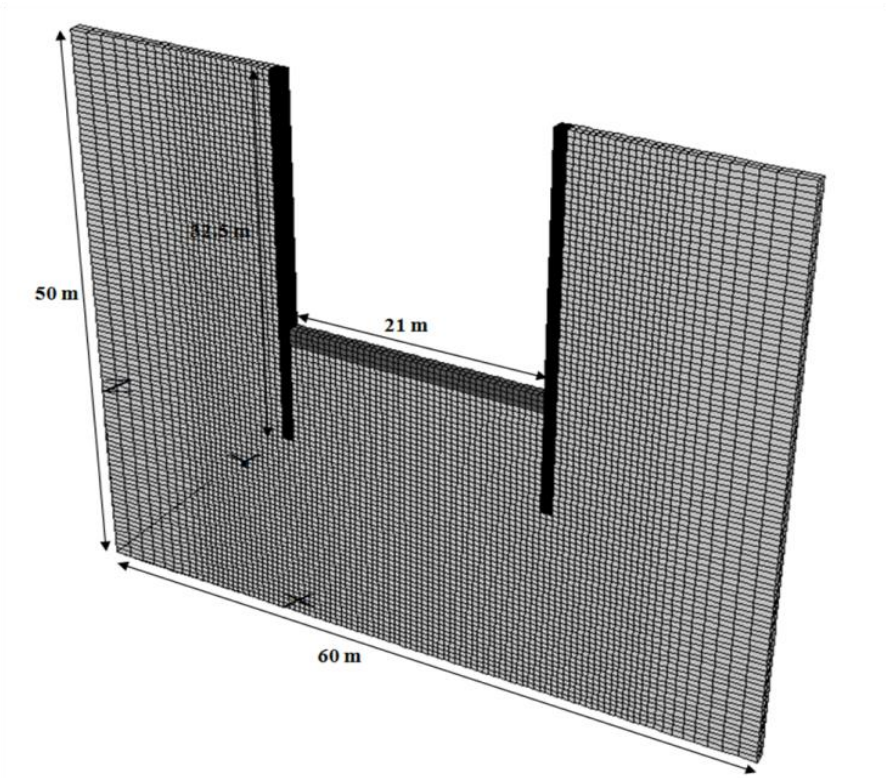

Figure 3.1 Geometry of the 2D model representing energy diaphragm walls constituting a metro station.

Concerning the thermal boundary conditions, adiabatic boundary conditions are imposed at the lateral boundaries, and at the metro diaphragm walls in contact with air at the interior side of the station. Imposing adiabatic boundaries at the contact with the external air inside the station may not represent real case conditions but it is considered as a conservative assumption. At the top, the surface is subjected to external air temperature following this equation:

$$T(z,t) = T_{ave} + A_0 e^{-\frac{z}{d}}\left(\sin\left(wt - \frac{z}{d}\right)\right) \tag{3.1}$$

where T_{ave} and A_0 are the average soil temperature and the annual amplitude of soil temperature, respectively, w is the annual radial frequency, and d is the damping depth ($d=(2D_T/w)^{1/2}$) and D_T is the thermal diffusivity of the soil.

At the bottom, a terrestrial surface flux 0.0544 W/m^2 is imposed, while the initial ground and wall temperature is set to 14 °C. All these thermal conditions are chosen to reproduce the variation of initial ground temperature for different seasons. Moreover, the raft foundation is assumed to be thermally null; it doesn't contribute in the thermal exchange phenomena, and the temperature of the energy diaphragm walls is uniformly fixed according to average values usually noted in these structures (Suryatriyastuti, 2013), Table 3.2.The assumption of imposing a uniform constant temperature in the geothermal structures and neglecting the presence of heat exchanger tubes seems to be sufficient and acceptable to study the thermal transfer with the ground because the difference between the inlet and outlet temperature is usually less than 4°C (Katsura et al. 2009, Ozudogru et al. 2012, Gashti et al. 2015, Di Donna & Barla 2016, Habert et al. 2016, Cui & Zhu 2016).

Table 3.2 Temperature imposed in the diaphragm walls (Suryatriyastuti, 2013).

Season	Imposed temperature (°C)
Summer	25
Autumn	9
Winter	5
Spring	21

Regarding the hydraulic boundary conditions, the top and the base of the model and the walls are considered impermeable, whereas hydraulic head is imposed at the left and right boundaries of the model to generate groundwater flow. The soil is considered homogeneous with a hydraulic conductivity value k_h that varies according to the considered case. Six cases are considered to take into account three types of boundary conditions and two values of hydraulic conductivity coefficient. For each case, the average Darcy velocities and the Péclet number are presented in Table 3.3.

Table 3.3 Hydraulic boundary conditions and flow velocity.

	Hydraulic head (m)		Average flow velocity (m/s)		Péclet number P_e	
	Left side (x=0 m)	Right side (x=60 m)	k_h=10^{-5} m/s	k_h=10^{-6} m/s	k_h=10^{-5} m/s	k_h=10^{-6} m/s
Case 1	50	30	3.34×10^{-6}	3.34×10^{-7}	7	0.7
Case 2	50	35	2.50×10^{-6}	2.50×10^{-7}	5.2	0.52
Case 3	50	45	8.34×10^{-7}	8.34×10^{-8}	1.75	0.18

3.3.2 **Approach 1**

This approach provides a simple, rapid, and practical tool for the evaluation of the exchanged conductive and advective heat. It is worth noting that in this approach, all the results are based on assuming that the water and heat flow are one dimensional along *x*-direction.

Influence of groundwater flow on the temperature profile

The simulations presented in this section are carried for one winter season; the temperature imposed into the energy diaphragm walls is 5℃. The influence of groundwater flow on the temperature profile at the end of the loading season is presented in Figure 3.2, which shows that the effect of advection becomes significant as the intensity of groundwater flow increases.

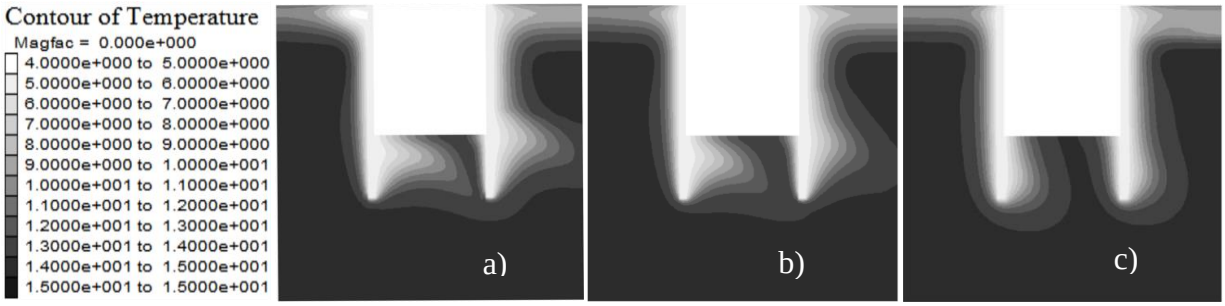

Figure 3.2 Temperature profile around the diaphragm walls-k_h=10^{-5} m/s - a) case 1 b) case 2 c) case 3.

Temporal and spatial variation of the allowable exchanged power

Figure 3.3 presents the variation of the allowable thermal power along the *x*-direction for case 1 (k_h=10^{-5} m/s) for the right and the left walls, along the downstream side. For each wall, along the downstream side, different horizontal levels which have the most significant ground temperature

variations are chosen; indicating that these levels are the ones which are mostly affected by the thermally activating the walls and thus by the heat exchange processes. At each level, the exchanged power is calculated and then the average of these levels is used to represent the allowable power exchanged by each wall. The allowable power shows high values at the beginning and then it decreases rapidly till a certain distance after which there is no thermal exchange since the temperature difference between adjacent soil zones will be null. Even though the left wall shows larger affected soil zones, however, the right wall imposes greater total thermal exchange due to the groundwater flow direction towards the downstream side.

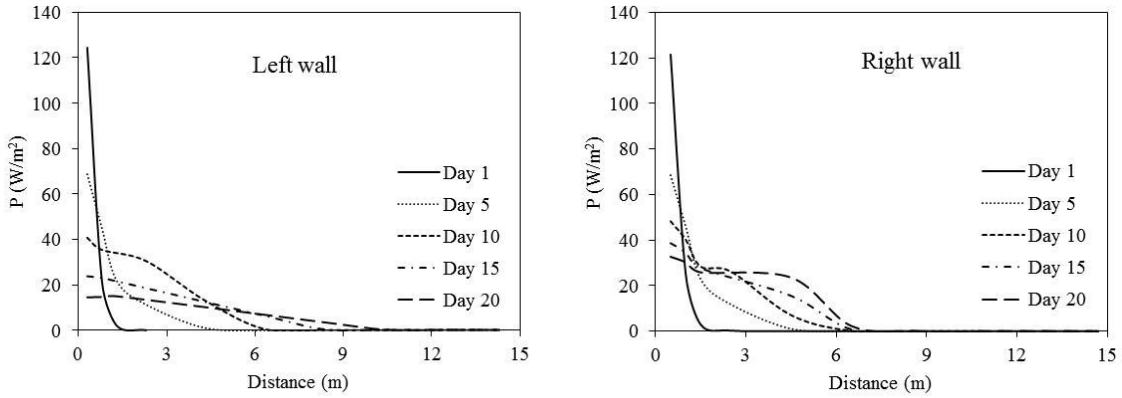

Figure 3.3Variation of the allowable thermal exchanged power along *x*-direction for the right and left walls (Case 1, $k_h=10^{-5}$ m/s).

Figure 3.4 presents the variation of the total allowable thermal power exchanged by conduction P_c and by advection P_v for the zones around the diaphragm walls that are being affected by the thermal exchange occurring during the cooling season. As time increases, the power exchanged by advection decreases, and thus the efficiency of the system. On the other hand, the conductive power can be considered of a constant trend with slight decrease during the whole thermal phase.

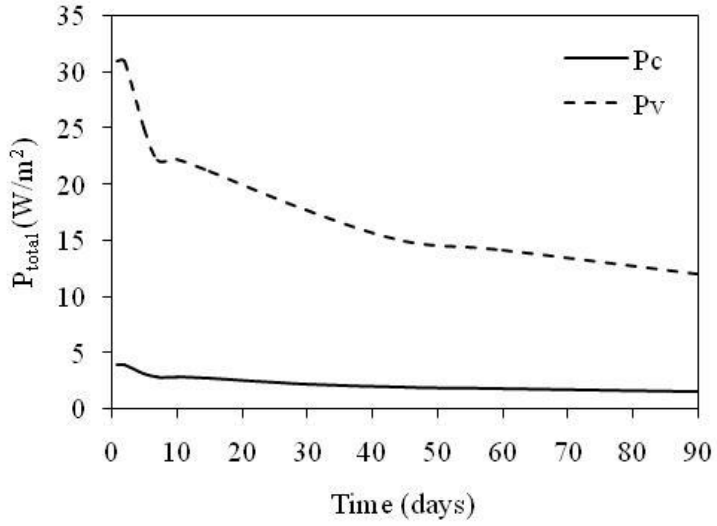

Figure 3.4 Variation of the total allowable thermal exchanged power during winter season (case 1, k_h=10^{-5} m/s).

Impact of groundwater flow on the exchanged thermal power

Figure 3.5 represents the variation of the total allowable thermal power P_{total} with Péclet number in logarithmic scale. P_{total} increases with P_e, in the considered cases, the total power doesn't exceed 15 W/m^2 despite of the high values of Péclet number reached. Knowing that it is recommended for an energy diaphragm wall to deliver a minimum of 35 W/m^2 (Brandl, 2006), then for the considered cases, external heat sources should be used if the power demand of the buildings surpasses that delivered by the energy diaphragm walls.

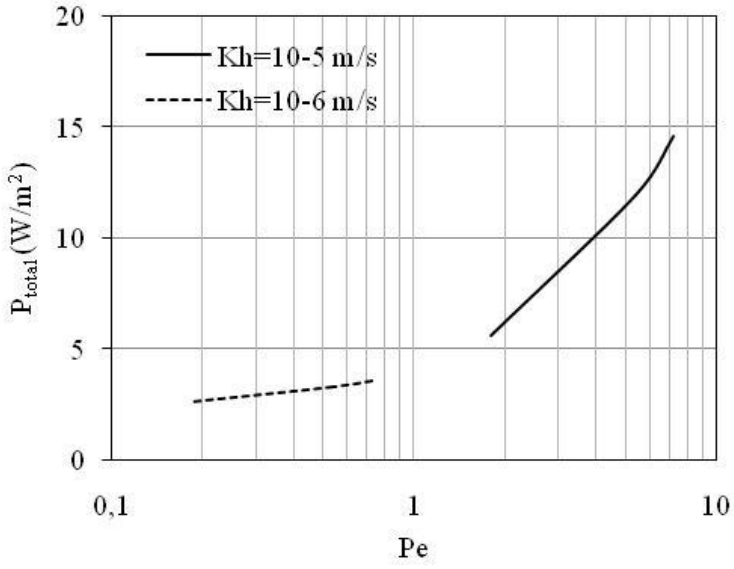

Figure 3.5 Variation of P_{total} with Péclet number.

The variation of the total allowable thermal power exchanged by conduction P_c and by advection P_v is presented in Figure 3.6. It can be noted that the thermal power exchanged by conduction is approximately constant and tends to decrease slightly as P_e increases, also the effect of conduction becomes more important as P_e decreases (for low hydraulic conductivity, k_h=10^{-6} m/s). On the other hand, the power exchanged by advection P_v increases linearly with P_e.

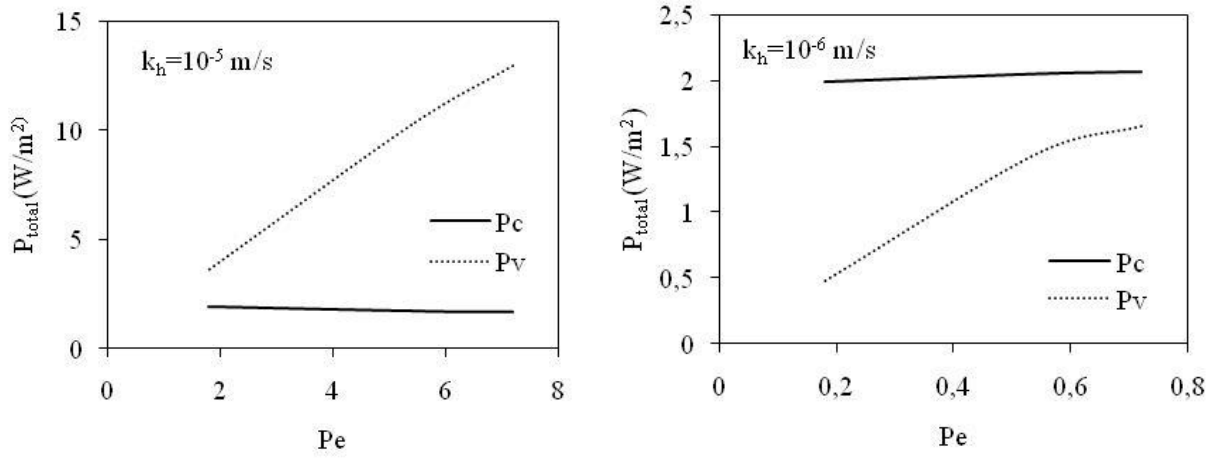

Figure 3.6 Influence of groundwater flow on the exchanged powers P_c and P_v.

Impact of cyclic thermal loading on the allowable exchanged thermal power

Cyclic temperature variations are imposed into the diaphragm walls, where the walls temperature during cooling and heating phases is set to 5℃ and 25℃ respectively (Figure 3.7).

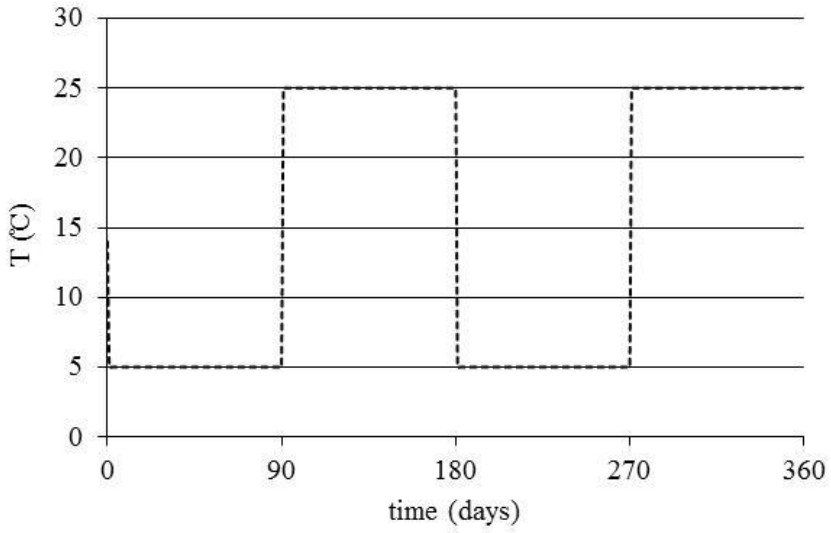

Figure 3.7 Temperature variations imposed into the diaphragm wall.

The temperature variation near an energy diaphragm wall affected by these cooling-heating cycles is presented in Figure 3.8. In this figure, the temperature variation is measured at the middle depth of the wall, from the edge of the right wall and for three cooling-heating cycles, where each cycle consists of a cooling phase followed by a heating phase (hi and ci are the heating and cooling phases of cycle i respectively where i varies from 1 to 3), and the duration of each phase is 3 months. It is worth noting that the groundwater flow conditions considered here are those of case 1.

Along the horizontal distance, as the distance from the edge of the wall increases, the temperature increases during the cooling phase and decreases during the heating phase till reaching a constant value for both phases equal to the initial ground temperature at a distance approximately 6 m away from the edge of the wall.

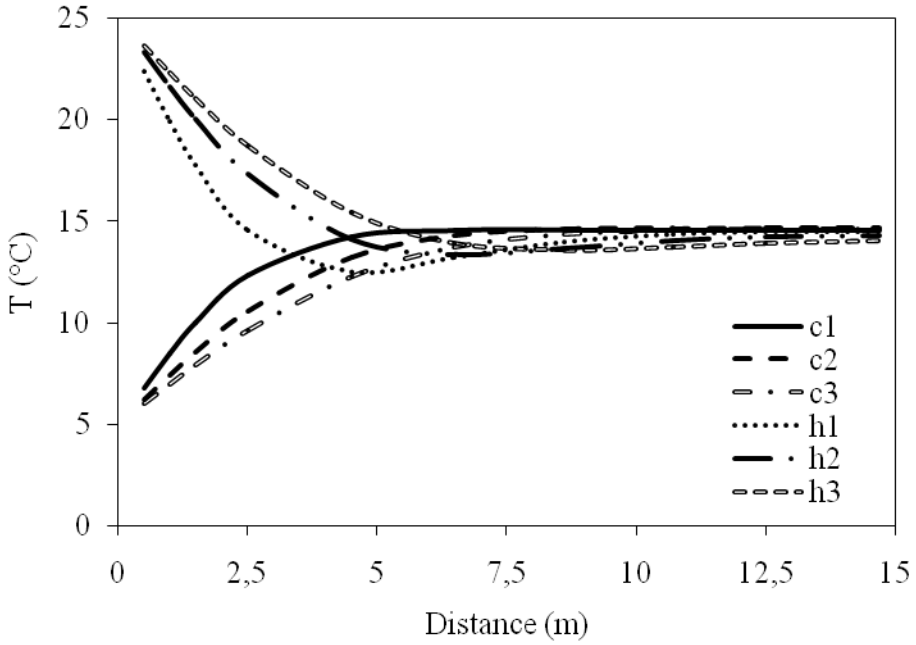

Figure 3.8 Variation of temperature during the loading cycles.

Concerning the allowable power exchange during the thermal cycles, for the first loading cycle, the power exchanged between the soil and the wall varies with time during each phase. Figure 3.9 presents the variation of the exchanged power for the three cooling-heating cycles in the zones near the structure which are being affected by the heat exchange process. Starting with the cooling phase, the exchanged power is approximately constant for small groundwater flow velocities, and for all cases it decreases at the end of this phase; the decrease is more remarkable for higher groundwater flow velocities. This can be interpreted by the fact that the temperature in the soil surrounding the wall starts to decrease during this phase due to continuous heat extraction from the soil.

Then for the following heating phase, negative values indicate that heat is being injected into the soil, thus increasing the soil temperature near the wall. The allowable exchanged power decreases during the heating phase. This slight decrease of the exchanged power during the heating or cooling phase is obvious for important water flow conditions, whereas for small groundwater flow, the variation has approximately a constant profile for each phase.

The exchanged power is slightly greater during the heating phase compared to that during the cooling one, this is due to the fact that at the beginning of the heating phase, the ground temperature is the lowest and thus the difference in temperature between the soil and the wall is the greatest, leading to the higher exchanged power. Then the soil temperature rises up causing a decrease in the heat exchange.

During the second thermal loading cycle, the heat transferred between the soil and the diaphragm wall decreases slightly in both phases, since the heat stored during the heating phase in the soil surrounding the diaphragm wall disseminates to points far away from the walls by the groundwater flow.

During the third cooling-heating cycle, the exchanged power during the two phases shows a slight increase compared to the second cycle, this is related to the heat that is transferred to the soil and that leads to enhance the heat absorption phenomenon at the beginning of the third cooling phase.

According to the obtained results and during the three considered cycles, the power exchange is greater in the heating phases than in the cooling phases. This may be related to the thermal properties of the soil that seems to exhibit a higher potential to gain heat during the heating phase than to lose heat during the cooling phase.

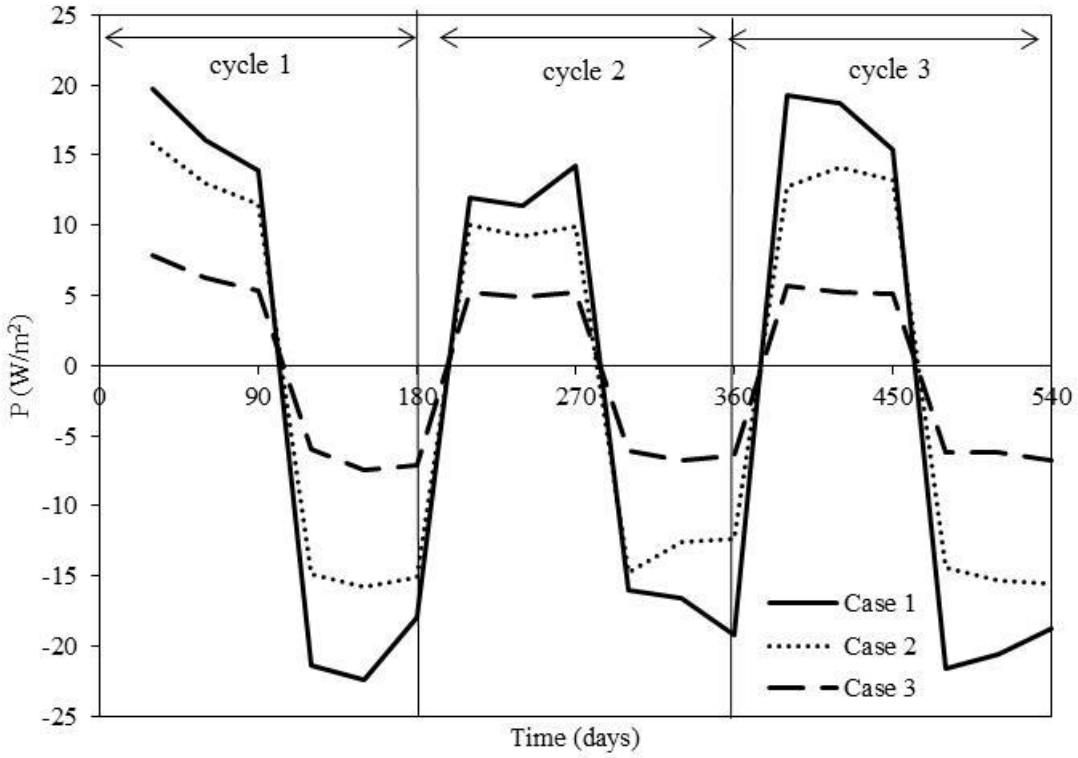

Figure 3.9 Variation of the exchanged power under cyclic loading (k_h=10^{-5} m/s).

Impact of the active length of the diaphragm wall

The effect of the total active length of the diaphragm wall is analyzed through the comparison of two different possible configurations: configuration W1 where the wall is totally equipped and configuration W2 (Figure 3.10) where the wall is partially equipped along its embedment depth with heat exchanger elements.

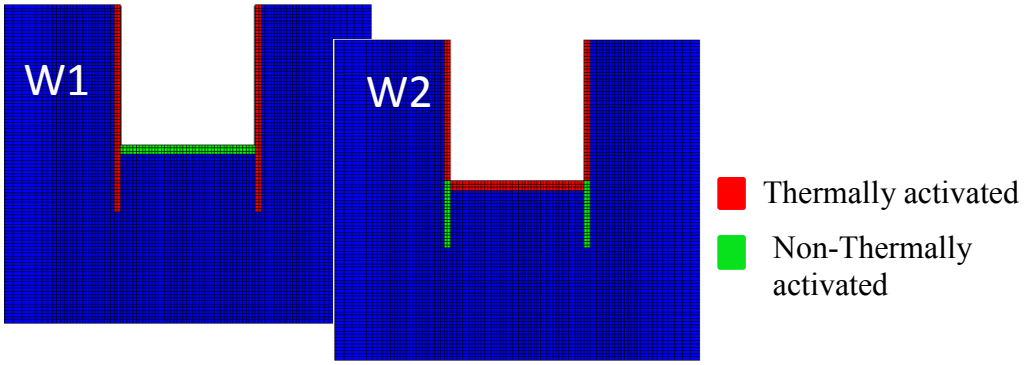

Figure 3.10 The modelled diaphragm wall with the two considered configurations.

Figure 3.11 shows the difference in the exchanged power between these two configurations. The equipment of the whole wall with heat exchanger tubes induces an enhancement in the allowable exchanged power which appears to be more important for high groundwater flow. For a groundwater flow velocity of 3.34×10^{-6} m/s, the exchanged power increases by about 25 %, and this increase only reaches 15 % for lower water flow velocities of the order 8.34×10^{-7} m/s.

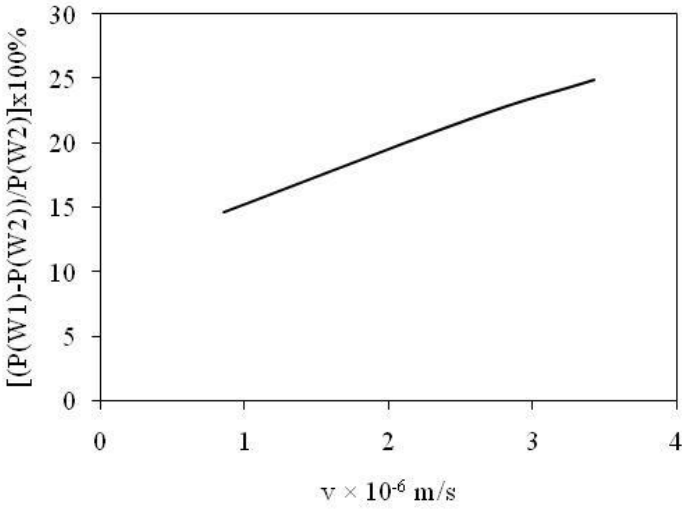

Figure 3.11 Ratio of the total thermal power between the configurations W1 and W2 (k_h=10^{-5} m/s).

3.3.3 **Approach 2**

A generalized approach capable of evaluating the exchanged heat for each soil and structural zone is presented in this section. This approach allows performing detailed and local calculations through its ability to calculate the conductive and advective divergences for each zone in the domain as explained in Chapter 2.

For this approach, FLAC3D (ITASCA, 2012) is used since this version of FLAC contains in its FISH library some gridpoint and zone variables that are needed in the calculation, knowing that those variables facilitate the calculation sequence and reduce the time needed for performing the analysis. In this approach, water and heat flow in the three directions are taken into account to perform the calculation of the allowable transmitted power between the geothermal structures and the surrounding soil.

The same cases (Cases 1, 2, and 3 with $k_h=10^{-5}$ m/s) considered in the first approach for the two dimensional energy diaphragm walls are modelled here in order to allow the comparison between both approaches.

Distribution of the divergence in the soil

The conducted model allows plotting the conductive and advective divergences. Generally, negative values of the divergence reveal that the corresponding zones act as heat sinks while positive values correspond to heat sources.

First, a reference case with pure conduction is presented to understand how the conductive divergence varies in the soil zones affected by the thermal load imposed into the diaphragm walls. Figure 3.12 shows the distribution of the total divergence; during winter (cooling phase), the soil acts as a heat source and then the divergence is positive and the opposite occurs during summer season (heating phase).

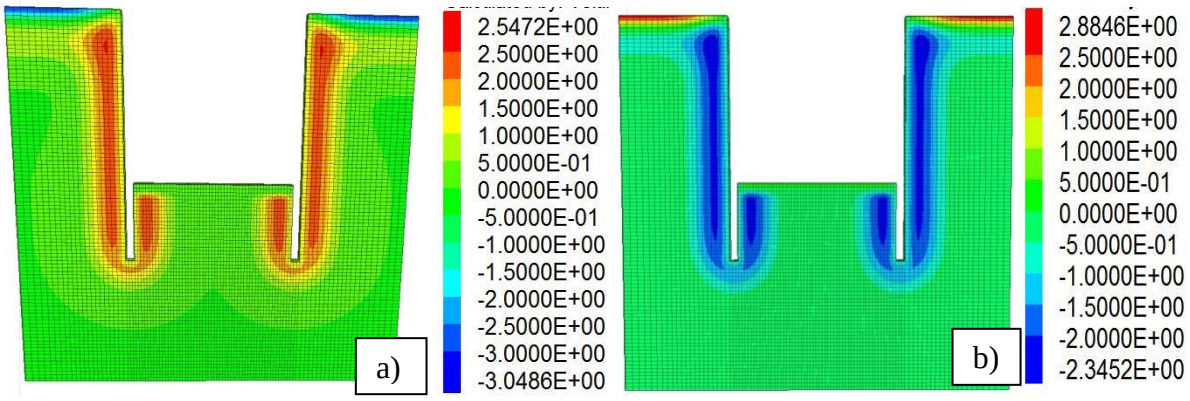

Figure 3.12 Distribution of the total divergence in the domain in the case of pure conduction a) Winter b) Summer.

Once groundwater flow exists, then the advective divergence plays an important role. Figure 3.13 presents the advective, conductive, and total divergences at the end of winter season. The conductive and advective divergences fall approximately in the same range of values but are of opposite senses. At the bottom of the wall, higher values are found where the groundwater flow hits the impermeable concrete obstacle and leads to higher heat exchanges there. In fact, the

analysis of the distribution of advective and conductive divergences becomes more difficult when the groundwater flow is present since and according to its intensity, this water flow will carry with it towards the downstream side the temperature being accumulated around the walls. Therefore, the surrounding soil will always act as heat source in winter (Figure 3.13c) and heat sink in summer.

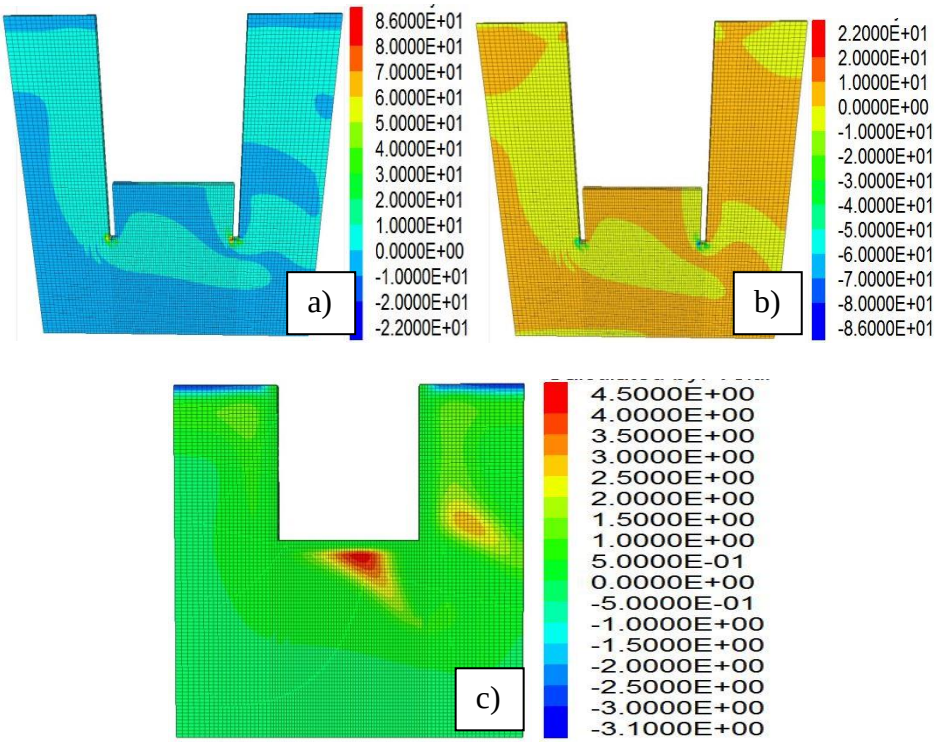

Figure 3.13 Evolution of the a) advective, b) conductive, and c) total divergences in the soil zones at the end of the winter season (cooling period).

Evolution of the total exchanged power during the winter season

Figure 3.14a represents the variation of the total exchanged power during one cooling phase for all soil zones. During the first days of the cooling phase, the exchanged power records high values due to the high difference in temperature between the diaphragm wall and the surrounding soil and then it rapidly decreases. Higher exchanged power is found for cases with higher groundwater flow velocities. Generally, the advective power contributes minorly in the total exchanged power due the small groundwater flow velocity as presented in Figure 3.14b.

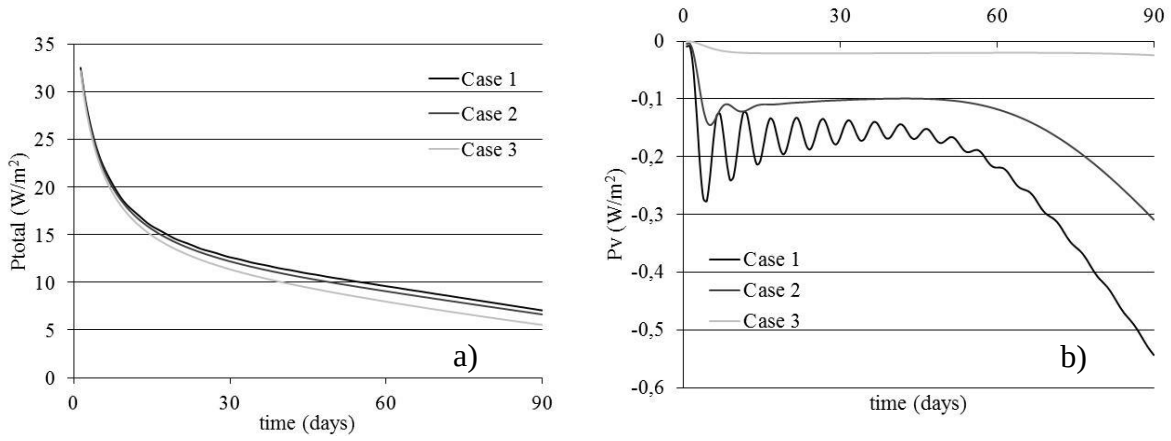

Figure 3.14 Total power a) and advective power b) exchanged by the whole domain during the winter season for the three considered cases with $k_h=10^{-5}$ m/s.

As obtained by approach 1, the conductive and advective powers tend to increase with Péclet number as shown in Figure 3.15.

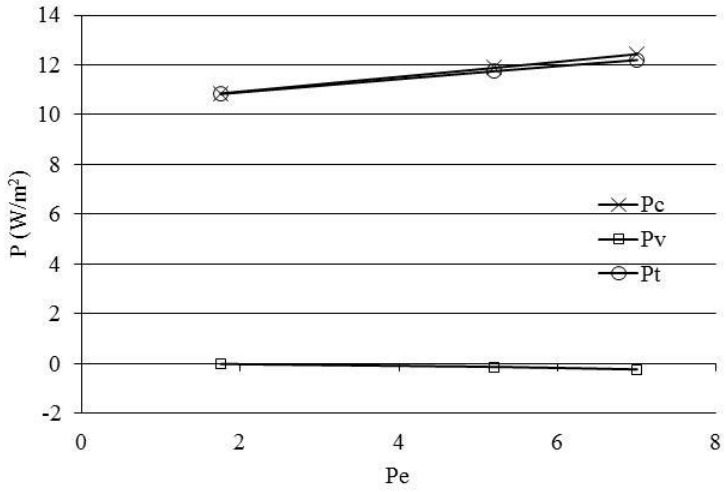

Figure 3.15 Evolution of the total, conductive, and advective powers of the whole domain with Péclet number.

Figure 3.16 shows the power exchanged by the soil zones that are in direct contact with the diaphragm walls. The zones that are in direct contact with the walls are the first mesh zones that surround the diaphragm walls. Compared to Figure 3.14a, it is clear that the zones surrounding the diaphragm walls contribute in about 42% of the total power exchanged by the whole domain. This means that as we go far from the walls, the exchanged power decreases due to the stabilization of the soil temperature in those zones. Figure 3.16 shows that as the groundwater

flow velocity increases, then the time needed to reach steady state decreases. After approximately 35 days of thermally activating the diaphragm walls, the total exchanged power reaches zero, meaning that the system no more transfers heat between the soil and the concrete elements; steady state is attained.

Figures 3.15 and 3.16 show that total average power exchanged by the whole domain including all the soil zones during a thermal phase is equal to the maximum power exchanged by the zones that are in direct contact with the energy walls. Thus analyzing the zones that surround the thermo-active walls gives an idea and can be sufficient for evaluating the total heat exchanged by the system.

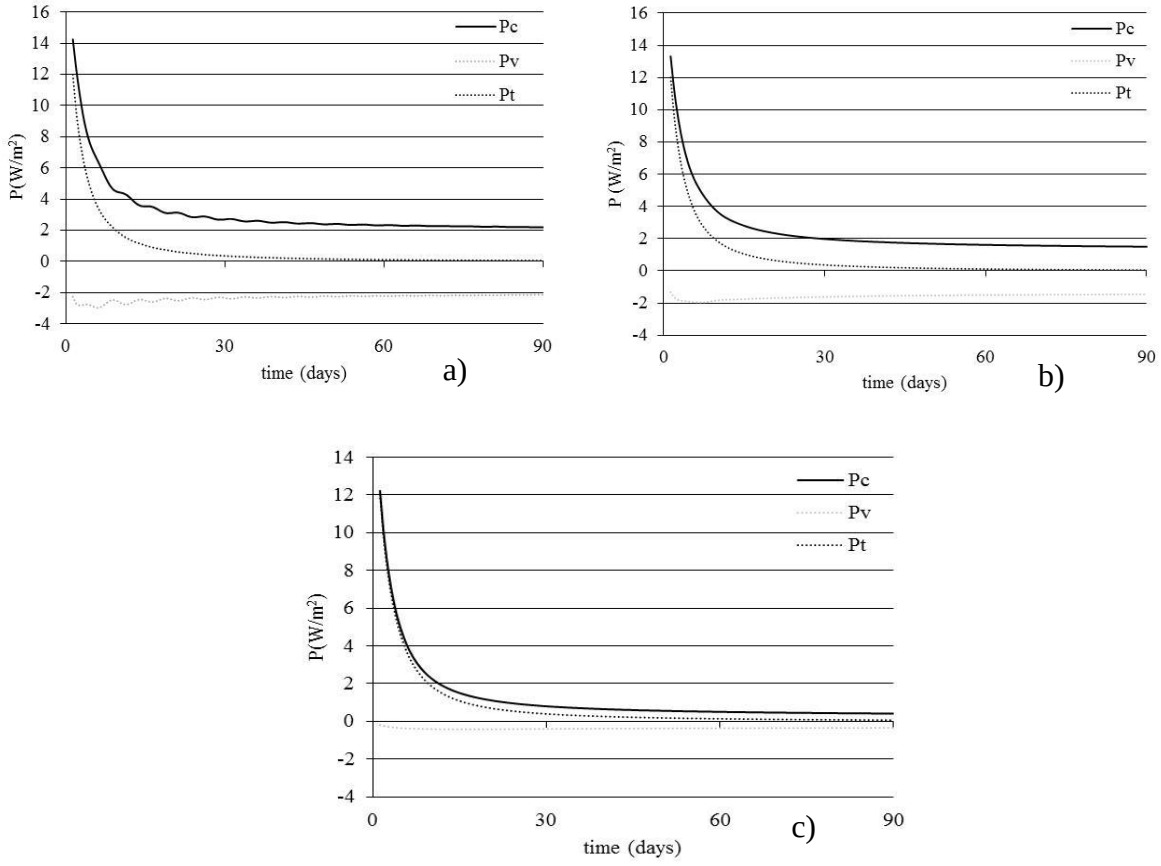

Figure 3.16 Variation of the power exchanged by the soil surrounding the walls for a) case 1 b) case 2 c) case 3.

Cyclic variation of the total exchanged power

Three consecutive cycles are considered in this section where each cycle consists of a cooling phase followed by a heating phase and the duration of each season is six months. Then each cycle consisting of two phases will represent one year of thermal loading.

As expected, the exchanged power decreases with time during each thermal loading phase (Figure 3.17). The total power exchanged by the soil zones that are in direct contact with the energy diaphragm walls (Figure 3.17b) has a similar trend and is approximately equal to that exchanged by the walls using approach 1 (Figure 3.9). Both approaches present logical results in comparison to the work carried by other researchers on energy diaphragm walls (Di Donna 2016, Cornelio et al. 2016, Bourne-Webb et al. 2016b).

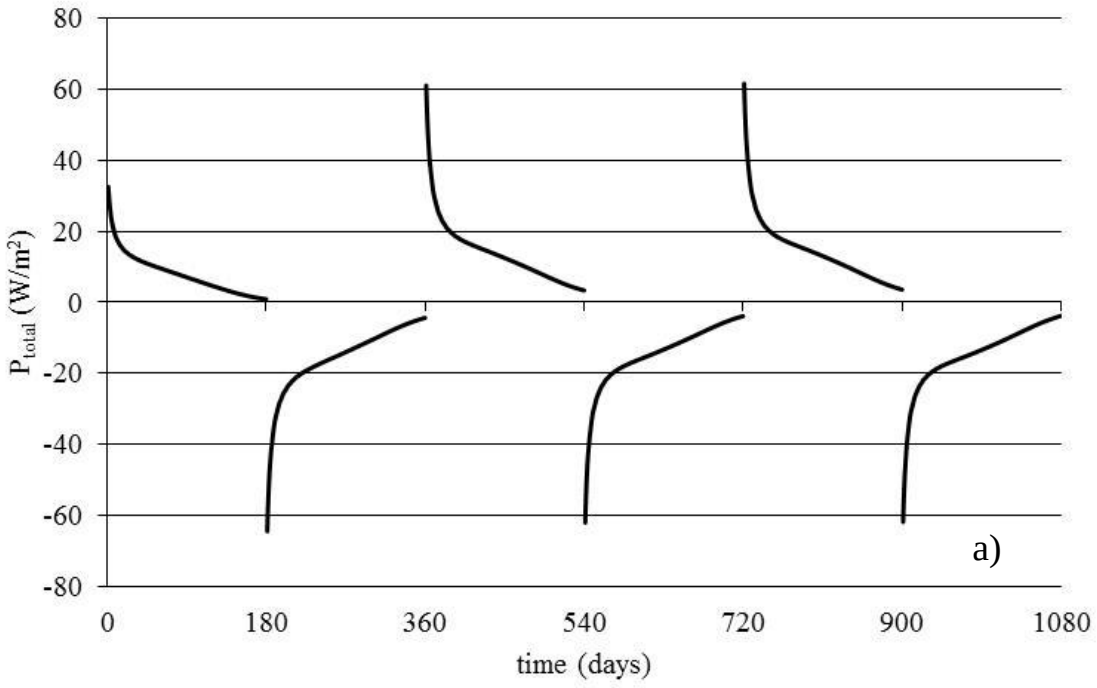

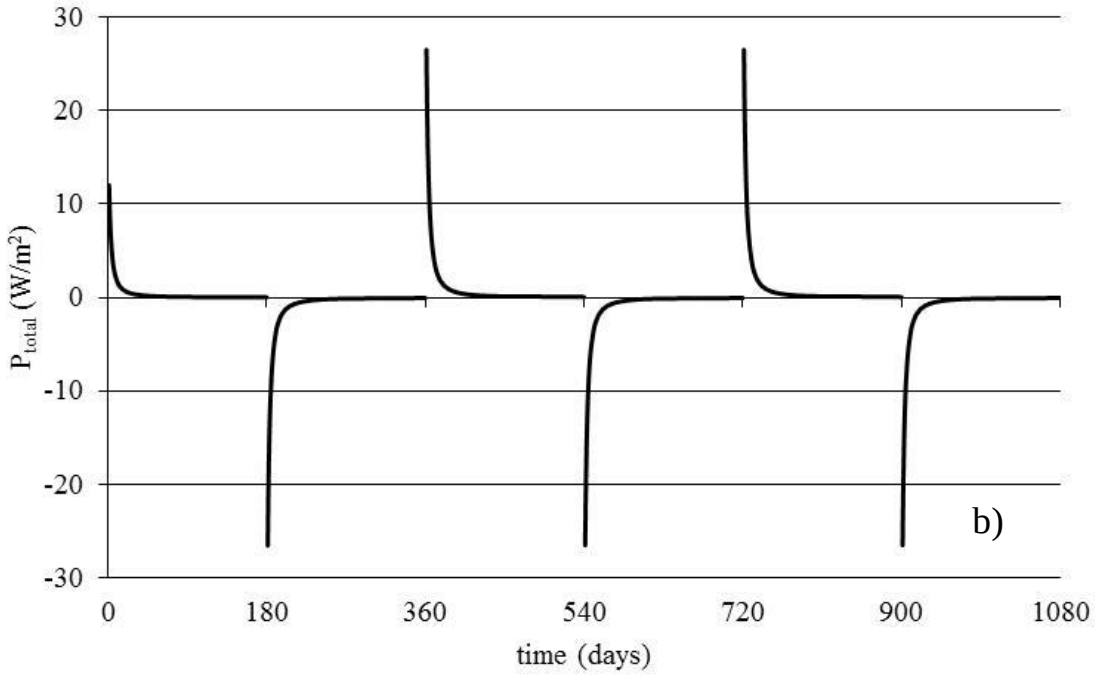

Figure 3.17 Total exchanged power a) for the whole domain b) for the zones surrounding the energy walls.

Figure 3.17b represents the variation of the total exchanged power for the zones that are in direct contact with the energy diaphragm walls. The power transmitted by these zones is about 41% of that of the whole domain. Adding to this, during each thermal loading phase, the total power attains zero, meaning that the thermal exchange is no longer taking place between the soil and the thermo-active parts. Moreover, the steady state is reached rapidly where no temperature changes with time are noted for these zones.

The total power constitutes of two terms, the conductive and advective exchanged powers that are plotted separately in Figure 3.18 in order to know the contribution of each term in the total exchanged power. Figures 3.18a and 3.18b present the variation of the powers for the whole domain and for the soil zones that are in contact with the diaphragm walls respectively. The diffusive process leads the heat exchange phenomenon; this is clear from the conductive power that has the same trend of variation as that of the total power and contributes almost by 98% in the whole heat exchange process.

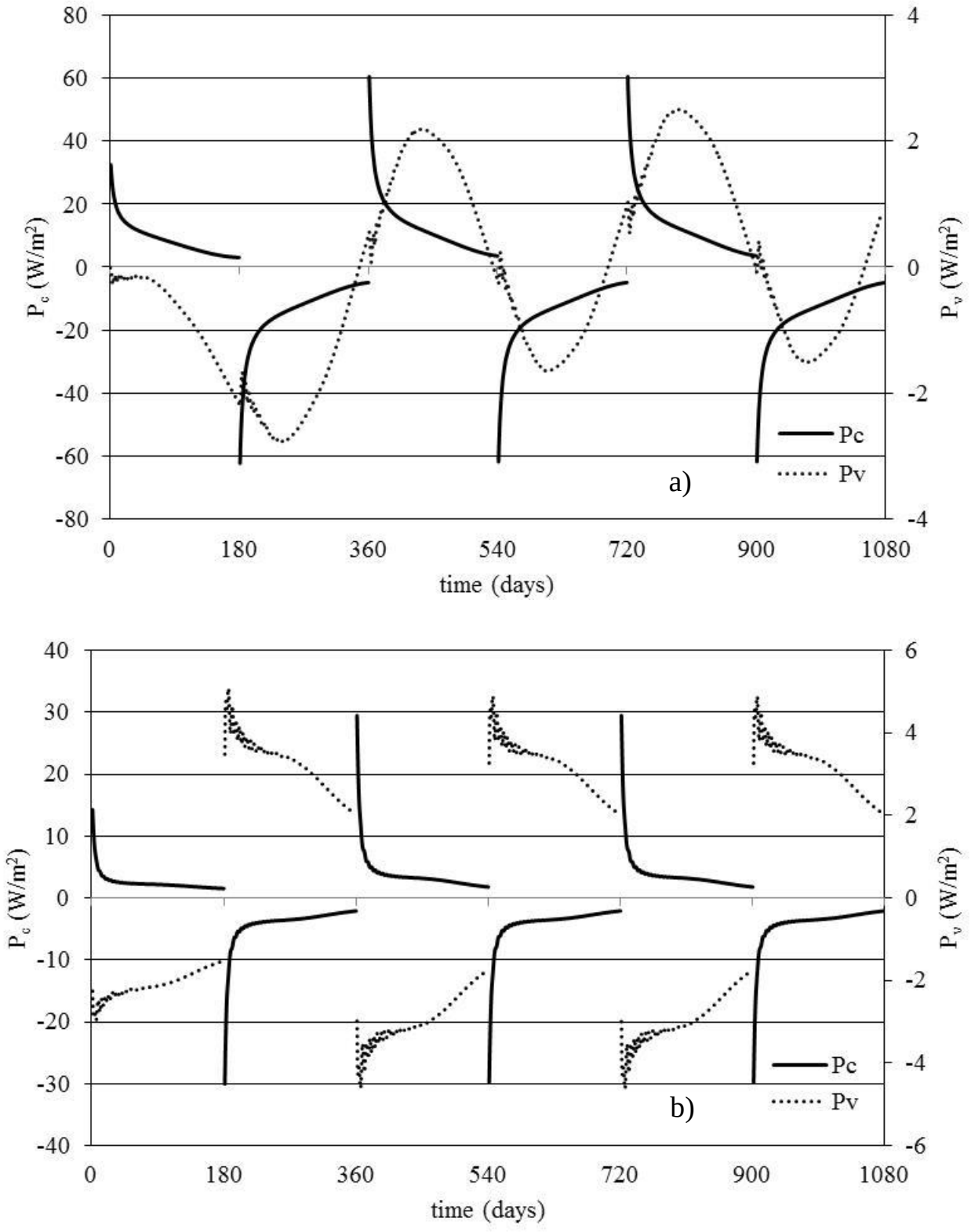

Figure 3.18 Exchanged conductive and advective powers, bold lines for conduction, and dotted lines for advection, a) for the whole domain b) for the zones surrounding the diaphragm walls.

Then the energy that could be delivered by the system is calculated according to Equation 11 presented in the Appendix of chapter two, and it is plotted in Figure 3.19. The maximum energy that could be delivered by the system reaches 6000 kWh, this value is relatively good for such systems knowing that the groundwater flow velocity is small and only one panel of 1 m length is considered.

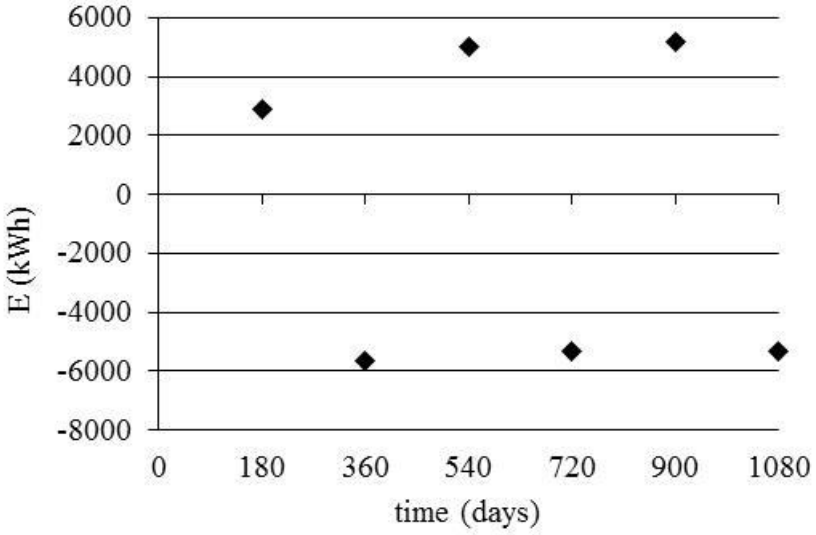

Figure 3.19 Energy supplied by the system during the three thermal cycles.

3.3.4 **Comparison between approach 1 and 2**

Slight differences are found between the two approaches especially at the level of the exchanged advective power, this may be related to several reasons:

- In the first approach, water and heat flows are considered as unidimensional along the *x*-direction only, whereas in the second approach they are considered in the three directions.
- Water flow velocity used in the calculation of the advective power in the first approach was the average Darcy velocity in the whole domain. On the other hand, in the second approach, water flow velocity of each soil zone is considered and this value may or may not be equal to the average Darcy velocity value.

- In the first approach, only zones close to the walls and being affected by the heat exchange phenomena are considered. However, in the second approach the power exchanged by the whole domain and the power exchanged by the surrounding zones are considered.

3.3.5 **Influence of the applied thermal load**

This section is devoted to examine the effect of the imposed thermal solicitation type on the total heat exchange capacity between energy diaphragm walls and the surrounding soil; it is treated through using approach 2. For this, a continuous sinusoidal temperature is imposed uniformly into the walls following this equation:

$$T_{wall} = T_{ave} + \Delta T_y.\sin(2\pi t/t_y) + \Delta T_d.\sin(2\pi t/t_d) + \Delta T_h.\sin(2\pi t/t_h) \quad (3.2)$$

where T_{ave} is the average soil temperature equals to 14°C, ΔT_y is the yearly temperature variation equals to 12°C, ΔT_d is the daily temperature variation 3°C, ΔT_h is the hourly temperature variation 2°C. t_y, t_d, and t_h are the duration of one year, one day, and one hour respectively, and t stands for time. Figure 3.21 represents the yearly fluctuations of the sinusoidal imposed temperature.

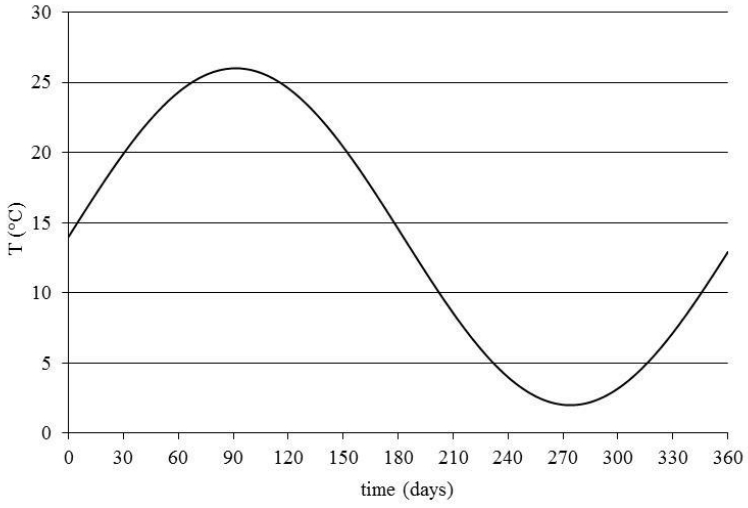

Figure 3.20 Variation of the sinusoidal temperature imposed into the wall.

This type of thermal solicitation is chosen based on the fact that in real case conditions, the temperature variation into geothermal structures is almost smooth and normally it should follow the external air temperature variation.

Figure 3.22 represents the variation of the thermally exchanged power caused by the sinusoidal temperature variation for one year of thermal loading in all soil zones. The maximum exchanged power does not exceed 20 W/m^2 which is less than that exchanged due to imposed constant wall temperature (previous section). In fact, when a constant temperature is imposed into the walls, a brutal drop in the exchanged power is observed just after the beginning of a thermal phase. Thus, as a global view, the exchanged power appears to be greater but this is valid only for the first few days; after that the exchanged power decreases rapidly and the range of values becomes the same as that obtained in the current case. Generally, the variation trend of the exchanged power is similar to that of the imposed temperature. It is worth noting that at the middle of spring and autumn, there is no need for external heating and cooling and this is illustrated by the null exchanged power (Figure 3.22).

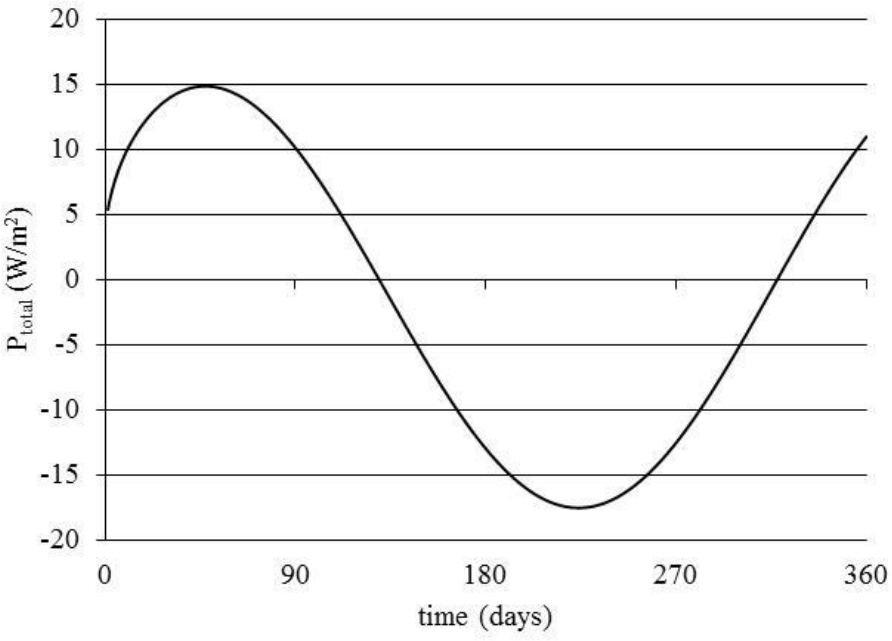

Figure 3.21 Power exchanged by the whole domain for one year thermal loading under sinusoidal thermal solicitation.

Figure 3.23 represents the variation of the thermally exchanged advective and conductive powers. As shown in this figure, both have the same trend of variation as that of the surface and diaphragm wall temperature. Nevertheless, the advective power has a minor contribution reaching 2.5% of the total heat exchange which can be attributed to the relatively low groundwater flow (~ 0.09m/day).

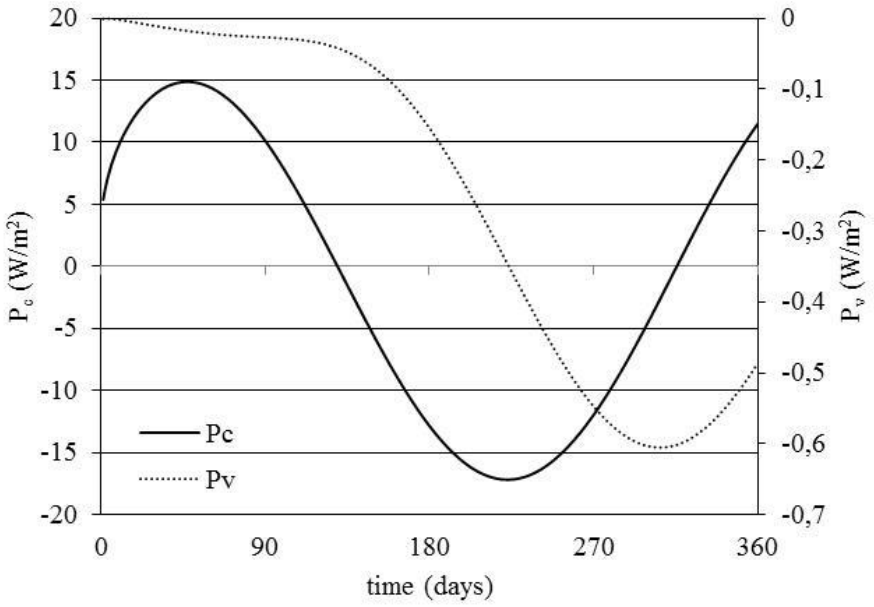

Figure 3.22 Conductive and advective power exchanged by the whole domain.

Imposing a sinusoidal temperature into the diaphragm walls allows the calculation of the thermally exchanged heat for the walls since their temperature varies with time. During one year of thermal cyclic loading, the walls' exchanged power doesn't exceed 5 W/m^2.

Regarding the exchanged energy, Figure 3.24 represents its variation. It reaches 3000 kWh but it is still lower than that generated by the case of imposed constant temperature.

Briefly, the energy exchanged during summer is higher than that exchanged during winter, meaning that the soil has a higher potential to gain heat than to lose it, and this confirms the results of the first approach.

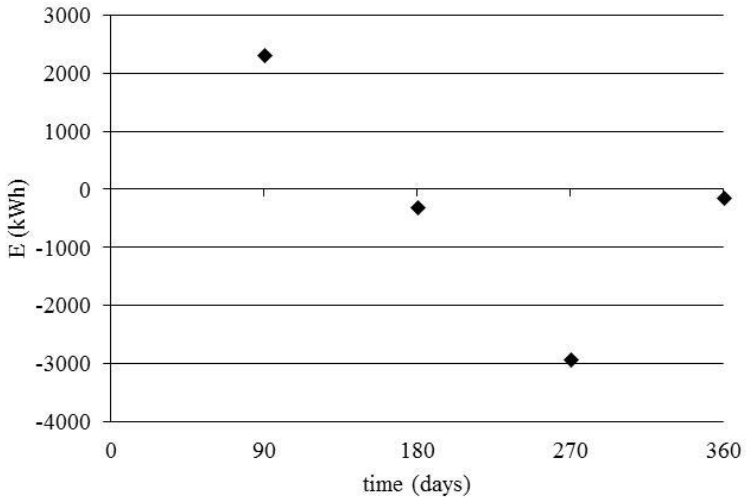

Figure 3.23 Energy delivered by the energy diaphragm walls.

It is worth noting that reversing the order of the thermal phases for a thermal cycle in a way that the thermal cycle will start by a heating season instead of a cooling season; this would affect directly the results regarding the exchanged heat (Figure 3.25). The exchanged energy in this case is higher in the cooling phase thus the soil has a higher potential to lose heat than to gain it. In fact, the potential capacity of the soil to gain or lose heat is a permanent property and thus the capability of the system to exchange heat in each phase relies on the order of the thermal phases, since when the thermal order of the phases is reversed then different soil thermal response is observed. As shown in Figure 3.25, the exchanged power for both cases is almost symmetrical and the efficiency of the system tends to increase slightly with time.

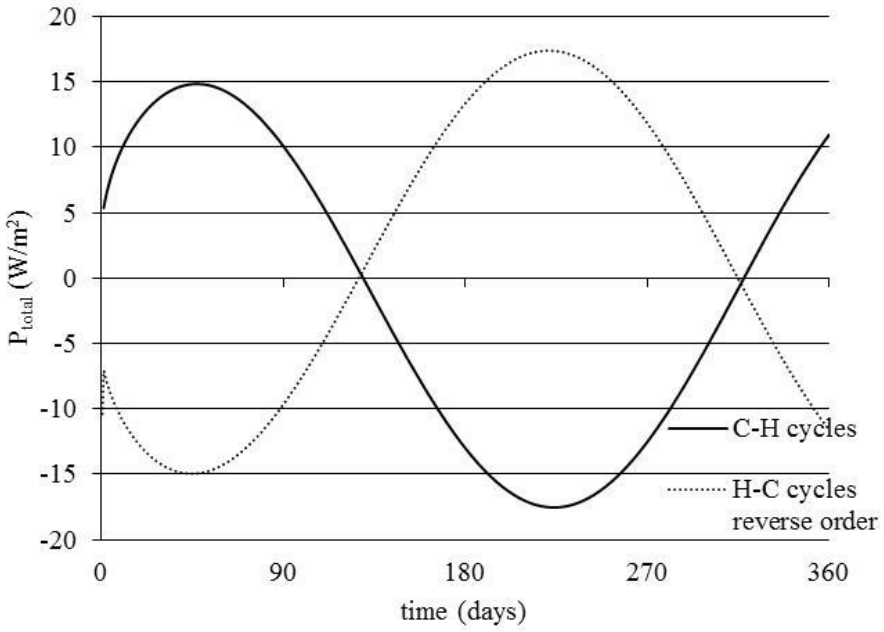

Figure 3.24 Variation of the thermal exchanged power for both types of thermal loading order.

In the case where the temperature is imposed brutally into the walls (case of constant temperature), the exchanged power shows high values at the beginning of the thermal phases and then drops rapidly, thus the total exchanged power is around the double of that exchanged by the contact soil zones. However, for the case of imposed sinusoidal thermal load, the power exchanged by the contact zones is approximately equal to one third of the power exchanged by the whole domain (Figure 3.26).

In general, the average power exchanged by the whole domain for both types of thermal loadings (constant and sinusoidal temperature) is equivalent to the maximum power generated by the soil zones in contact with the diaphragm walls.

Both thermal loading types are time and memory consuming; nevertheless the case with sinusoidal temperature variation is more realistic. Therefore, modelling energy diaphragm walls through imposing sinusoidal temperature variation into the walls is better for their design.

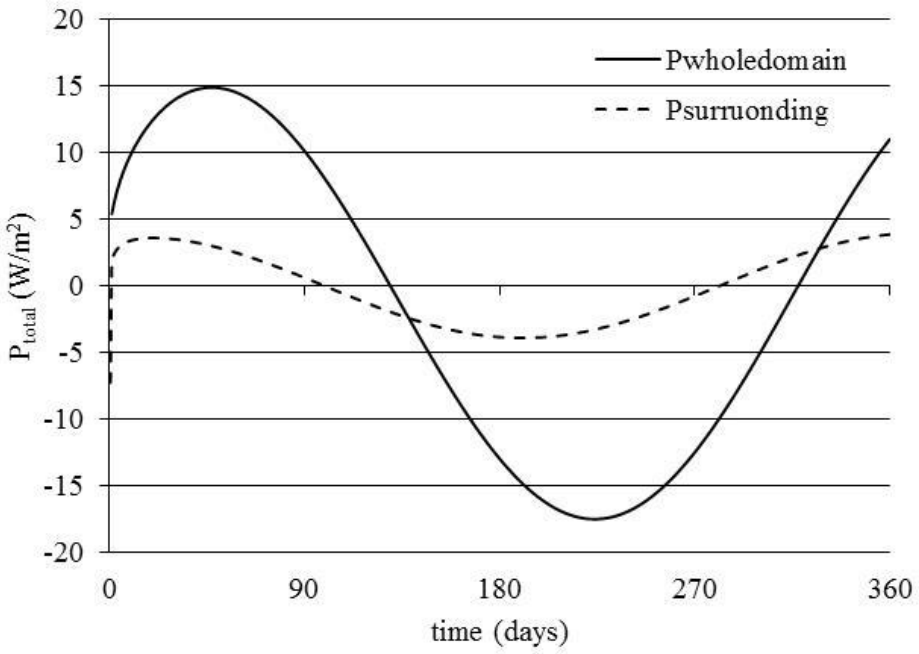

Figure 3.25 Thermal power exchanged in the whole domain and in the zones surrounding the energy walls.

Regarding the provided exchanged thermal energy by thermo-active diaphragm walls; in France, according to the French thermal regulations (RT 2012), it is advised that buildings should use between 40-65 kWh/m^2 of energy per year depending on the climatic zone and the type of the building. Thus considering an average building area of 80 m^2, it consumes 4200 kWh. Therefore, the considered energy diaphragm walls could be able to satisfy approximately all the needs for the case where constant temperature is imposed into the walls and 72% of the thermal needs for the case of sinusoidal imposed temperature, knowing that only one panel of 1 m length is considered here.

3.4 Three dimensional energy diaphragm wall model

The simulation of real case diaphragm walls with all the appropriate boundary conditions is better achieved using three dimensional models. For this reason, and since slight differences are found between approaches 1 and 2, then in this part, the energy diaphragm wall is modeled in three dimensions using approach 2 as shown in the following figure (Figure 3.27). Only one

panel of length 2.5 m is modeled, and at the back side, the retaining wall has a thickness of 1 m. The left, right, and the back walls are thermally activated. As an approach to understand the heat exchanged between the energy walls used as retaining elements for metro stations, the power exchanged by the whole domain as well as the power exchanged only by the zones which are in direct contact with the energy diaphragm walls are calculated as provided in the previous sections using approach 2. It is worth noting that the velocity of underground water flow considered in this case is approximately 10^{-6} m/s.

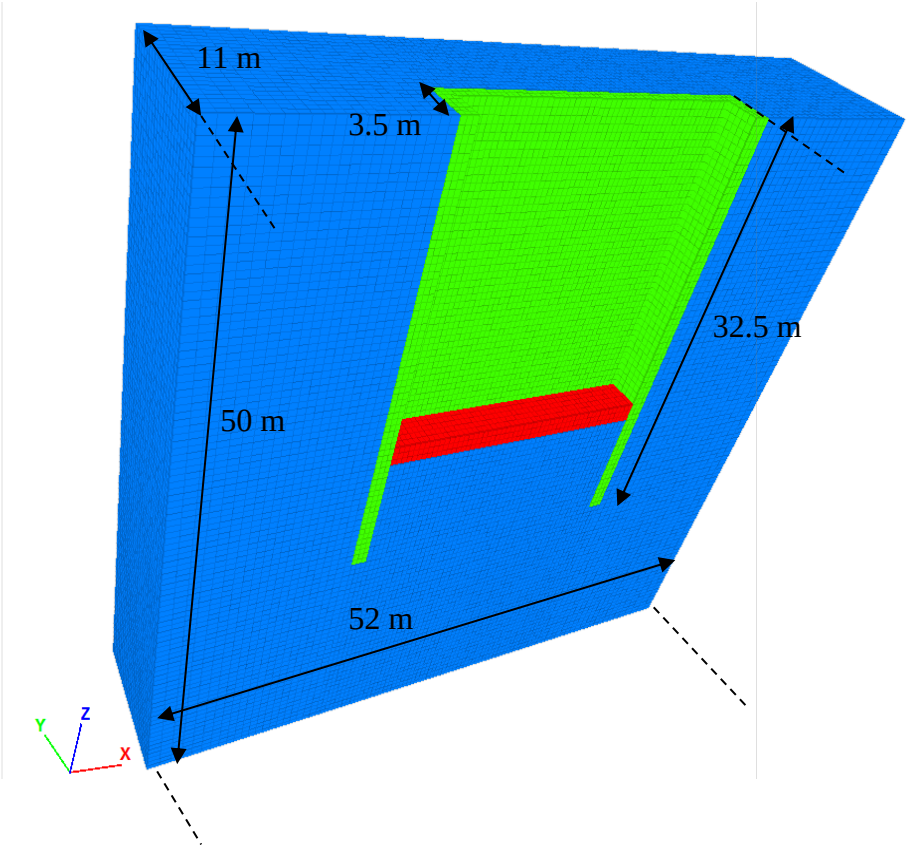

Figure 3.26 Geometry of the 3D modeled metro stations with the energy diaphragm walls in green.

In this three dimensional model, the number of zones and gridpoints are 222200 and 236946 respectively, these last lead to decrease the efficiency of the calculation sequence and increase the time needed to perform the required calculations, and thus only two thermal phases are modelled.

Therefore in the following, a heating load followed by a cooling load is imposed into the walls knowing that the thermal solicitation is the continuous sinusoidal temperature variation (Figure 3.21).

At the end of the first thermal phase, the soil is expected to act as a heat sink absorbing the temperature imposed into the wall, then the total divergence should have negative values; this is confirmed by the obtained results as presented in Figure 3.28.

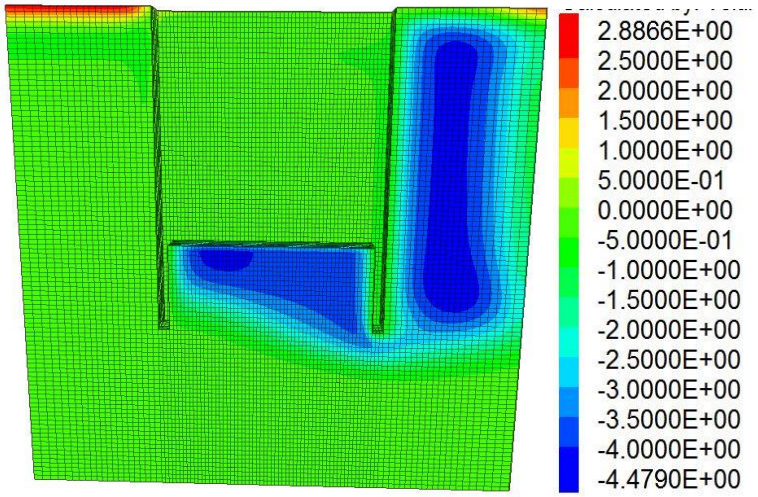

Figure 3.27 Distribution of the total divergence in the domain.

Figure 3.29 represents the variation of the exchanged power in the whole domain except in the thermally activated elements. The impact of groundwater flow becomes significant as time increases where the advective power reaches about 45% of the total exchanged power.

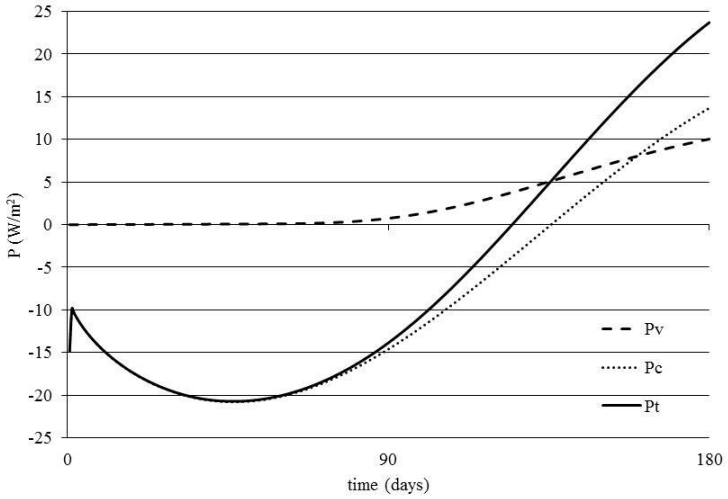

Figure 3.28 Exchanged power for the whole domain without the thermally activated elements.

On the other hand, Figure 3.30 represents the variation of the exchanged power for the zones that are in contact with the energy diaphragm walls. At the end of the second thermal phase, the power exchanged by the surrounding zones reaches 33% of the total power exchanged by the whole domain. It is worth noting that the advective power contributes in delivering more than the half of the total power.

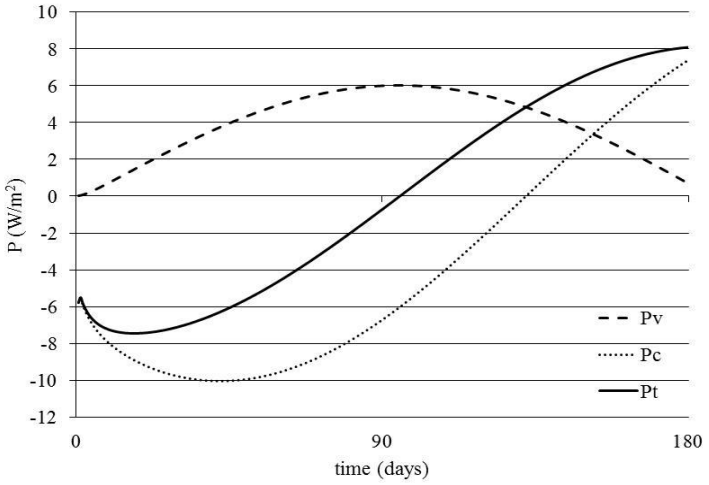

Figure 3.29 Exchanged power by the surrounding zones only.

The energy diaphragm walls are divided into three parts, left, right, and back walls. Each part is surrounded by soil zones that have their own conductive and advective powers as shown in Figure 3.31. The left and right walls are perpendicular to the groundwater flow whereas the back

is the wall is parallel to the groundwater flow. Figure 3.31 shows that the advective power exchanged by the zones that are in contact with the perpendicular walls is higher than that exchanged by the zones that are in contact with the wall that is parallel to the groundwater flow, this is in accordance with the work of several researchers (Diao et al. 2004, Choi et al. 2012, Tolooiyan & Hemmingway, 2012). For the conductive power, also higher exchanged power is found for the zones that are in contact with left and right walls, this is due to the direction of the groundwater flow too.

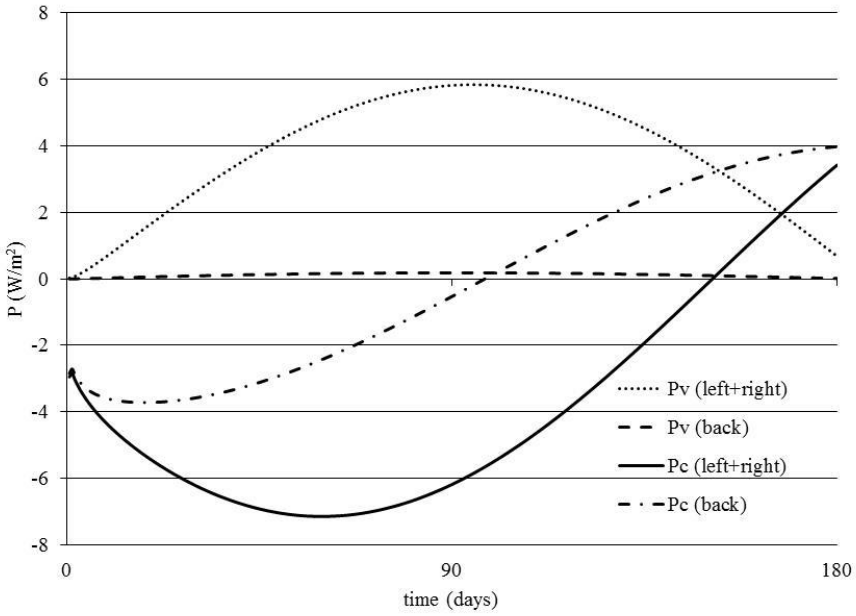

Figure 3.30 Distribution of the conductive and advective powers in the surrounding zones.

Figure 3.32 represents the variation of the conductive powers for the energy diaphragm walls for two seasons. The advective power of the walls is null since no heat exchanger tubes are modelled. On the other hand, since there are more zones in the back wall than in the left and right walls, then the exchanged conductive power is higher for the back walls. It is shown that the power exchanged by the energy diaphragm walls is approximately 22% of that exchanged by the whole domain, and it exceeds that exchanged by the surrounding zones by 25%.

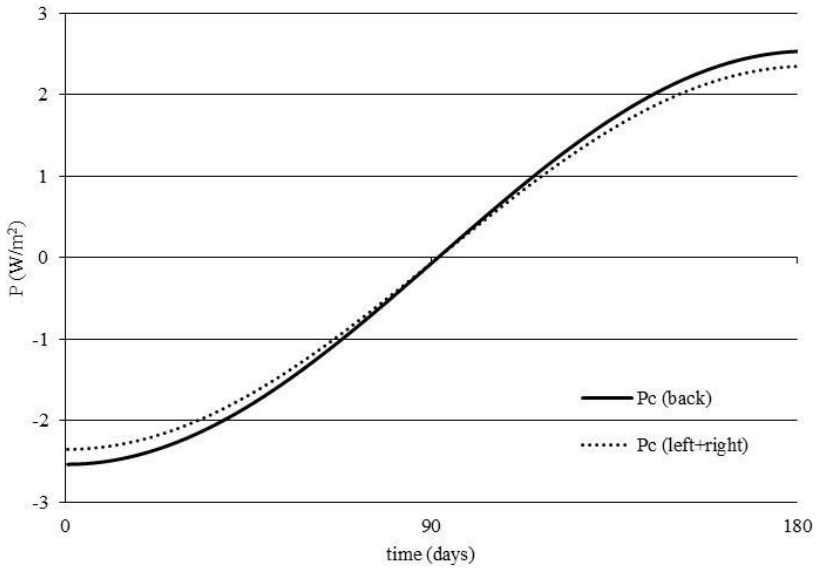

Figure 3.31 Conductive power exchanged by the energy diaphragm walls.

The two dimensional energy diaphragm wall model can be considered as a simple model that can be done to get preliminary results concerning the exchanged heat. However, a three dimensional model simulates real cases conditions and thus could provide more realistic results. Moreover, the impact of groundwater flow becomes obvious along the different parts of the wall. Regardless of the time and memory consumption caused by modelling in three dimensions, this method should be considered when designing the thermal performance of energy diaphragm walls.

3.5 Three dimensional energy pile model

The wide implementation of energy piles around the world drives the attention of researchers and design engineers to focus more on their thermal and mechanical performance. In this manner, to evaluate their thermal efficiency, approach 2 is used to calculate the power that could be exchanged between energy piles and their surrounding soil. Approach 2 is adapted in this section since as mentioned before, approach 1 and 2 almost lead to the same results.

A square energy pile of 12 m length and 41 cm side width is modeled in this section. Due to symmetry, only half of the domain is modelled, and the geometry of the domain is presented in

Figure 3.33. The initial thermal conditions, thermal properties, hydraulic properties, and fluid flow assumptions are the same as those considered for the energy diaphragm wall. However, for the temperature imposed into the pile, it is the continuous sinusoidal temperature presented in Figure 3.21. Regarding the underground water flow, it has a velocity of $3x10^{-6}$ m/s.

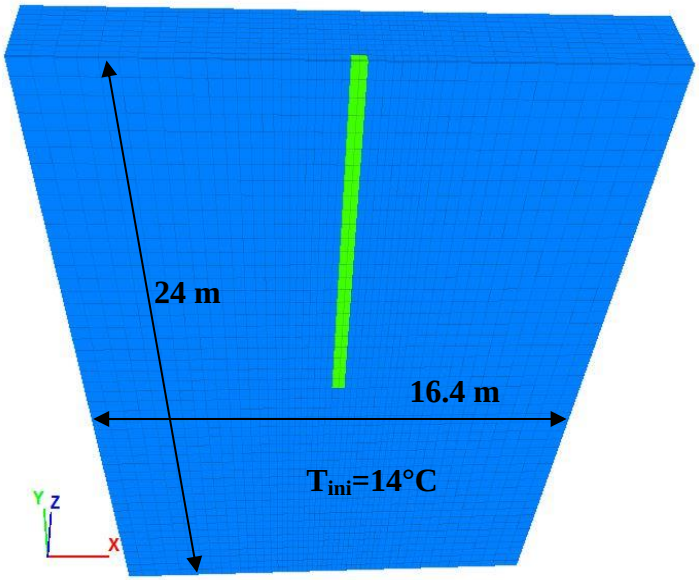

Figure 3.32 Geometry of the three dimensional energy pile model.

Figure 3.34 shows the distribution of the total divergence in the zones around the pile at the end of the first heating and cooling phases. For example, during summer (heating phase), the pile transfers its heat to the surrounding soil, then the soil acts as a heat sink and thus its divergence is negative, and the opposite occurs during the cooling phase. It is worth noting that the total divergence is affected by the direction of groundwater flow and its intensity.

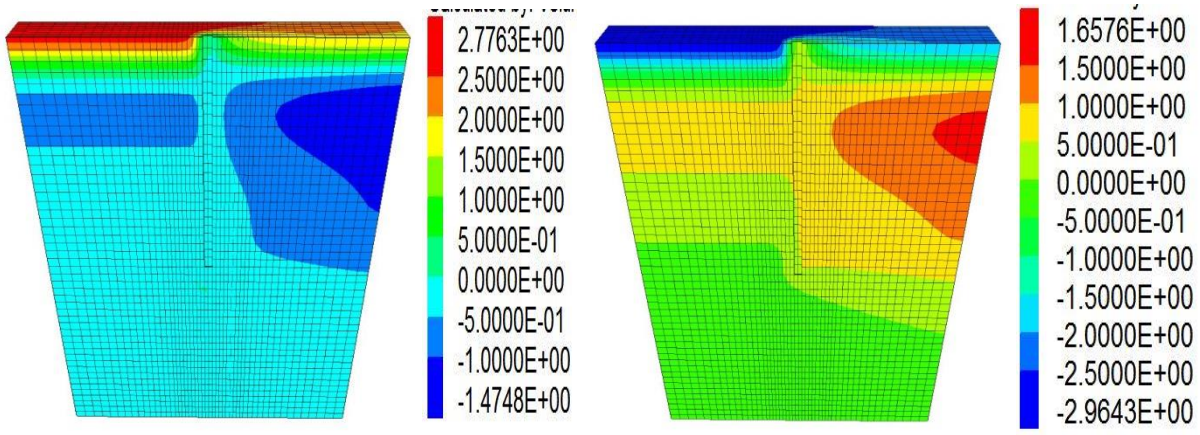

Figure 3.33 Distribution of the total divergence in the zones around the pile at the end of the first a) heating phase b) cooling phase.

3.5.1 **Cyclic thermal loading of 3-D energy pile**

Three consecutive thermal cycles are considered such that each cycle consists of four phases. After three thermal cycles, the total power exchanged by the whole domain seems to have a constant variation over an entire cycle and produces a maximum total power of 35 W/m^2 (~700 W) in the whole domain (Figure 3.35). In this manner, Gashti et al. 2015 assessed the power exchanged by energy pile installed in silty sandy soil and found that during winter, the maximum power reaches 500 W whereas during summer it reaches 1500 W. In their study, the presence of groundwater flow was found to have a slight impact on the exchanged power.

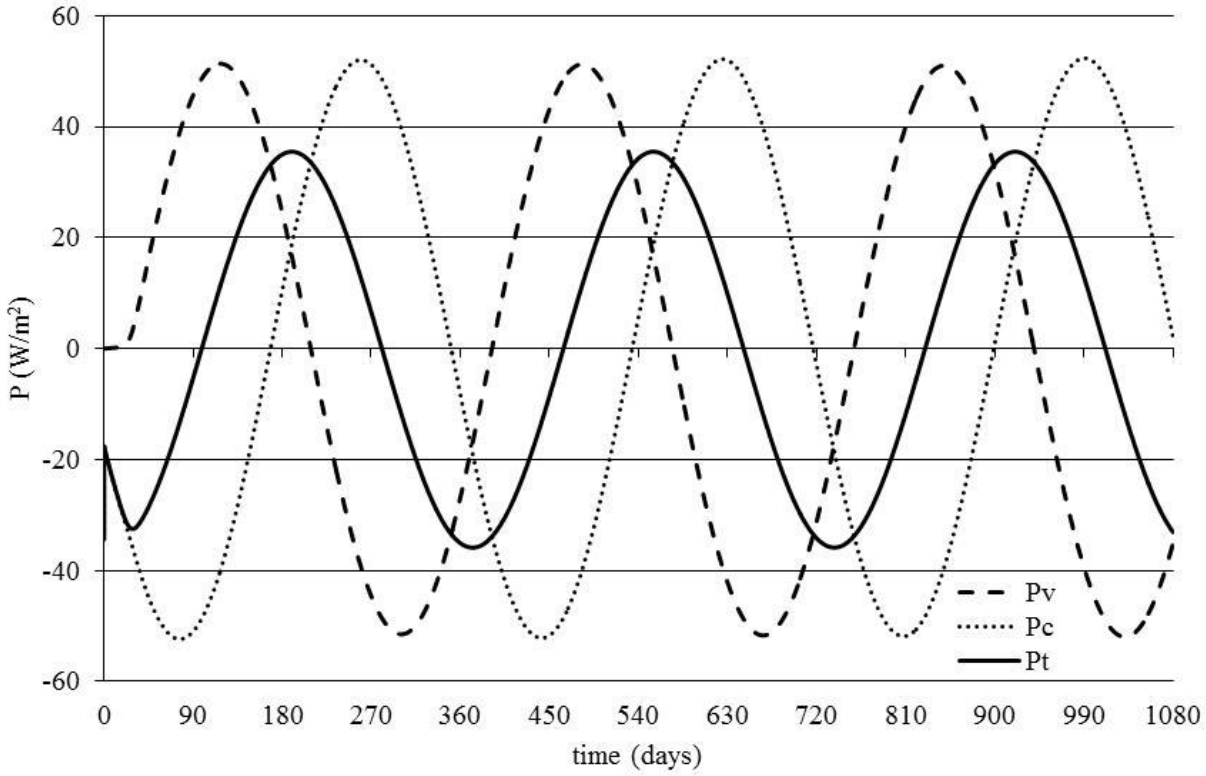

Figure 3.34 Power exchanged by the whole domain during three thermal cycles.

Now, the power exchanged by the zones which are in contact with the energy pile is considered. The power exchanged by the contact zones represents one third of that exchanged by the whole domain. What is remarkable in Figure 3.36 is that Pc and Pv are approximately symmetrically opposite leading to very small values of the total exchanged power, meaning that the variation of the temperature for the surrounding zones is very small. In fact, it is less than 4.4°C between each two thermal steps.

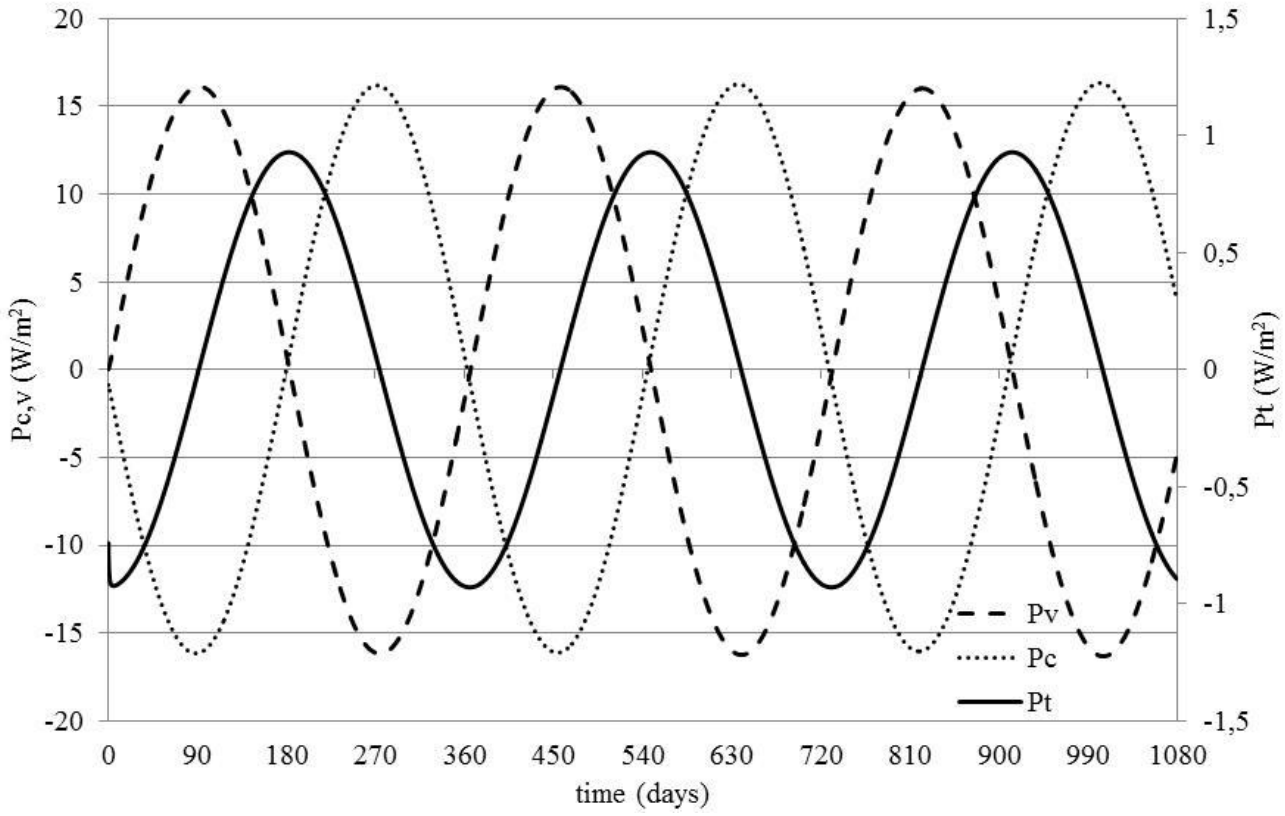

Figure 3.35 Power exchanged by the zones surrounding the energy pile only.

3.5.2 **Comparison between 3-D energy diaphragm walls and energy piles**

The higher number of concrete and soil elements in the case of energy walls compared to those of the energy piles doesn't allow the comparison of the total exchanged power. However, the distribution of the advective power shows different behaviour between energy walls and energy piles. For the case of energy diaphragm walls, it has a slight contribution, whereas it is remarkable for energy piles and almost symmetrical to the conductive power. This significant difference can be attributed to the geometry of each configuration where the length of the energy diaphragm walls works as an obstacle to the groundwater flow and causes this advective power distribution.

3.6 Conclusion

New methods have been proposed to evaluate the exchanged energy based on the assessment of the conductive and advective powers separately; these methods allow understanding the influence of each component on the total exchanged heat.

The hydro-thermal behaviour of energy diaphragm walls as well as energy piles has been studied in this chapter. The aim is to evaluate the allowable exchanged thermal energy between these energy geo-structures and the surrounding soil. The impact of the presence of groundwater flow has been examined and proved to have a positive influence on the exchanged energy through enhancing heat transfer by advection.

2D and 3D finite difference numerical models of energy diaphragm walls and energy piles were conducted. Simulations and the obtained results show that 2D models for both approaches are much simpler than 3D models, they require less memory allocations, and reduce significantly the time required for performing the calculations and analyses, yet they are don't offer precise results. However, even though 3D models are memory and time consuming, they prove to be more accurate and representable of real case examples.

CHAPTER 4 : Thermo-mechanical behaviour of energy piles: Impact of imposed thermal loads

4.1 Introduction

Despite of the early usage of energy piles since 1980's (Brandl 2006) and their wide implementation, still there are some ambiguities regarding their design, which requires efficient and unambiguous approaches to provide the most appropriate verifications.

Several questions regarding the mechanical design of energy piles require deep and accurate responses as the number of cyclic thermal loadings in terms of heating and cooling needed to be considered, the amplitude and the mean of thermal loadings, the shape of the thermal loading as crenel solicitations or sinusoidal solicitations, the necessity to perform a transient analysis. Most studies consider only permanent situations or the greatest temperature difference for designing energy piles (Bourne-Webb et al. 2009). A coupled transient thermo-mechanical approach enables to account for the possible effects of changes in the pile and in the ground in terms of temperatures, strains and stresses throughout the thermal cycles (Di Donna et al. 2016a), but the choice of thermal solicitations is not clearly addressed. The spatial and the temporal evolutions of the temperature into the ground are difficult to be considered, but the design of energy piles requires a clear overview about its influence. For example, Laloui et al. (2006) show that the

applied thermal load leads to increase twice the total axial load in the pile. Gashti et al. (2015) find higher stresses at the pile toe resulting from higher temperature variations caused by the thermal fluctuation around the U-tubes, and Rotta Loria et al. (2015) present non-linear response of the pile foundation due to increasing thermal loads. Bourne-Webb et al. (2016a) assured through conducted numerical simulations that the contribution of the affected surrounding soil should not be ignored in the design of energy piles especially in the case of moderately to highly over-consolidated clays.

This chapter focuses on the importance of considering and analyzing the temporal and spatial distribution of temperature for energy pile design in order to propose an appropriate way to design energy piles. It aims to focus on the influence of the thermal solicitations on the design of energy piles. For this objective, the study of a single energy pile installed in saturated sandy soil affected by coupled thermo-mechanical loads is proposed. Several forms of thermal solicitations are examined to assess their influence on the pile reaction with the aim to provide some insights for the choice of the appropriate thermal solicitations for a precise project. Especially, the influence of the rest period is considered as well as real continuous sinusoidal temperature variations. These different alternatives in terms of thermal solicitations can account for the difference between the seasons or even passive cooling. Some recommendations are provided at the end of the chapter to help the designer to choose the most appropriate thermal solicitations in order to ensure the robustness and the reliability of the energy piles under design.

4.2 Numerical model

The pile geometry and the soil mechanical properties are adapted from the full scale loading tests carried by Szymkiewicz et al. (2015) near Dunkerque, northern France (among the three tested piles, two are energy piles). The considered pile is a continuous flight auger (CFA) pile of 12 m length and 52 cm in diameter.

The behaviour of energy piles under only mechanical then thermo-mechanical loading is studied through numerical modelling via the finite difference code FLAC3D (ITASCA, 2012). The modelled pile has a square section with equivalent width of 41 cm and of 12 m length. Due to symmetry, only one quarter of the domain is modelled. Concerning the mechanical boundaries, the lateral sides are normally fixed whereas the model is fully fixed at the bottom as shown in Figure 4.1.

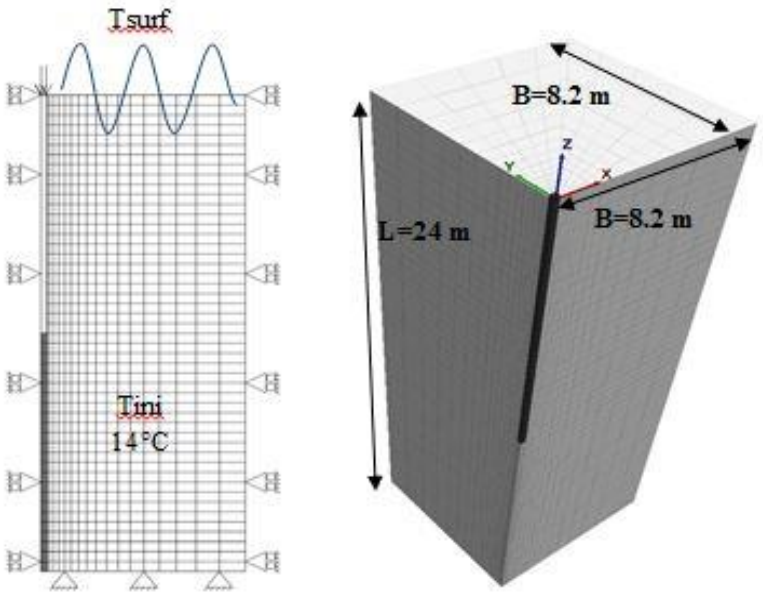

Figure 4.1 Model geometry, thermal and mechanical boundary conditions.

The soil is considered as a saturated sandy soil with a water table of hydrostatic regime situated at 1.5 m depth.

The soil behaviour is described using an elastic perfectly-plastic model, with an isotropic elastic part and a Mohr-Coulomb failure criterion combined to a non-associated flow rule. The pile is supposed to have an isotropic linear elastic behaviour.

The mechanical properties for the soil including the cohesion, friction angle, and density are those measured at the experimental site (Szymkiewicz et al. 2015). The elastic modulus can be obtained by correlations with pressuremeter tests or the cone resistance tests. No information is known about the dilation angle; consequently, several parametric studies have been performed in

order to determine the dilation angle of the soil best fitting the experimental data. Table 4.1 presents the values of the mechanical parameters considered for soil and pile.

Table 4.1 Mechanical parameters of the soil and the pile.

	Soil		Pile
Density ρ (kg/m^3)	0-1.5 m	1581	2500
	1.5-24 m	1910	
Elastic modulus E (MPa)	73		20000
Poisson's coefficient ν	0.3		0.2
Cohesion c (kPa)	3		-
Friction angle φ	31		-
Dilation angle ψ	6		-

Figure 4.2 shows the results of the experimental and numerical static load tests where the soil with a Young modulus E equal to 73 MPa, and a dilation angle ψ equal to 6° are found to have a good agreement with the experimental load-settlement curve. It is worth noting that in this figure, $P_{ultimate}$ stands for the pile ultimate capacity which is 2450 kN and the dotted horizontal line represents the allowable pile head settlement which is 10% of the pile's diameter.

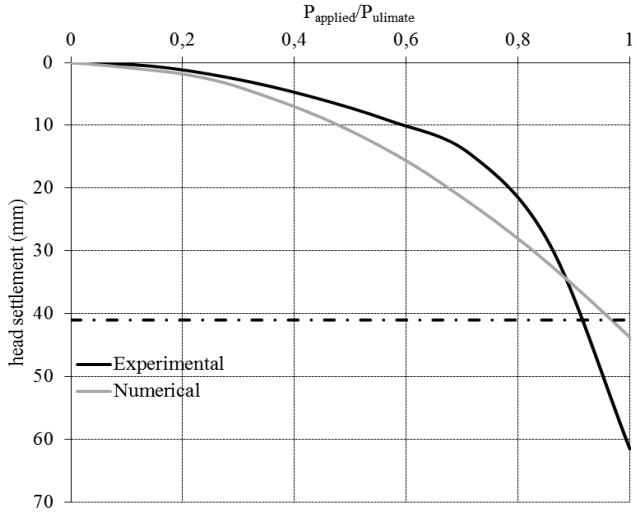

Figure 4.2 Load ratio-head displacement variation.

The difference between numerical results and experimental data is not negligible but can be assumed to be sufficiently low for the following of the study, especially, as the mechanical load applied is around 33% of the pile bearing capacity. It is important to note that perfect contact is

considered between the pile and the soil, therefore no interface elements are modelled. No cyclic parameters are also considered in the constitutive law of the soil since the loading level is low and should not lead to mechanical cyclic accumulation of displacements or strains.

It is worth mentioning that in all of the presented figures, negative axial forces represent tensile forces, and positive axial forces represent compressive forces.

4.3 Thermal solicitations under consideration

A sequential transient thermo-mechanical analysis is carried out to examine the impact of applied mechanical and imposed thermal load on the behaviour of an energy pile installed in saturated sandy soil. A mechanical load equivalent to 33% of the pile bearing capacity which is about 800 kN, is applied at the head of the pile prior to the imposed thermal cycle. This loading level corresponds to the serviceability limit state in many pile design codes. The pile head is supposed to move without any fixity (free conditions).

For the thermal boundaries, the initial temperature is 14°C corresponding to the soil constant temperature at a depth 10-12 m in most European countries. The surface is exposed to the external air temperature following equation 3.1 defined in chapter 3, while a constant or sinusoidal variable temperature is imposed into the pile.

The thermal parameters of the pile and soil are those used for concrete and saturated sandy soil; their values are summarized in (Table 4.2).

Table 4.2 Thermal parameters of the soil and the pile.

	Soil	Pile
Thermal conductivity λ (W/m.K)	2	1.8
Specific heat capacity (J/kg.K)	1550	880
Thermal expansion coefficient α_T (/°C)	$5x10^{-6}$	$12x10^{-6}$

Regarding the imposed thermal solicitations into the pile, ten consecutive periodic thermal cycles corresponding to ten years are simulated. This thermal load is applied uniformly into the pile

since the presence of the heat exchanger tubes is neglected. For the following cases to be considered, the low difference in temperature between the inlet and outlet heat exchanger tubes embedded in energy piles makes the assumption of a uniform pile temperature a feasible hypothesis for designing energy piles.

Three types of thermal solicitations are considered and compared in order to cover various climatic conditions and provide some insights regarding the choice of the thermal load to be imposed into the pile (Figure 4.3). The first solicitation TS1 corresponds to a constant pile temperature with rest phases. This solicitation includes four main parts during a year: one part for heating and one part for cooling with two rest phases. The second solicitation TS2 corresponds to a constant pile temperature without rest phases. This solicitation only includes two main parts during a year: one part for heating and one part for cooling. The third solicitation TS3 corresponds to a continuous sinusoidal temperature variation taking into account various scales: the year, the day and the hour.

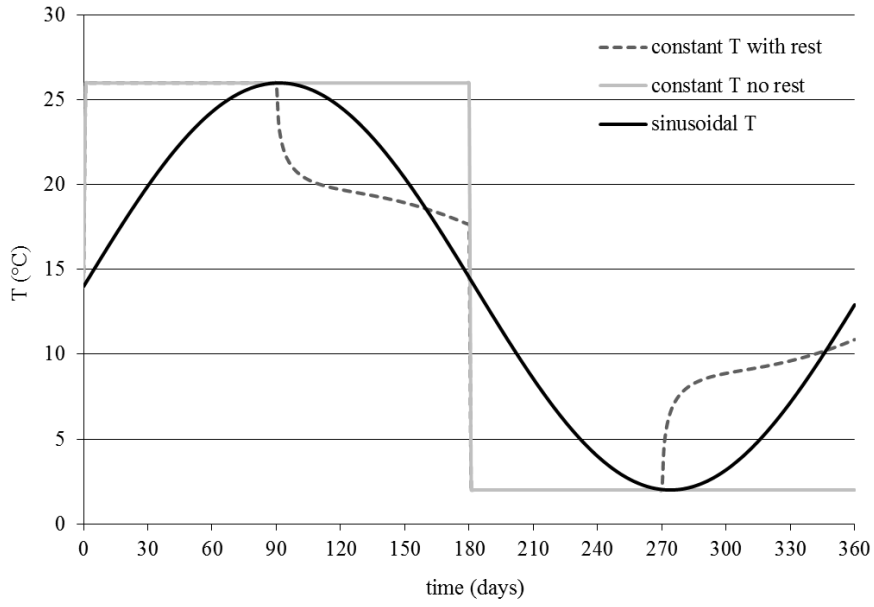

Figure 4.3 Variation of the pile temperature for the three types of thermal solicitations.

The comparison of these three cyclic periodic thermal solicitations is interesting in order to understand how the additional thermal displacements and axial forces vary. Indeed, due to the

irreversible strains induced by the mechanical dead-load, nonlinear effects are expected. For this reason, reversed heating and cooling phases are also analyzed for the three cases presented above (in Figure 4.3, the thermal solicitations start with heating phase).

Furthermore, a reference case TS0 has been also defined and it corresponds to a pure mechanical calculation where the temperature into the pile is applied by considering only volumetric strains ε_v:

$$\Delta\varepsilon_v = \alpha_c.\Delta T \tag{4.1}$$

In this case, consecutive heating and cooling phases are simulated through imposing the corresponding volumetric strains. This procedure is used a lot in practice and corresponds to a situation where a sudden temperature variation is applied into the pile without any temperature diffusion in the surrounding ground. As previously, reversed heating and cooling phases are also analyzed. At time t=0, TS0 provides the same results as TS1 and TS2.

4.4 Thermal volumetric strain: TS0

Thermal volumetric strains are imposed into the pile for ten thermal cycles, in order to account for the temperature variation in a pure mechanical model. It is supposed that the temperature is varying between 2°C and 26°C ($\Delta T=\pm$ 12°C) during cooling and heating phases respectively.

4.4.1 **Pile head displacement**

The pile head displacement is plotted in Figures 4.4a and 4.4b for TS0 and TS0 with reversed heating and cooling phases respectively, in order to focus on the influence of the order of thermal loading. The head displacement slowly increases during the ten consecutive thermal cycles and is almost stabilized at the end of this period. In these figures, w_{th} and w_{mech} are the displacements induced by the thermal solicitations and the applied mechanical load which is 33% of the pile bearing capacity. There is a low ratcheting effect whereas the constitutive law used includes no cyclic parameter. A slight heave is calculated during the first cycle (Figure 4.4a) when the pile is

subjected firstly to a heating load showing that the effect of the thermal loading variations order is only significant during this first cycle. After two cycles, the two figures show the same trends with a discrepancy of six months. In this example, the thermal induced displacement reaches the initial pile head displacement (the relative increase is about 100%). The obtained results may not represent the response of all cases of energy piles; they are specific for the considered soil and concrete thermal and mechanical parameters, for the assumed soil mechanical behaviour under cyclic loading, for the assumed soil-pile interface type, and for the imposed thermal solicitations.

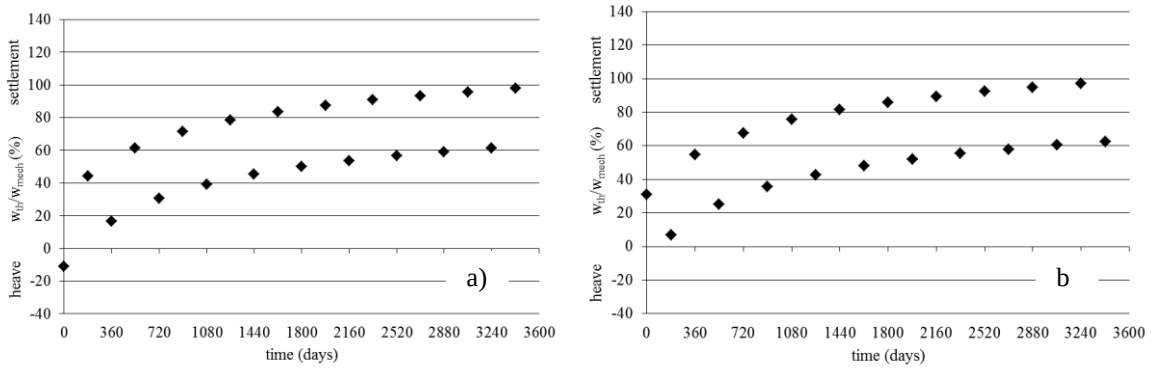

Figure 4.4 Variation of the thermally induced pile head displacement for a) TS0 b) TS0 with reversed heating and cooling phases.

4.4.2 **Normal force distribution**

Considering heating and cooling sequences and then reversed sequences, Figure 4.5 shows the axial force distribution at the end of the first and tenth cycles while Figure 4.6 presents the thermally induced axial force evolution with time at 6.25 m depth.

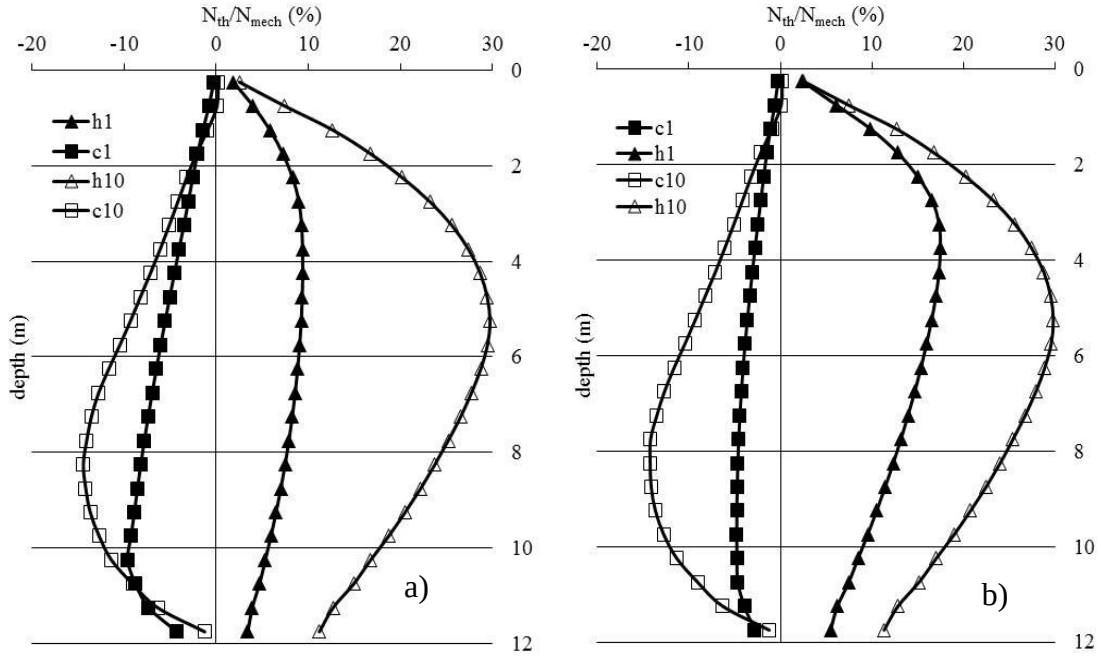

Figure 4.5 Axially induced forces at the end of the first and tenth cycles a) TS0 b) TS0 with reversed heating and cooling phases.

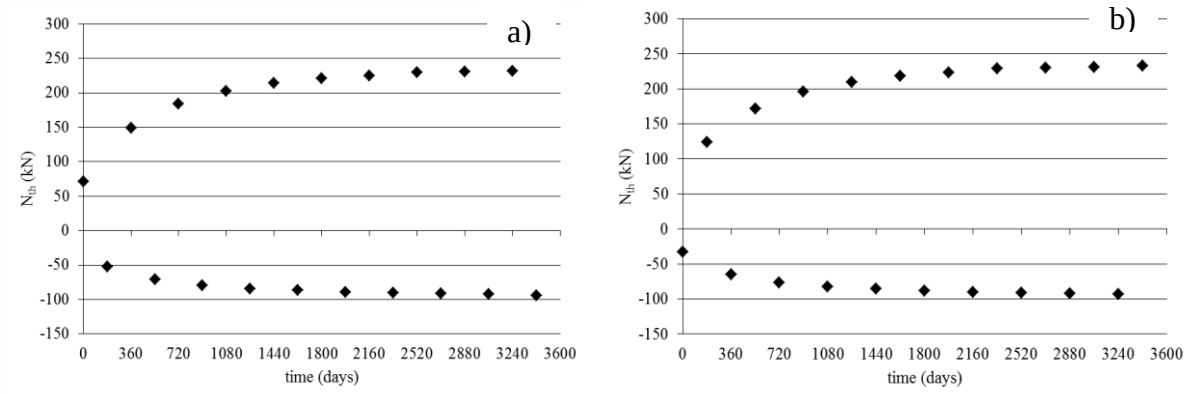

Figure 4.6 Thermally induced axial force a) TS0 b) TS0 with reversed heating and cooling phases.

N_{th} designates the variation of the axial force due to the thermal solicitations while N_{mec} is the initial axial force due only to the mechanical loading applied at the pile head. In this figure as for the following, the legend 'h' and 'c' stand for heating and cooling phases respectively whereas the figure just after goes for the number of the thermal cycle. The trends are similar and point out an increase of the maximum axial force both in compression and tension. After two cycles, the

influence of the thermal loading order is not noticeable. The results obtained after one phase of heating or cooling underestimates the additional axial forces but give a good trend in terms of compression and tension.

4.5 Constant pile temperature: TS1 and TS2

For several climatic conditions, there is a period of time during spring and autumn where the energy needs in the buildings are very low and the heat pump can be turned off for passive cooling to take place. This period is called in this study a rest phase and its impact on the thermo-mechanical pile behaviour is analyzed. Therefore, two cases are considered (Figure 4.3): TS1 where rest phases exist; i.e. the thermal cycle consists of heating and cooling phases separated by rest phases. During cooling and heating, the pile temperature is constant and equal to 2°C and 26°C respectively (corresponding to $\Delta T = \pm 12°C$), whereas it is allowed to vary freely during the rest phase. In this case, the duration of each thermal phase is three months. In case TS2, no rest phases are considered between heating and cooling phases, and the duration of each thermal phase extends to six months.

4.5.1 **Pile head displacement**

Figure 4.7 represents the variation of the thermally induced pile head displacement for TS1 and TS2.

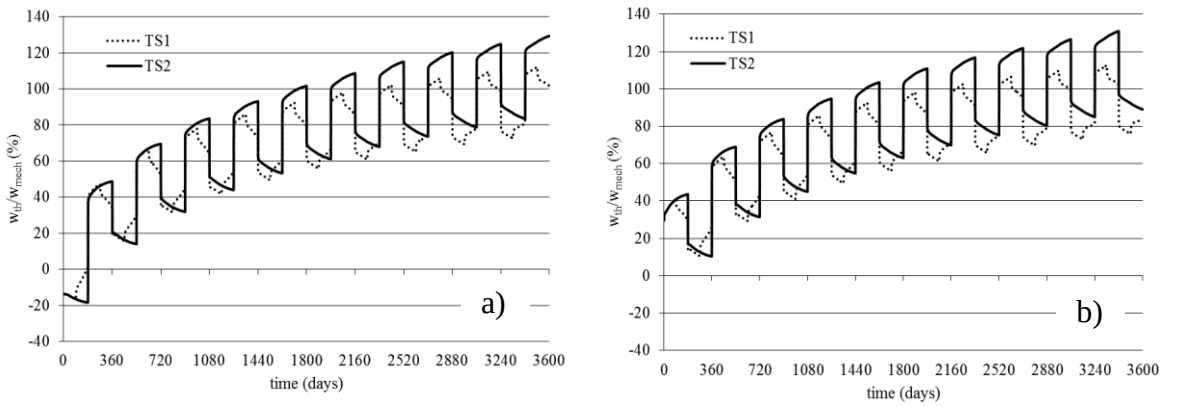

Figure 4.7 Variation of the pile head displacement for the cases of constant pile temperature; a) TS1 and TS2 b) TS1 and TS2 with reversed heating and cooling phases.

The displacement indicates a head heave during the first six months due to the thermal pile expansion where the thermally induced displacement reaches 20% of the mechanically induced settlement (approximately 1 mm) for both cases, then it decreases during the following phases of the first cycle where a negative displacement (settlement) is developed as presented in Figure 4.7a.

For the following consecutive cycles, the pile settlement increases with time but the settlement rate decreases without being null. At the end of the tenth cycle (equivalent to 10 years duration), the maximum thermally induced pile head settlements reach 112% (-5 mm) and 130% (-6 mm) of the mechanical displacement for TS1 and TS2 respectively. Along time, the difference between TS1 and TS2 increases until reaching 28% at the end of the thermal cycles. The higher settlement induced for TS2 can be attributed to the absence of the rest phases which tend to recover the pile temperature and thus relieve the impact of the imposed thermal load. Whereas no cyclic constitutive law is used, the pile head displacement is not stabilized after 10 cycles while the rate and the amplitude of displacement tend to decrease indicating similar effects to those of ratcheting. In terms of energy pile design, these results are quite interesting and significant since they show that cyclic effects can be observed even if the constitutive law considered to simulate the ground behaviour does not deal with these aspects.

Another interesting point is the low displacement variation following the sudden temperature change. This result is due to the diffusion of the temperature in the surrounding ground, which modifies the friction conditions at the soil-pile interface and shows how thermal transient effects can affect the behaviour of energy piles.

It is worth noting that after each rest phase in TS1, the displacement is not totally recovered since the temperature of the pile is not recovered too (Figure 4.3). This raises the question about the duration of the rest phases needed to fully recover the temperature and thus the thermally induced displacement. Anyway; this issue depends also on climatic conditions and the building thermal needs; therefore, a detailed study could be done to better understand the induced mechanisms behind the presence of the rest phase.

Figure 4.7b shows the displacement variation of the pile head considering TS1 and TS2 with reversed heating and cooling phases. The trends between Figures 4.7a and 4.7b are almost the same after two cycles. They show that at least two full cycles have to be simulated to account for a steady state situation into the pile. Considering two separate cases, one for heating and one for cooling, without taking into account the interactions between the two phases of heating and cooling can provide a wrong view for the design. Recommendations for the energy pile design should highlight this aspect.

4.5.2 **Normal force distribution**

The thermally induced axial forces generated in the pile at the end of the first and the tenth cycles of thermal loading for TS1 and TS2 are represented in Figures 4.8a and 4.8b respectively.

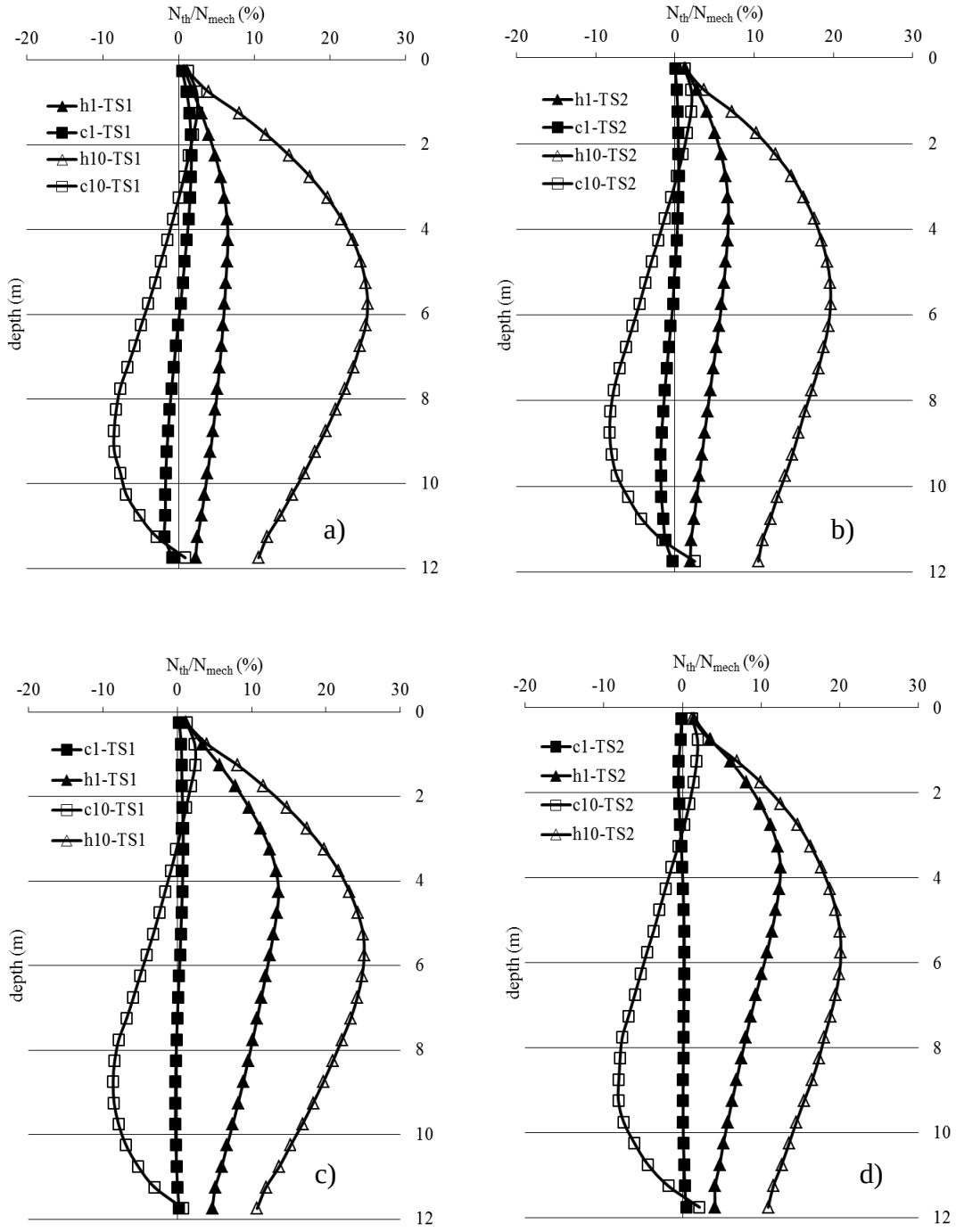

Figure 4.8 Variation of the axial force at the end of the first and tenth thermal cycles for the case of constant pile temperature a) TS1 b) TS2 c) TS1 with reversed order d) TS2 with reversed order.

For the two cases, the absolute values of axial forces increase between the first and the tenth cycle. TS1 shows higher absolute values of axial forces which are 25% and -8.5% of the mechanically imposed load for heating and cooling respectively. For TS2, the maximum values

are 20% and -8.2% for heating and cooling respectively. The variation of the axial forces is higher during the heating phases compared to the cooling phases for both cases; this can generate higher compressive stresses and avoids the development of tensile stresses, which is good for the pile design since it reduces the steel reinforcements.

Figures 4.8c and 4.8d show the axial force distribution at the end of the first and the tenth cycles of thermal loading considering reversed heating and cooling phases for both cases TS1 and TS2 respectively. The results are similar to those obtained previously and only a slight difference in the axial normal force can be viewed at the end of the first cycle: with reversed heating and cooling phases, the axial normal force is slightly higher.

Figures 4.9a, 4.9b, 4.9c and 4.9d show the variation of the axial force at 6.25 m depth with time. The differences are very slight; the role of the rest phase is limited and the thermal load history has an effect only during the first two cycles. Nevertheless, at each temperature change into the pile, it is interesting to underline that TS2 provides higher absolute values especially for cooling phase. As for the pile head displacements, the normal forces into the energy pile slowly vary after each sudden temperature change due to the diffusion of the temperature in the surrounding ground. This result shows that axial force calculated just after the sudden temperature change is not representative since it decreases with time. For the design of an energy pile, it is very conservative to consider this maximum additional force and add it to the other transient actions (wind, snow, variable loadings) since its duration is very short. It confirms that only a part of this maximum additional axial force has to be considered for the design.

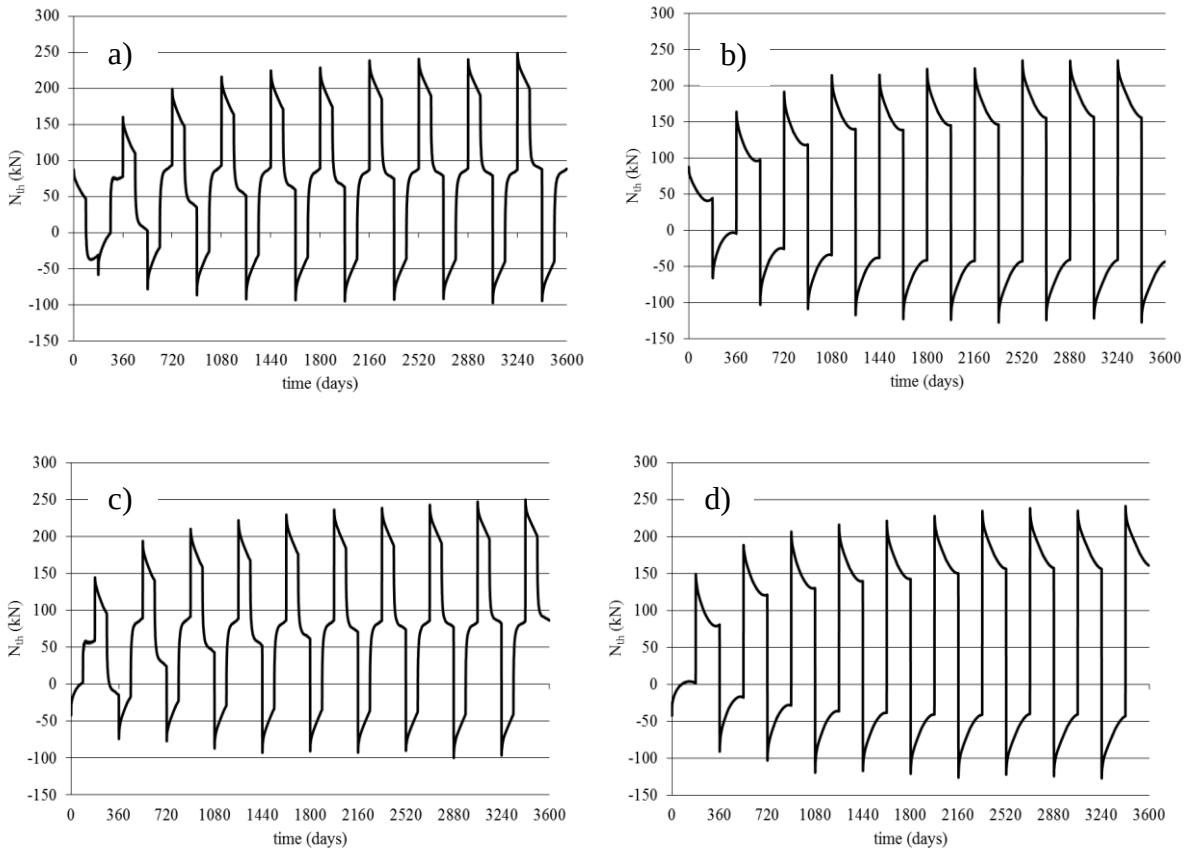

Figure 4.9 Variation of the thermally induced axial force with time a) TS1 b) TS2 c) TS1 with reversed heating and cooling phases d) TS2 with reversed heating and cooling phases.

4.5.3 **Comparison between TS0, TS1, and TS2**

As a partial conclusion, the presence of the rest phase has a slight effect on the head displacement variation where it shows a decrease by around 28% compared to TS2 without rest phases. On the contrary, thermally induced axial forces are slightly higher for the case with rest phases (by around 5%). The low difference in the induced axial forces, compared to the more significant difference regarding the pile head displacement between both cases, leads to consider TS2 as the more unfavorable case that may lead to slightly more conservative results.

The results obtained for TS1 and TS2 are close to those obtained considering TS0 and show that a transient analysis with a crenel solicitation including or not rest phases does not enable to improve the design, but it can just give an idea about the thermal diffusion of temperature in the pile and in the surrounding soil with time.

4.6 Continuous sinusoidal pile temperature: TS3

In order to cover more real cases, in many situations, the rest phase is not really present and the pile temperature is not constant during each thermal loading phase, however it tends to vary depending on the external temperature fluctuations. In these cases, usually the temperature inside the pile does not change (increase or decrease) suddenly as for the assumed cases TS1 and TS2 before. Therefore, a sinusoidal temperature variation is supposed to be applied uniformly inside the pile according to the relationship presented through equation 3.2 in chapter 3. The chosen values of this thermal load are representative of some typical measured data in some energy piles (Brandl, 2006; Pahud & Hubbuch, 2007; Suryatriyastuti, 2013; Habert et al., 2016).

4.6.1 **Pile head displacement**

The calculation of the pile head displacement provides lower values in this case compared to the previous cases where uniform constant temperature is imposed into the pile. In addition, in this case the rate of the head displacement increase is lower. With sinusoidal pile temperature variations, the head displacement starts to stabilize rapidly after the fourth cycle (Figure 4.10a). This means that if realistic cases of thermal conditions are considered then the pile behaviour does not show any trend of displacement accumulation. The thermally induced pile head displacement does not exceed 80% of the mechanical displacement even after 10 cycles in comparison to 112% and 130% for TS1 and TS2.

Figure 4.10b shows the displacement variation of the pile head with reversed heating and cooling phases. The results present very similar trends to those obtained previously with TS1 and TS2 (see, Figures 4.7a and 4.7b). The upper and lower bound values in terms of displacements after five cycles are the same for the two types of solicitations (TS3 and TS3 with reversed heating and cooling phases).

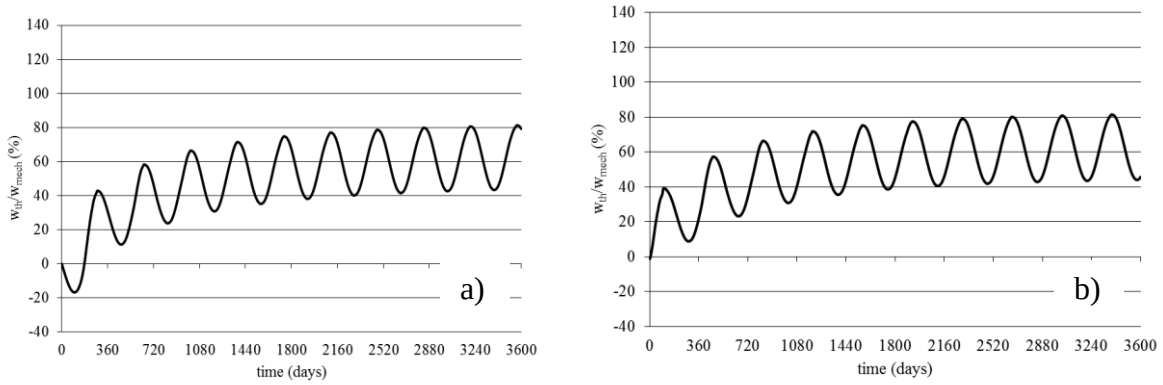

Figure 4.10 Variation of the thermally induced pile head displacement a) TS3 b) TS3 with reversed order of heating and cooling phases.

4.6.2 **Normal force distribution**

Figure 4.11a represents the variation of the total axial force along the thermal cycles.

Unlike cases TS1 and TS2, now for each phase, the pile generates tensile stresses during cooling and compressive stresses during heating. The maximum axial force ranges between -7.5% and 22% of the mechanical load, due to cooling and heating respectively. Figure 4.11b represents the variation of the axial force with reversed heating and cooling phases. Similar to the previous cases, slight difference is found between both thermal loading types. With reversed phases, the axial forces are slightly higher especially at the end of the first heating phase.

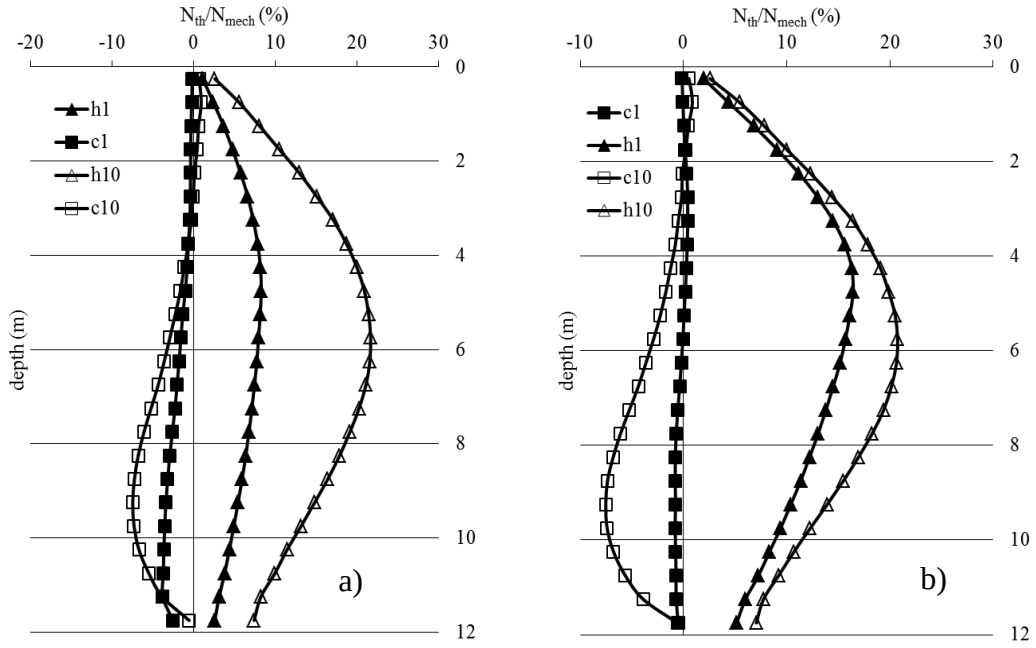

Figure 4.11 Variation of the axial force at the end of the first and tenth cycles a) TS3 b) TS3 with reversed order of heating and cooling phases.

Figures 4.12a and 4.12b show the variation of the thermally induced axial force with time at a depth of 6.25 m for TS3 without and with reversed heating and cooling phases, respectively. Almost negligible differences are found between both figures. These results confirm that at least three full cycles have to be simulated to account for a steady state situation into the pile. From the fifth cycle (2160 days), the maximum axial force does not vary anymore. The comparison with TS0, TS1 and TS2 enables to assess the equivalent thermal solicitations that will be applied to the pile to obtain the same results.

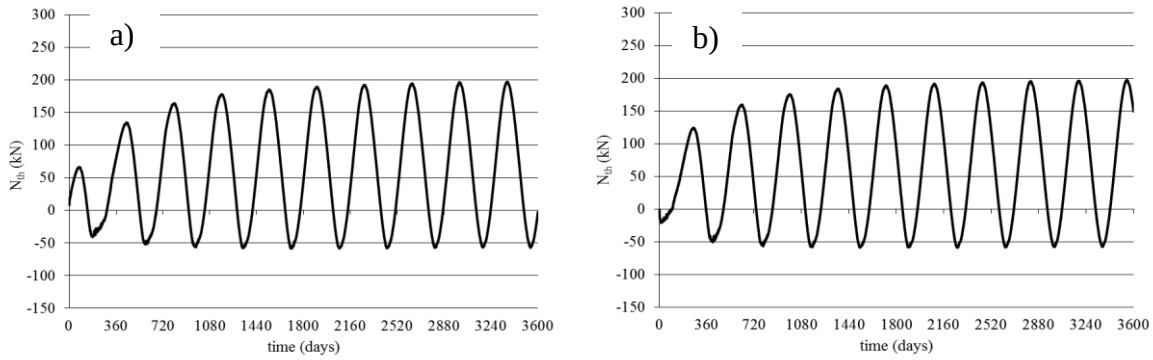

Figure 4.12 Variation of the thermally induced axial force with time a) TS3 b) TS3 with reversed order of heating and cooling phases.

4.7 Comparison between the four thermal solicitations

Four types of thermal solicitations have been considered, to take into account various simulation possibilities (pure mechanical and transient thermo-mechanical analysis) and different climatic conditions, in order to be able to choose the best type when designing energy piles. The results obtained concerning the head displacement and distribution of axial forces may give an idea about the type of thermal solicitation that should be imposed in an energy pile for an appropriate design.

Regarding the pile head displacement, for the four considered cases, the mean value of the displacements is still increasing while the amplitude of the pile head displacement decreases with time. Ratcheting effects at the pile head are obvious where the head displacement continues to increase with time. For the case of constant pile temperature (TS1 and TS2), the rest phase has a positive impact on the head displacement. For the considered duration of each phase, the rest phase is not capable to recover the pile temperature but attenuates the impact of the applied thermal load. On the other hand, the third type of thermal solicitation (sinusoidal pile temperature; TS3) shows less pile head displacements and rapid stabilization after four cycles. For TS3, the maximum induced thermal displacement is approximately the half of that induced by the case of constant pile temperature.

Concerning the distribution of axial forces, for the case of constant pile temperature the presence of the rest phase has a small impact where the axial forces increase slightly. However, lower axial forces are found for TS3 since the temperature has a continuous sinusoidal trend of variation similar to the soil temperature variation in the shallower zones and at the surface. The analysis of Figures 4.12a and 4.12b shows that the stabilized thermal forces generated after three cycles for case TS3 are almost equivalent to those generated due to constant pile temperature just after the first cycle for cases TS0, TS1 and TS2.

All these calculations performed with a simple constitutive law for the ground underline the important role of the thermal solicitations on the thermo-mechanical behaviour of an energy pile. The temperature amplitude is a key parameter in the analysis and the design but the temperature variation rate seems to be more important: sudden and instantaneous thermal variations induce very high values of additional axial forces and do not permit a stabilization of the pile settlement with the cyclic thermal solicitations. On the contrary smooth temperature variations induce lower values of additional axial forces and a stabilization of the pile settlement. These results show that the cyclic soil-pile interface behaviour is very complex: very different numerical results can be obtained by considering apparent similar thermal variations.

Choosing either TS0, TS1 or TS2 as a thermal solicitation type for energy piles design, leads to higher displacements and axial forces and to a too conservative approach. Case TS3 with continuous sinusoidal pile temperature seems to be more realistic, avoids conservatism and thus the over design of energy piles. This as a consequence, affects the design of the energy pile and may reduce initial investment costs. On the other hand, from a practical point of view, adopting case TS3 is time consuming and not very common in the engineering practice. Adopting case TS0 for only four thermal cycles is sufficient for the design of energy piles in terms of displacements and additional axial forces, since these latter are close to those obtained by considering a continuous sinusoidal pile temperature. Case TS0 could be only adopted with a very cautious choice of the temperature variation.

4.8 Impact of pile head fixity

The pile end restraints represented by the connection with the super structure and applied mechanical loading at the pile head on one hand, and the presence of stiff bearing layer at the base on the other hand; influence the mechanical behaviour of piles. The variation of the pile axial forces and strains strongly depends on its end restraints. As a thermal load is imposed into

the pile to simulate energy piles, then in addition to the thermal contractions and dilations induced by this load causing modifications in its behaviour, the presence of end restraints will also affect its global thermo-mechanical behaviour (Amatya et al. 2012, Suryatriyastuti 2013, Saggu et al. 2015, Bourne-Webb et al. 2009). Energy piles being connected to the super structures, means that they are partially or totally fixed at their heads and thus their head fixity should be taken into account while performing their thermo-mechanical design. For this reason, in this section, the impact of restrained pile head fixity coupled with the various types of thermal solicitations (TS0R, TS1R, TS2R, TS3R where R stands for restrained pile head) is studied to better understand their behaviour.

4.8.1 **Case TS0R**

High axial stresses are obtained at the pile head due to the fixed head condition; the induced thermal stresses range between -87 % and 15 % of the mechanical load during cooling and heating respectively (Figure 4.13). Slight differences are found when reversing heating and cooling cycles. This difference is remarkable only at the end of the first cooling phase where the axial stress decreases in the case of reversed order.

Smooth thermal axial force increase is registered for both thermal cases as shown in Figure 4.14 that presents the variation of the thermally induced axial force in the upper pile zone, and after three thermal cycles, the difference between both becomes negligible.

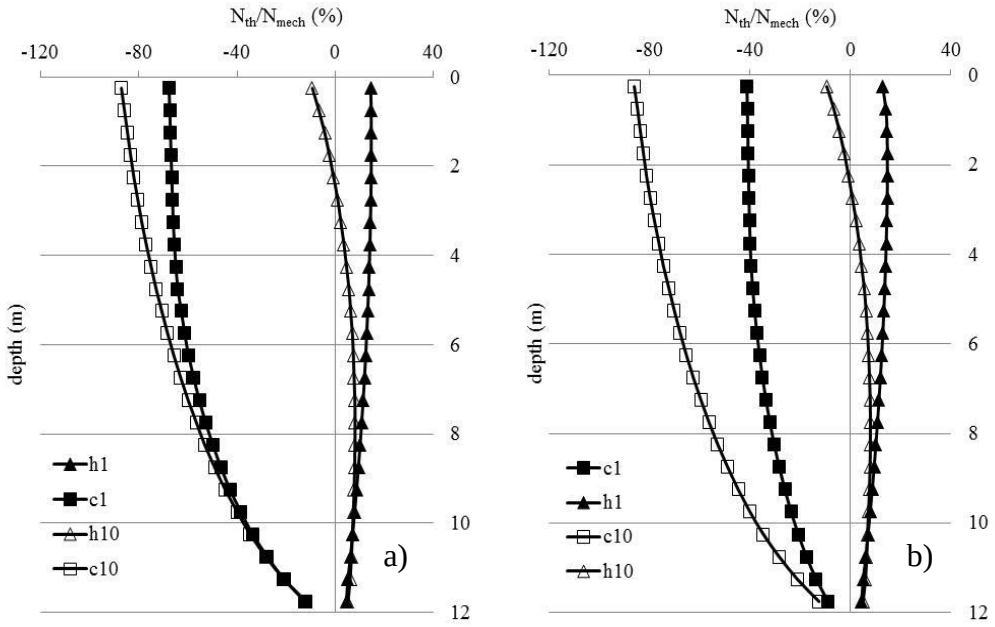

Figure 4.13 Variation of the axial stress for the fixed pile head a) TS0R b) TS0R with reversed order.

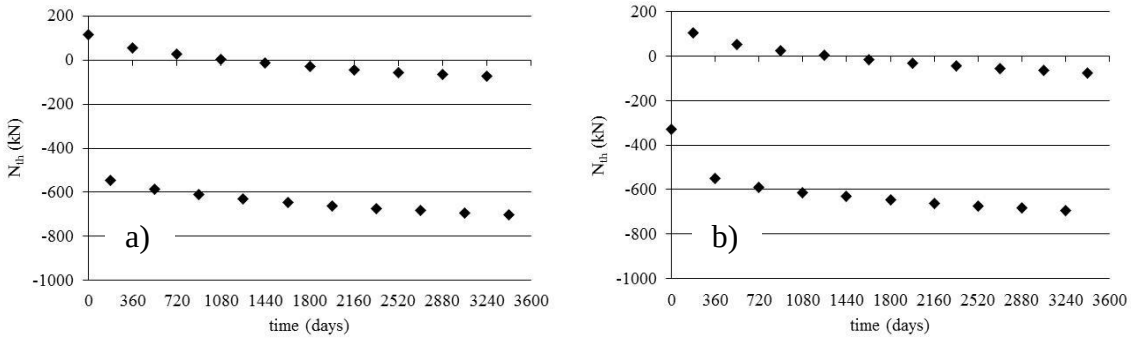

Figure 4.14 Variation of the thermal axial force with time for the fixed pile head a) TS0R b) TS0R with reversed order.

4.8.2 **TS1R and TS2R**

Figure 4.15a and 4.15b shows the variation of the thermal axial stress for TS1R and TS1R with reversed order of heating and cooling phases respectively. Similar axial stress variations to those obtained for TS0R are found for TS1R. On the other hand, Figure 4.15c and 4.15d presents the variation of the thermal axial stress for case TS2R and TS2R with reversed order. Generally, higher axial stresses are induced in case TS2R compared to the previous thermal cases. Tensile

stresses are generated in the upper zones at the end of the tenth cooling cycle. These tensile stresses don't exceed 0.36 MPa and thus are lower than the tensile strength of concrete (1.2MPa). However, they should be taken into account at the design stage of energy piles. Moreover, having different thermal and mechanical loads may pose a threat regarding the tensile failure and the development of cracks, then special attention should be paid regrading this issue.

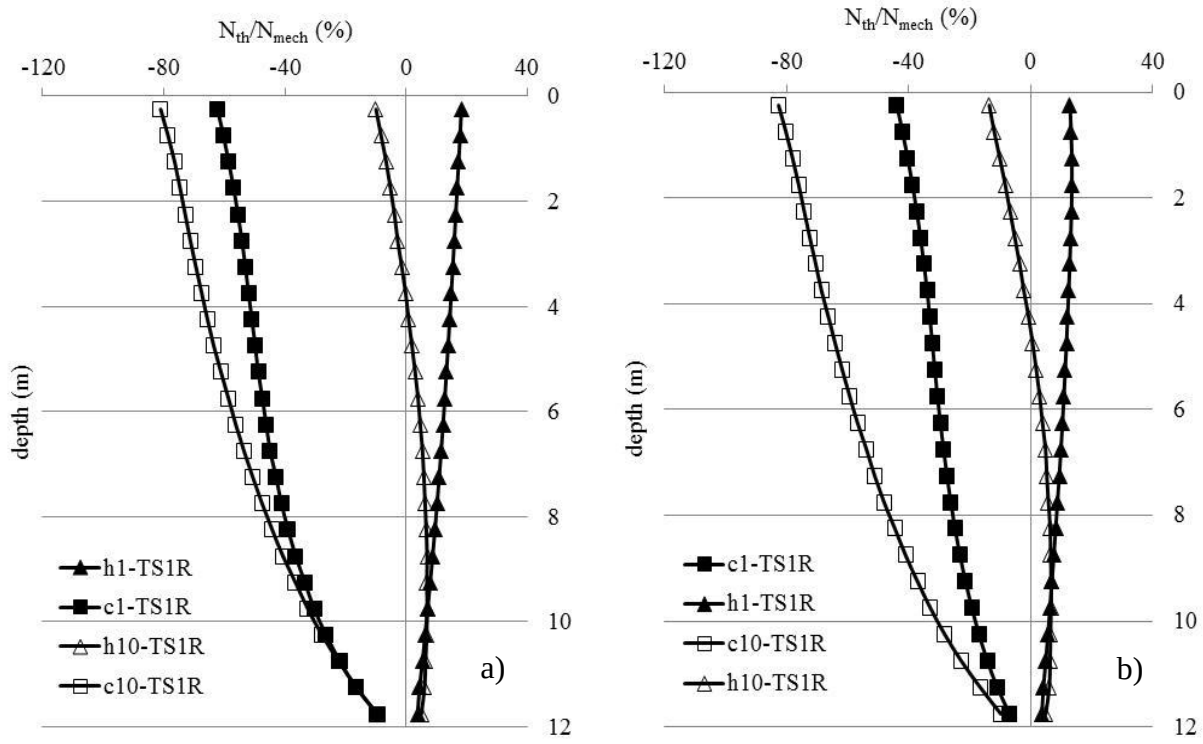

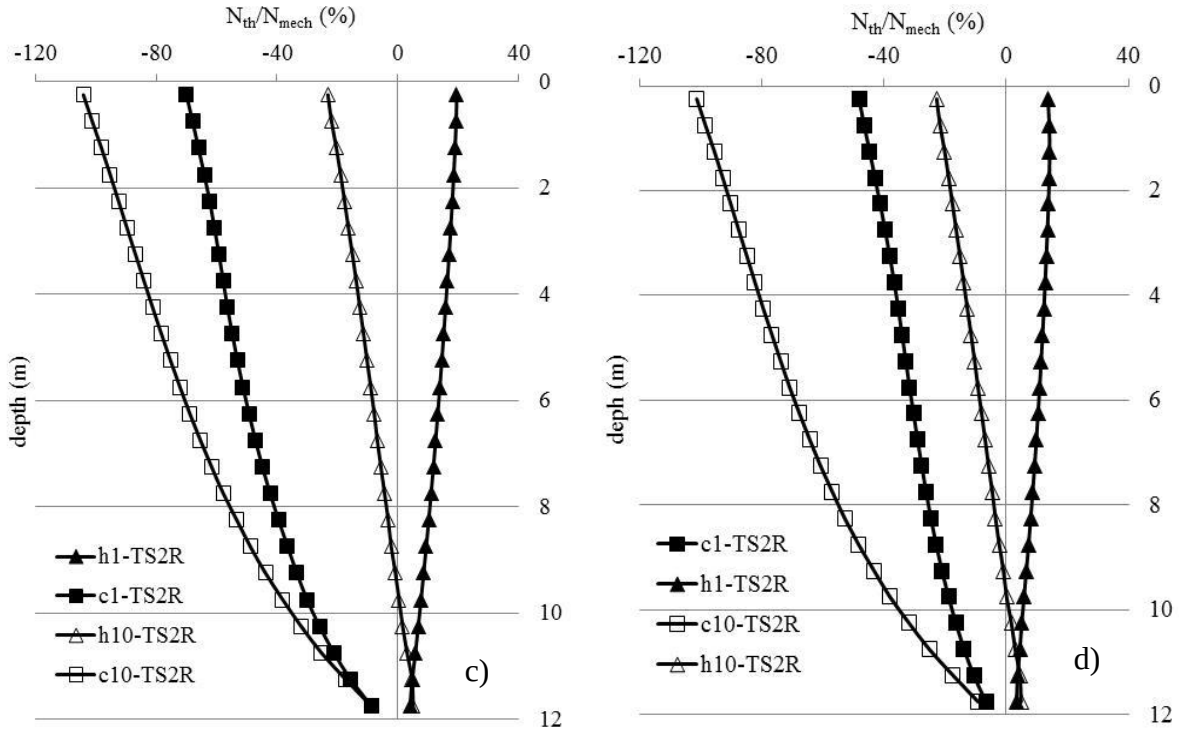

Figure 4.15 Variation of the axial stress for fixed pile head a) TS1R b) TS1R with reversed order c) TS2R d) TS2R with reversed order.

Figure 4.16 represents the variation of the thermally induced axial force in the upper zone of the pile. It can be said that after two thermal cycles, the impact of the thermal load history disappears for TS1R and TS2R; which is similar to the results obtained for the case of free pile head.

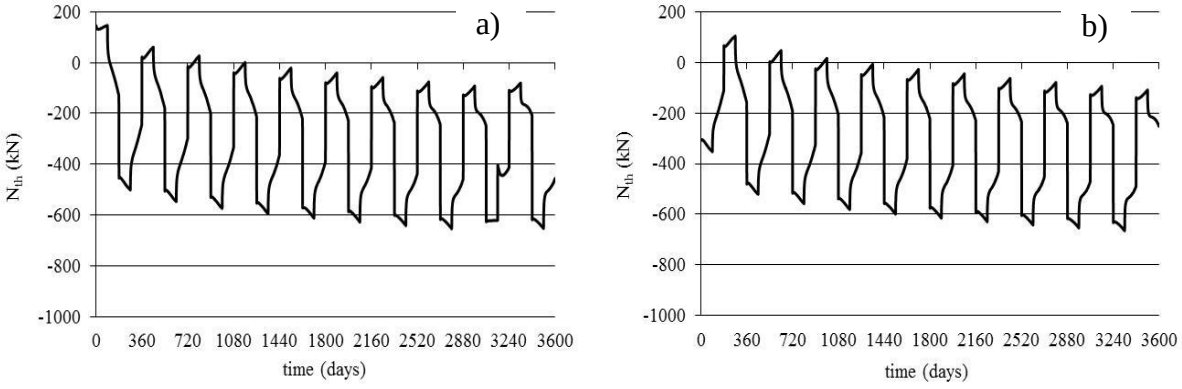

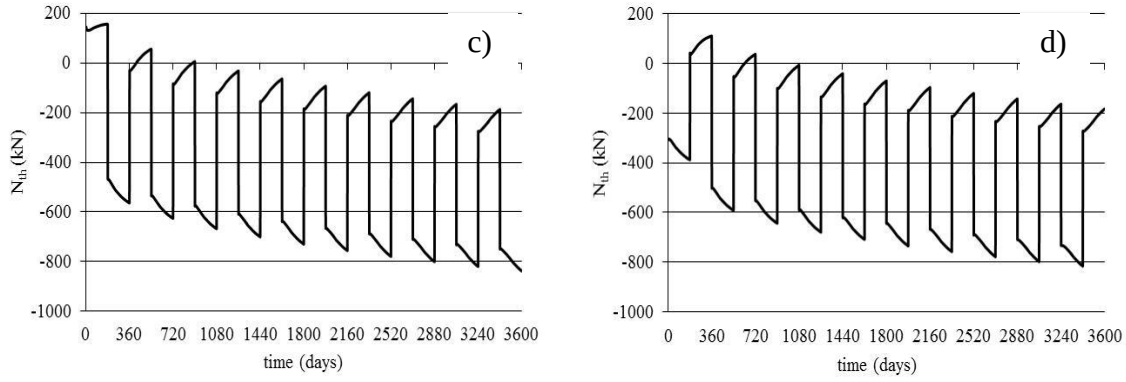

Figure 4.16 Thermally induced axial force for fixed pile head a) TS1R b) TS1R with reversed order c) TS2R d) TS2R with reversed order.

4.8.3 **TS3R**

With continuous sinusoidal variable pile temperature, axial stresses induced by thermal loads significantly show lower values compared to cases TS0R, TS1R, and TS2R as presented in Figure 4.17. The normal axial stress does not exceed 56% of the mechanical stress during cooling, and 20% during heating.

Almost from the second cycle, the variation of the thermal axial force at the upper zone stabilizes with time (Figure 4.18).

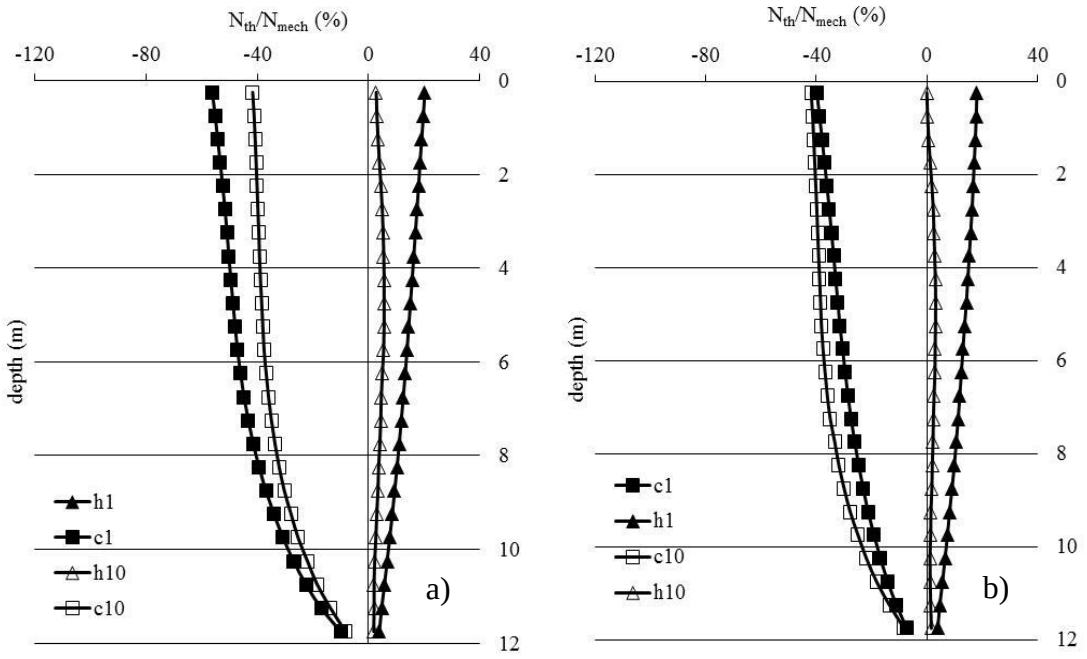

Figure 4.17 Variation of the axial stress for fixed pile head a) TS3R b) TS3R with reversed order.

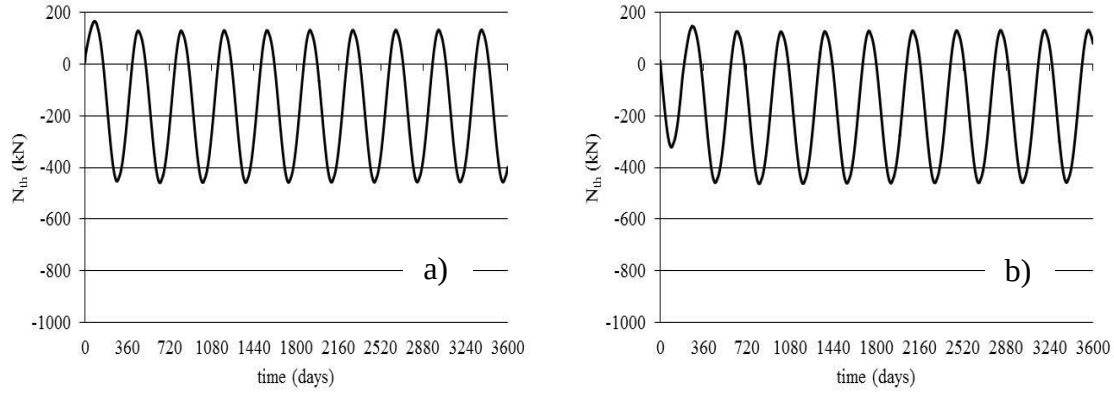

Figure 4.18 Thermally induced axial force for fixed pile head a) TS3R b) TS3R with reversed order.

4.8.4 **Comparison between different pile head fixities under variable thermal loads**

Regarding the impact of various types of thermal solicitations on the mechanical behaviour of fully restrained head pile, it is found that case TS2R without rest phases has the highest induced axial stresses. Tensile stresses appear in this case and require attention while designing energy piles. Case TS0R with imposed strains gives a general idea about the distribution of the axial

forces but it could underestimate the axial forces depending on the real type of imposed thermal solicitation.

Regarding the influence of the end-restraint on the mechanical and thermal behaviour of energy piles, it is clear that in the case of fixed pile head, the presence of the rest phase affects the distribution of axial forces and could not neglected (Figure 4.8 and 4.15). Adding to this, rapid stabilization of the axial stresses occurs almost after the first cycle for TS3R in the case of fixed pile head, and it is worth noting that the stabilized values for case TS3R are equivalent to those obtained during the first cycle for other cases (TS0R, TS1R, and TS2R), however for the case of free pile head, after three thermal cycles, the normal stress for TS3 stabilizes and becomes equivalent to the stress generated after the first cycle in TS0, TS1, and TS2.

4.9 Influence of soil thermal and thermo-mechanical properties

Soil surrounding energy piles affects directly their mechanical behaviour. Mechanically, the presence of stiff soil layer beneath the pile or/and the plastic properties of the soil would absolutely affect the soil structure interaction through the mobilization of shaft friction and base resistance. These would influence the thermal contractions and dilatations of the energy pile and thus its mechanical behaviour.

Thermally, the soil thermal properties and specifically its thermal conductivity and specific heat capacity play an important role regarding the thermo-mechanical behaviour of energy piles since they affect the thermal exchange process between the soil and the concrete piles. On the other hand, the soil thermo-mechanical property which is its thermal expansion coefficient affects the structural behaviour of energy piles (Bodas Freitas et al. 2013, Bourne-Webb et al. 2016a). In this context, Bourne-Webb et al. (2016a) confirmed that the coefficient of thermal expansion of the soil surrounding energy piles affects their mechanical behaviour especially for moderately to highly over-consolidated clay and granular soils.

This section is devoted to study the influence of the soil thermal properties on the mechanical behaviour of free energy pile through the assessment of the variation of the pile head displacement and normal forces.

Four different cases were considered as listed in Table 4.3 and are compared to the reference case that is studied in the previous sections. In each case, one value or more of the thermal parameters is varied to configure its influence on the mechanical behaviour of the energy pile.

Table 4.3 Thermal parameters of the four studied cases.

	λ (W/m.K)	C_p (J/kg.K)	α_T ($^\circ C^{-1}$)
Case a	2	1550	$10x10^{-6}$
Case b	2	2100	$5x10^{-6}$
Case c	3	1550	$5x10^{-6}$
Case d	3	2100	$5x10^{-6}$
Reference case	2	1550	$5x10^{-6}$

4.9.1 **Pile head displacement**

Figure 4.19 represents the variation of the head displacement for each case with respect to the reference case. The results illustrate that increasing the thermal conductivity (case c) and the specific heat capacity (case b) by 50% and 35% respectively leads to a slight variation in the pile head displacement especially in the first two cycles and beyond the second cycle, the impact becomes negligible (Case b, c, d). On the other hand, doubling the thermal expansion coefficient of the surrounding soil (case a) in a way that it still falls in the possible range of values for granular soils (Mukhopadhyay et al. 2007), this leads to remarkable variations in the pile head displacement. In the first two cycles, the head displacements increases largely by around 45%, and then starts decreasing till stabilization at values higher by 25% from those obtained in the reference case.

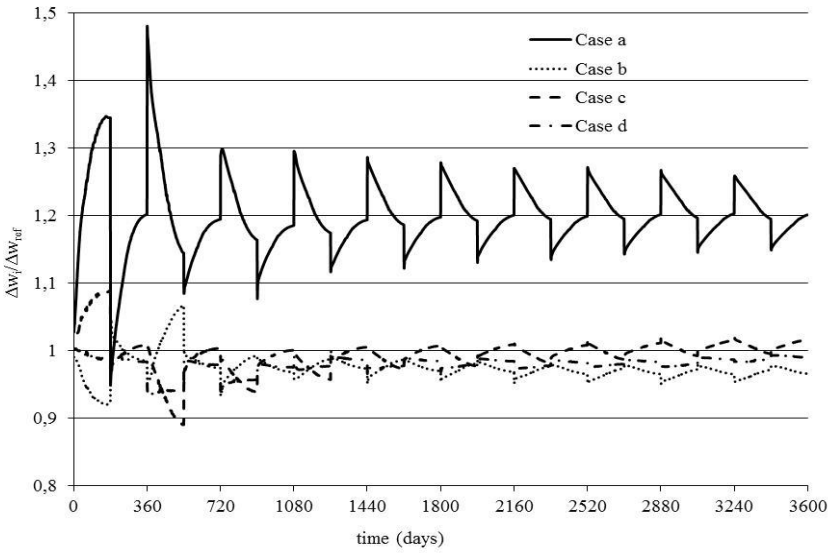

Figure 4.19 Variation of the pile head displacement for the four cases with respect to the reference case.

Figure 4.20 shows clearly how the displacement in the vertical direction is affected when the soil thermal expansion coefficient varies. It represents the variation of the vertical displacement at the end of the tenth cooling phase. As the soil experience higher volumetric deformations in case a, the shear stresses at the pile-soil interface will be affected and cause higher deformations along the pile length.

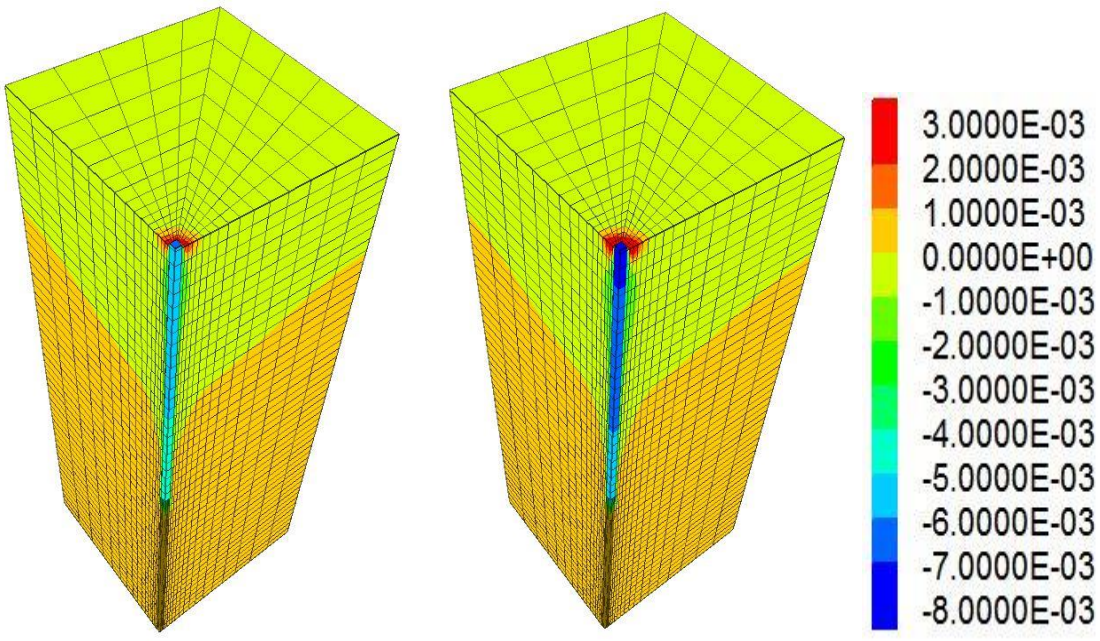

Figure 4.20 Vertical displacement (in m) at the end of the tenth cooling phase for a) reference case (α_T=5x10^{-6}°C^{-1}) b) case a (α_T=10x10^{-6}°C^{-1}).

4.9.2 **Normal force distribution**

The distribution of the axial normal forces along the pile length proves to be dependent on the thermal properties of the surrounding soil. Figure 4.21 presents the variation of the axial forces at the end of the first and tenth thermal phases for the cases presented in the above table and for the reference case. In contrary to the pile head displacement variation, for cases b, c, and d, during the first cycles, the impact of increasing the thermal properties appears to have negligible influence. At the end of the tenth cycle, this influence arises but still can be considered negligible since it does not cause a variation greater than 2%. For case a, the impact of increasing the thermal expansion coefficient is clear. During heating, this leads to a decrease in the compressive stresses and could lead to the generation of tensile axial stresses depending on the applied thermal load; these results confirm those obtained by Bourne-Webb et al. (2016a) and Bodas Freitas et al. (2013). On the other hand, during cooling, the opposite occurs, higher soil thermal expansion coefficient leads to decrease the tensile stresses and produces compressive stresses. The significant impact of the thermal expansion coefficient on the mechanical behaviour of energy piles is related to the volumetric changes of the soil under the effect of the applied thermal load and the heat exchange process. These volumetric changes affect the soil-pile interface and therefore influence the pile behaviour.

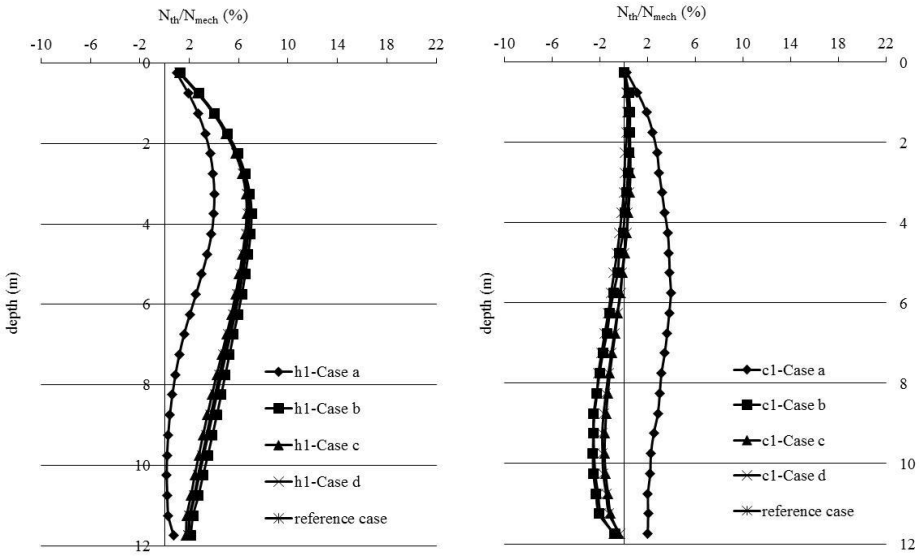

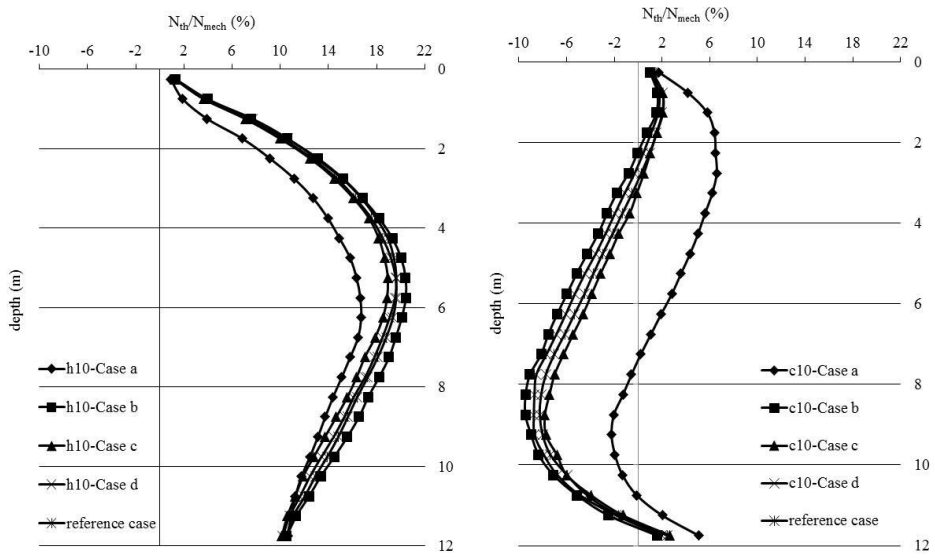

Figure 4.21 Variation of the axial normal forces of the four cases and the reference case.

Generally, for the different considered cases, it can be said that the soil thermal expansion coefficient and thus its volumetric variation affected by thermal loading must not be neglected while designing energy piles as this may lead to under or over design depending on other thermal and mechanical assumptions and conditions.

4.10 Recommendations for the energy pile design

This section summarizes the main conclusions for the choice of the thermal solicitations to consider for the design of an energy pile:

- Regarding pile displacements, the interaction between heating and cooling phases, rather than separate heating and cooling phases should be considered. Separate calculations can lead to wrong views; they underestimate the evolution of the displacement during each thermal loading phase.
- Regarding axial force distribution, the interaction between heating and cooling phases can be neglected. Nevertheless, if only two separate calculations are done, one for heating and one for cooling, it is important to underline that the additional axial forces

are underestimated. In order to correct this bias, large variations of temperature have to be considered.

- Transient calculation can be considered not necessary, but it enables to improve the design, especially to have a good assessment of additional axial force caused by the imposed thermal loads and to account for the impact of the thermal diffusion with time.
- The role of the rest phase can be neglected from a mechanical point of view; it has almost a slight influence on the global response of the energy pile for the case of free pile head. However, for a fully fixed pile head, the impact of the rest phase could not be ignored.
- Modelling an energy pile subjected to uniform constant temperature variations for four thermal loading cycles is equivalent to the stabilized behaviour of an energy pile subjected to sinusoidal variable temperature, and thus this is sufficient for the design of free head energy piles. On the other hand, for fixed pile head, one thermal loading cycle of uniform constant temperature is enough to simulate the same stabilized behaviour induced by sinusoidal variable temperature.
- Special attention should be paid to the soil thermal properties and specifically its thermal expansion coefficient to avoid incorrect predictions for the mechanical behaviour of energy piles.

4.11 Conclusion

This chapter deals with the behaviour of energy piles under different combinations of thermal loadings. It highlights the influence of the choice of the thermal solicitation on the design of energy piles. Despite of the head restraint condition, piles subjected to continuous sinusoidal temperature consistent with the external air temperature variation prove to be more safe leading to lower axial displacements and forces; this is due to the non-sudden temperature variation compared to the cases where constant temperature is imposed into the pile. In this manner, the

presence of a rest phase is found to have a slight impact that can be considered to be negligible on the behaviour of free head energy piles, whereas for the fixed head energy piles, the influence of the rest phase is remarkably favorable and should be accounted for. Nevertheless, detailed study could be conducted regarding the duration of the rest phases in climates where they are needed, to better understand their impact on the structural behaviour of energy piles. In this manner, imposing a constant temperature under transient conditions and fixed thermal strains prove to be conservative. Regarding the thermal properties of the soil, the volumetric changes that occur due the thermal load should not be neglected, and attention should be paid for the estimation of the soil thermal expansion coefficient.

The design of energy piles remains a complex exercise that requires considering thermal and mechanical solicitations. In addition, further studies should be carried to analyze the influence of the thermal solicitation type on the behaviour of group of energy piles.

CHAPTER 5 : Thermo-mechanical behaviour of energy diaphragm walls

5.1 Introduction

Energy diaphragm walls are gaining interest nowadays due to the augmentation in their usage and implementation in several projects and in different countries as in Italy, UK, and Austria (Cornelio et al. 2016, Di Donna 2016, Amis et al. 2010, Brandl 2006), and recently in France for the construction of the new Paris metro stations. Metro stations require bearing structural elements capable to retain soil stresses. For this reason, diaphragm walls could be used as bearing elements, and thus could be accompanied by heat exchanger tubes to act as energy walls. Mechanically, their structural behaviour affected by imposed thermal loads and the thermal exchange with the surrounding soil is rarely studied till now. Among the few studies, Sterpi et al. (2016) confirmed through different conducted numerical models that the influence of thermal load does not lead to detrimental effects but only requires to be considered in the design. Moreover, Bourne-Webb et al. (2016b) studied the impact of different thermal boundary conditions and soil properties on the mechanical behaviour of energy walls through evaluating the bending moments and the lateral displacements. Habert & Burlon (2015) highlighted on the influence of thermal loading on the mechanical behaviour of energy wall.

Chapter 3 dealt with the thermal performance of energy diaphragm walls. This chapter focuses on the impact of various thermal loading types and different soil thermal and thermo-mechanical

properties on the structural performance of energy diaphragm walls used for the construction of metro stations. On the other hand, a special attention is paid regarding the impact of the soil constitutive model used in non-linear calculation. Thus, it is interesting to use complex constitutive model capable to take into account shear and volumetric hardening acting during the diaphragm wall installation.

5.2 Numerical modelling

Energy diaphragm walls are modelled numerically by the aid of the finite element numerical software, Plaxis 2D. They are modelled through a fully coupled thermo-hydro-mechanical analysis, represented by fully coupled flow-deformation and thermal transient calculations. The geometry of the model, as well as the mechanical properties of soil and concrete are adapted from the work conducted by Habert & Burlon (2015), as they assure the mechanical validity of the model. Table 5.1 presents the values of the mechanical parameters of soil and concrete used in the model. However, regarding the thermal properties of soil and concrete, they are those used in the hydro-thermal model presented in Chapter 3. Table 5.2 presents the assumed values of the thermal parameters of soil and concrete.

Table 5.1 Mechanical parameters of concrete and soil.

	Concrete	Soil
Density ρ (kg/m^3)	2500	2000
Elastic modulus E (MPa)	20000	20
Porosity n	0.25	0.25
Friction angle φ	-	35
Dilation angle	-	5
Cohesion (kPa)	-	1
Interface coefficient	-	0.67

Table 5.2 Thermal parameters of concrete and soil.

	Concrete	Soil
Thermal conductivity λ (W/m.K)	1.8	2
Specific heat capacity (J/kg.K)	880	1000
Thermal expansion coefficient ($^{o}C^{-1}$)	$12x10^{-6}$	$5x10^{-6}$

Due to symmetry, half of the domain is modelled knowing that water flow is assumed to be static with the water table located at the bottom of the excavation. Figure 5.1 represents the numerical model and the simulated mesh. The model consists of a diaphragm wall of length 20 m and of 10 m embedment depth with 1 m thickness. A strut is situated at 2.5 m depth and a slab at 9.5 m depth. Regarding the boundary and initial conditions; mechanically, standard fixities represented by fully blocking the displacement at the bottom and horizontally blocking the displacement on the lateral sides are assumed. Thermally, initial temperature is set to 14°C and the same assumptions used for the numerical model in Chapter 3 are assumed here (surface temperature, thermal condition at the bottom, etc.). It is important to note that closed thermal boundaries are assumed at the interface with the inside metro station.

The construction of the energy diaphragm walls is done through the staged construction method which consists numerically of the main following parts. The first step starts by mechanically activating the wall, then excavating till the first strut level (here 2.5 m) through deactivating the upper soil zone and installing the strut through activating it. Following is the excavation till the base slab and installing the slab. After assuring the mechanical stability, thermal loads are imposed into the diaphragm wall for five consecutive cycles where each cycle lasts for one year.

It is worth noting that the strut and the slab are considered as non-thermo-active concrete elements; it is only the diaphragm wall that is thermally activated.

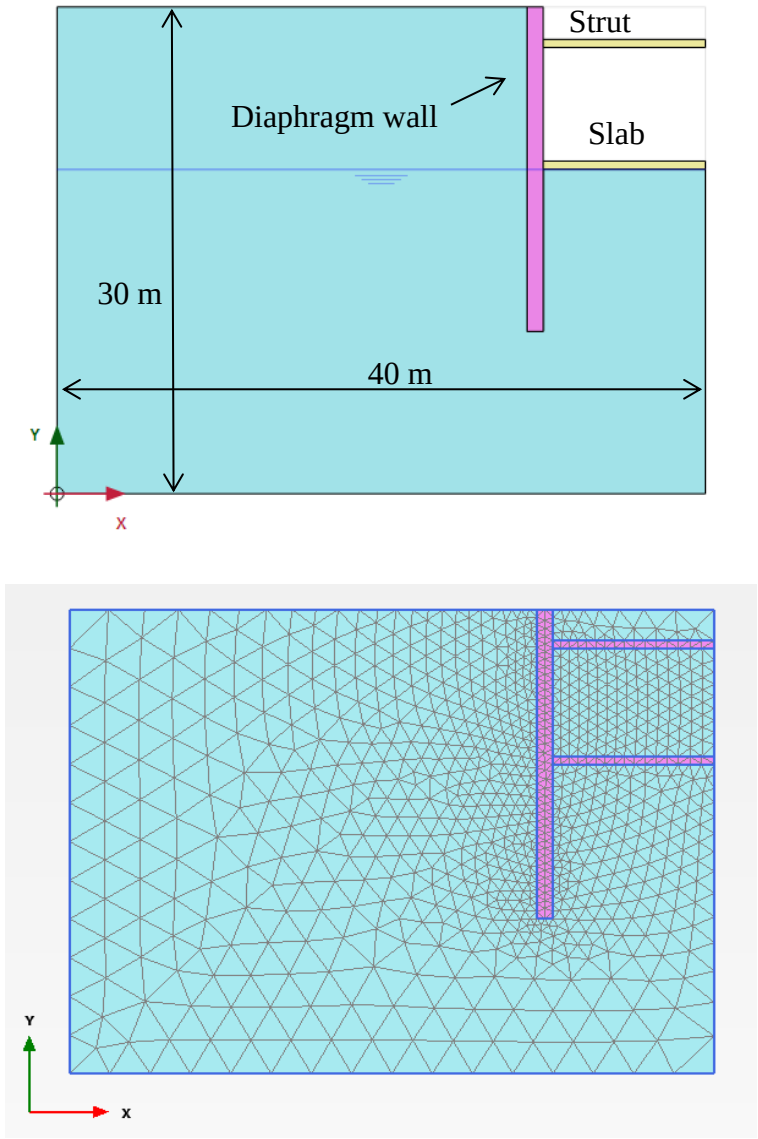

Figure 5.1 Geometry and the mesh of the model.

The diaphragm wall is supposed to behave thermo-elastically, while the behaviour of the soil follows Mohr-Coulomb failure criterion with non-associated flow rule.

5.3 Impact of thermal loading type on the mechanical behaviour of energy diaphragm walls

As the implementation of energy diaphragm walls is being popular recently, then several questions arise regarding the type of thermal load to be imposed into the walls and its duration. For this reason, and based on the results of the analysis done in Chapter 4, two types of thermal

solicitations, TS2 and TS3, are modelled in this section to evaluate the influence of the thermal loading type on the mechanical behaviour of energy diaphragm walls through assessing the variation of the structural forces. Moreover, to evaluate the influence of the thermal loading order, TS2 is considered with reversed order; the thermal phases are reversed in each cycle. As mentioned above, five consecutive cycles are modelled; each cycle consists of two thermal phases where the duration of each thermal phase is six months (Figure 5.2).

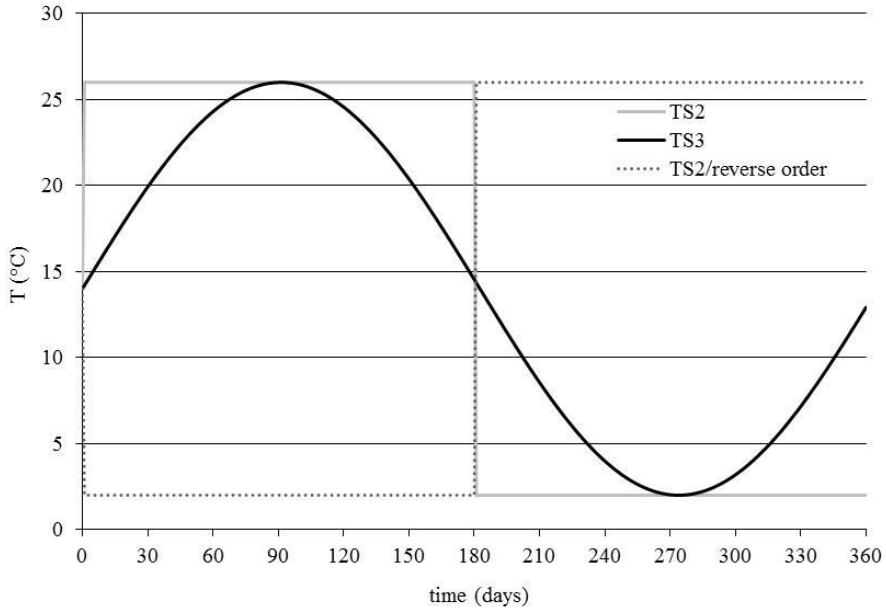

Figure 5.2 Different types of the considered thermal loads.

5.3.1 **Normal forces distribution**

Figure 5.3 represents the variation of the normal forces along the diaphragm wall for TS2 and TS2r with reverse order of heating and cooling phases. The normal forces are calculated along the wall's axis based on the variation of the vertical stresses. Figure 5.3 shows the variation of the axial forces at the end of the excavation phases (before thermally activating the wall), at the end of the first heating and cooling phases, and at the end of the fifth heating and cooling phases. In all the figures, h and c stand for heating and cooling respectively and the figure following the letter corresponds to the cycle number.

At the end of the excavation phases, compressive forces develop at the upper part of the wall, whereas tensile forces develop along its embedded part. With the thermal loads, negative forces indicating compression, develop during heating and positive forces indicating tension, appear during cooling. The normal forces distribution is not influenced by the cyclic thermal loading; this is illustrated by the negligible difference between the normal forces at the end of the first thermal cycle and those obtained at the end of the fifth thermal cycle. Slight difference is noticed between TS2 and TS2 with reversed order, thus the order of the thermal load proves to have a negligible impact on the distribution of axial forces along energy walls.

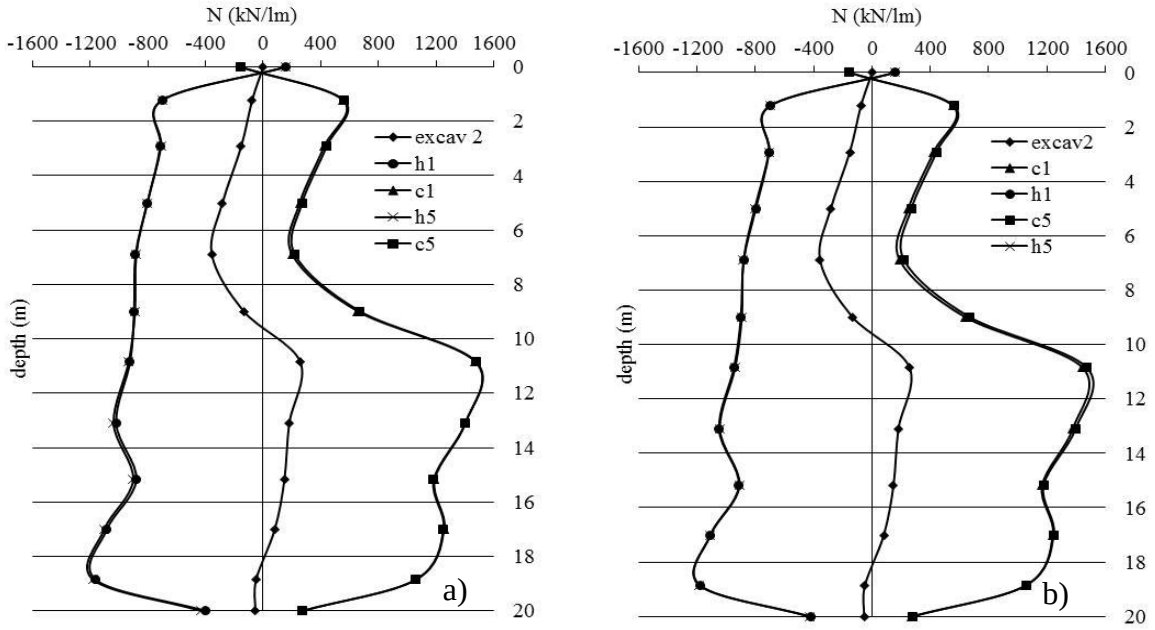

Figure 5.3 Variation of the axial normal forces along the diaphragm wall for a) TS2 b) TS2r.

Figure 5.4 represents the distribution of the axial forces for case TS3. In the case of sinusoidal variable temperature, the influence of the thermal loading becomes negligible. Moreover, no difference is noticed between the end of excavation phase and the thermal loading phases, since the temperature is not imposed brutally into the diaphragm walls as for the case of TS2. Compared to TS2, the axial force is lower and it is less than the half of that induced by TS2; it ranges between -400 and 400 kN/lm.

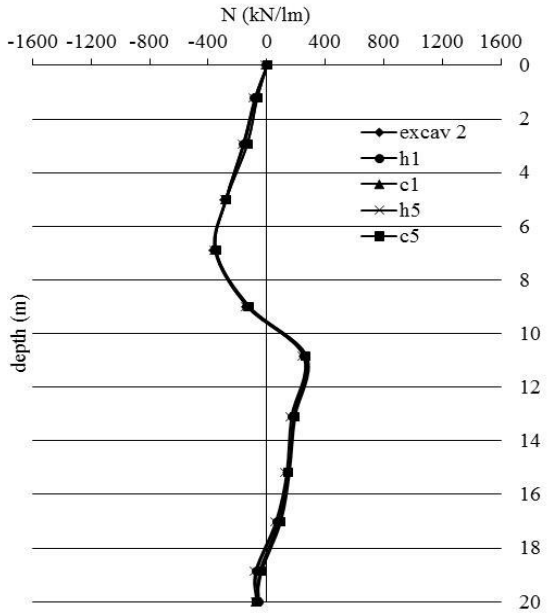

Figure 5.4 Axial normal force for case TS3.

5.3.2 **Shear forces**

Regarding the distribution of shear forces for the considered cases; Figure 5.5 represents their variation. The thermal loading type or its order proves to have no impact on the shear forces distribution. Adding to this, imposing continuous sinusoidal temperature variation into the wall does not lead to great modifications; only slight decrease in the shear forces is observed. These results agree with those obtained by Habert & Burlon (2015) regarding the shear forces variation. As for the normal forces, the shear forces are not influenced also by the cyclic thermal loading.

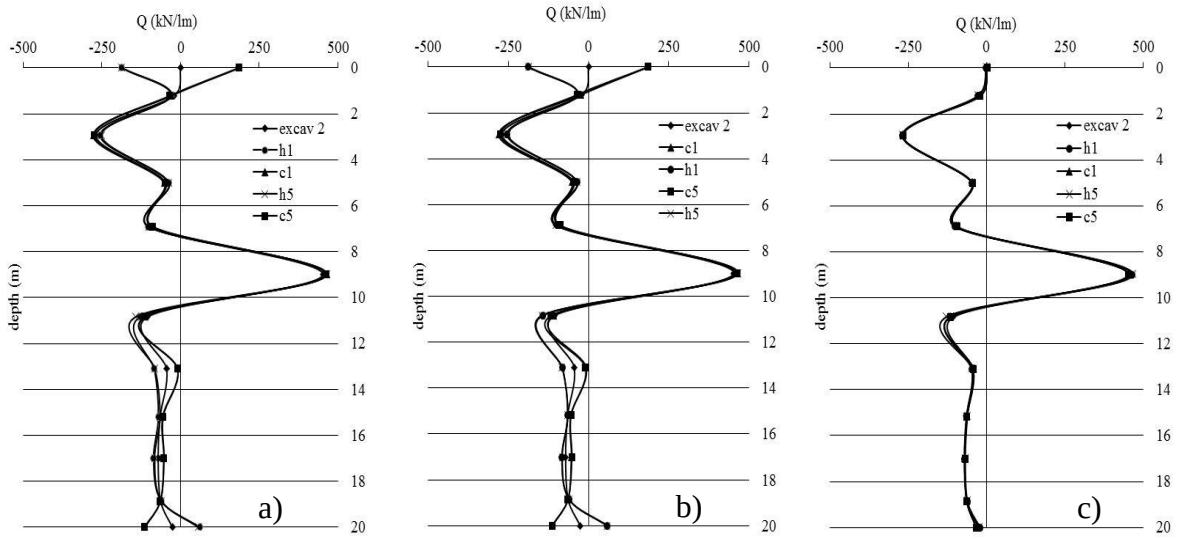

Figure 5.5 Shear forces along the diaphragm wall for a) TS2 b) TS2r c) TS3.

5.3.3 **Bending moment**

Figure 5.6 represents the variation of the bending moment along the wall length for TS2, TS2r, and TS3. As for the normal forces distribution, the bending moment shows no variation between TS2 and TS2r with reverse order; moreover, it is not affected by the cyclic thermal loading. It tends to develop positive moment during heating phases and negative moment during cooling phases. During heating, positive moment develops at the upper part since concrete expansion leads to the development of negative shear stresses at the interface that in turn leads to the development of positive moment; and the opposite occurs during cooling.

On the other hand, for TS3, the impact of the thermal loading disappears and lower moment is generated compared to TS2.

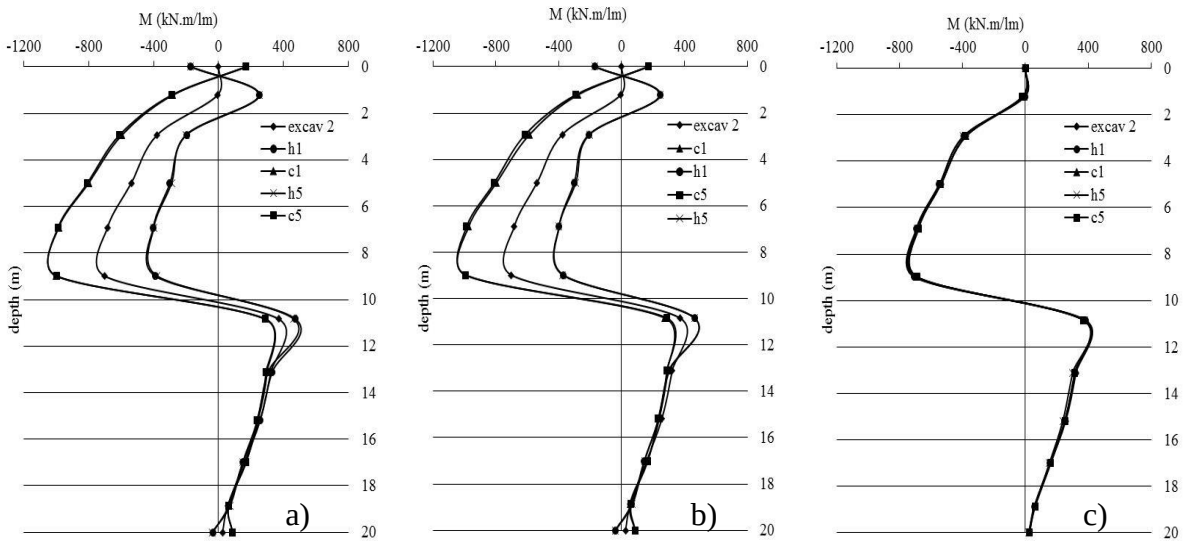

Figure 5.6 Bending moment of the diaphragm wall for a) TS2 b) TS2r c) TS3.

5.4 Impact of soil thermal properties on the mechanical behaviour of energy diaphragm walls

The soil thermal properties may affect the structural behaviour of energy diaphragm walls since they have a direct impact on the heat transfer between the soil and the concrete structures. In this section, case TS2 with constant wall temperature is considered as it represents the unfavorable case. Concerning the thermal properties of the soil, the thermal conductivity and the specific heat capacity are increased to 3 W/m.K and 2000 J/kg.K respectively. Compared to TS2 studied in the previous section, increasing the thermal conductivity of the soil by 50% and doubling its specific heat capacity does not lead to significant variations (Figure 5.7). This is in agreement also with the results obtained in Chapter 4 regarding the impact of the soil thermal properties on the mechanical behaviour of energy piles.

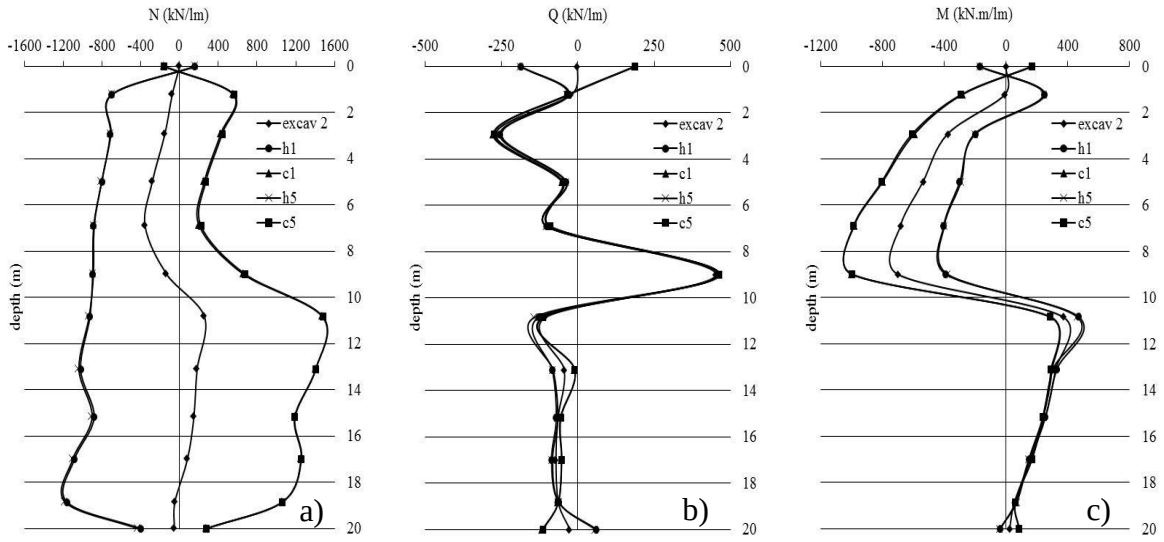

Figure 5.7 Variation of the a) normal forces b) shear forces c) bending moment of the diaphragm wall for TS2 with new soil thermal properties.

5.5 Impact of the soil thermo-mechanical property on the mechanical behaviour of energy diaphragm walls

Soil thermal expansion coefficient is a thermo-mechanical property that affects the interaction between the soil and the energy diaphragm walls and therefore it may influence the structural behaviour of the walls. Increasing the soil thermal expansion coefficient leads to some modifications regarding the distribution of the forces along the diaphragm wall length.

The soil thermal expansion coefficient assumed in this section is $10x10^{-6}$ $^{\circ}C^{-1}$, which is the double of the original value. Slight variations in the distribution of the normal and shear forces are obtained. However, for the bending moment, it tends to increase by 39% and decrease by 22% at different positions (Figure 5.8). It is worth noting that the position of the maximum bending moment remains intact since the temperature is imposed uniformly along the wall length. Similar results are obtained by Bourne-Webb et al. (2016b) who studied the impact of different soil thermal expansion coefficient values on the mechanical behaviour of energy diaphragm walls. They found variations of 45% in the bending moment for a soil having double of the concrete thermal expansion coefficient compared to a thermally inert soil.

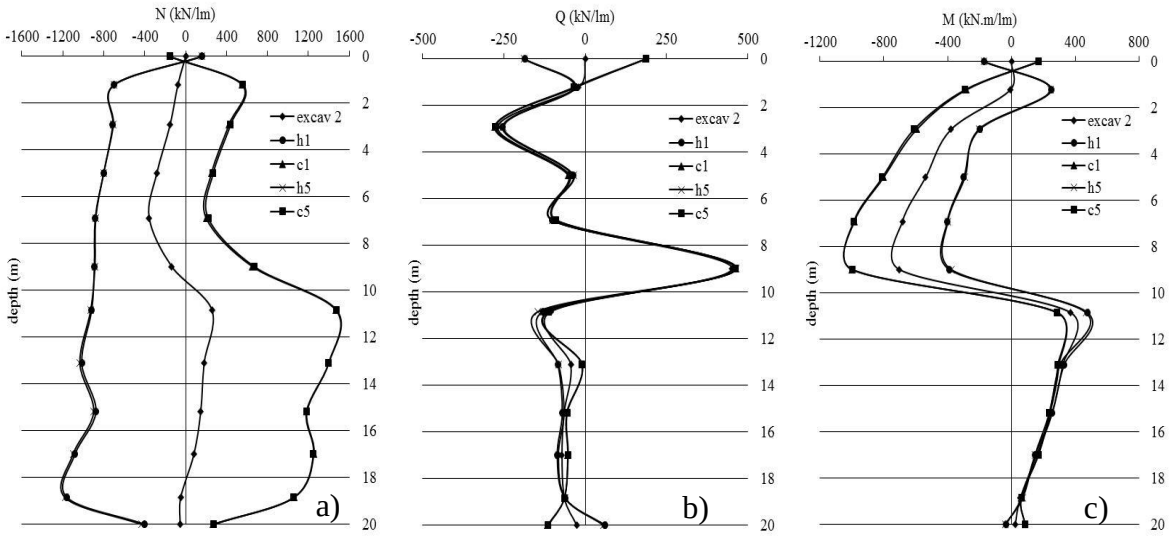

Figure 5.8 Variation of the structural forces along the diaphragm wall for $\alpha=10x10^{-6}\ ^{\circ}C^{-1}$.

5.6 Accounting for the soil hardening

The previous sections model the mechanical behaviour of the energy diaphragm wall through assuming a simple constitutive law for the soil behaviour which is the elastic perfectly plastic law represented by Mohr-Coulomb. Herein, the hardening plasticity model is assumed for the soil behaviour in order to provide an idea about the impact of the soil constitutive law on the general behaviour of the system and to determine if it would affect the thermo-mechanical response of the diaphragm walls in return.

Compared to Mohr-Coulomb, the hardening soil model uses the theory of plasticity, includes soil dilatancy, and introduces a yield cap. Moreover, the hardening soil model is capable to describe the soil more accurately through using three different input stiffnesses; reference triaxial loading stiffness E_{50}^{ref}, reference oedometric stiffness E_{oed}^{ref}, and reference unloading/reloading stiffness E_{ur}^{ref}.

Thus, the soil behaviour is assumed to follow the hardening soil model. To achieve this aim, the first step is to calibrate the soil mechanical parameters in order to obtain the homogenous stress schemes. After trying several set of parameters, the following values summarized in Table 5.3

are considered as they show close response to that induced by the Mohr-Coulomb failure criterion (Figure 5.9).

Table 5.3 Values of the considered mechanical parameters.

	value
E_{50}^{ref}	27 MPa
E_{oed}^{ref}	27 MPa
E_{ur}^{ref}	55 MPa
m	0.5
K_0^{nc}	0.48

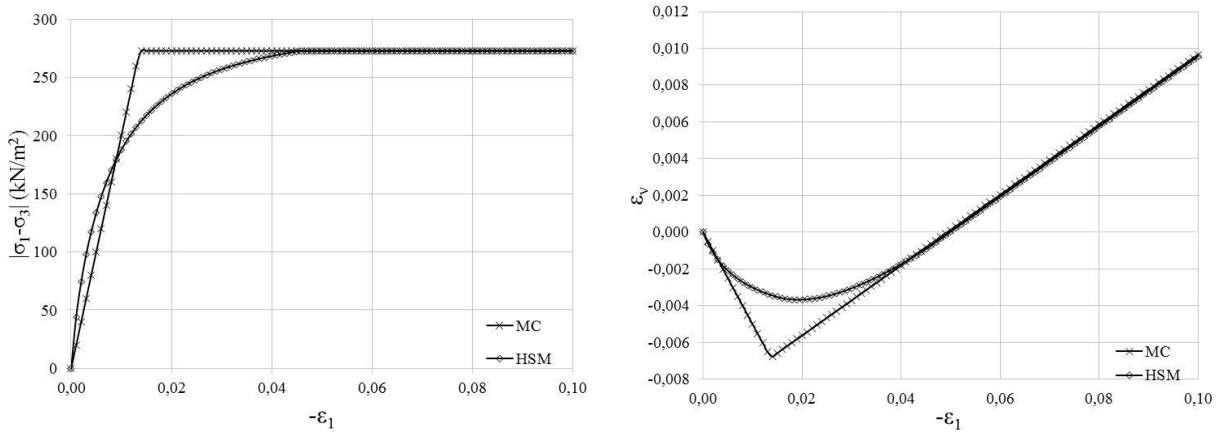

Figure 5.9 Variation of the a) principal stress difference and axial strain b) volumetric strain and axial strain.

After calibrating the soil mechanical properties, the numerical analysis starts following the same steps mentioned before which are summarized by the staged construction method followed by imposed thermal cycles.

In this context, it is worth noting that at the end of the last excavation step, the behaviour of the soil and the structural elements is different according to the assumed constitutive law as presented in the following figures. The deformed shape of the model is significantly distinct and the induced displacement decreases remarkably as the hardening soil model is applied (Figure 5.10); its maximum value reaches 4.4 cm compared to 10 cm induced when Mohr-Coulomb failure criterion is assumed. Briefly, it could be said that the hardening soil model provides more reliable and realistic predictions of the engineering system response.

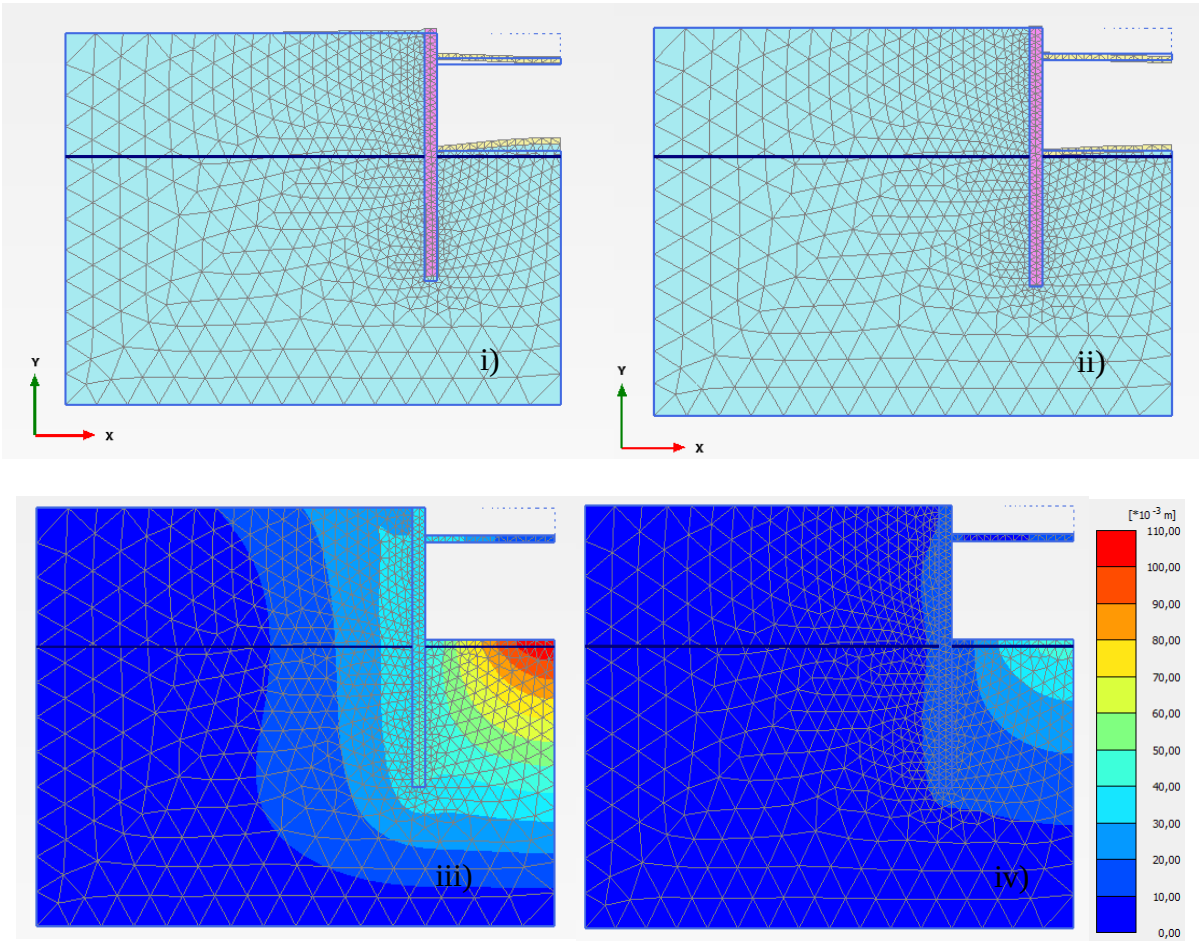

Figure 5.10 Deformed mesh and deformation contours for Mohr-Coulomb i and ii, and for Hardening soil model iii and iv.

On the other hand, the distribution of the structural forces along the wall is not the same for both types of constitutive laws (Figure 5.11). When hardening soil model is assumed for the soil behaviour, the structural forces decrease almost to the half compared to those when Mohr-Coulomb is considered.

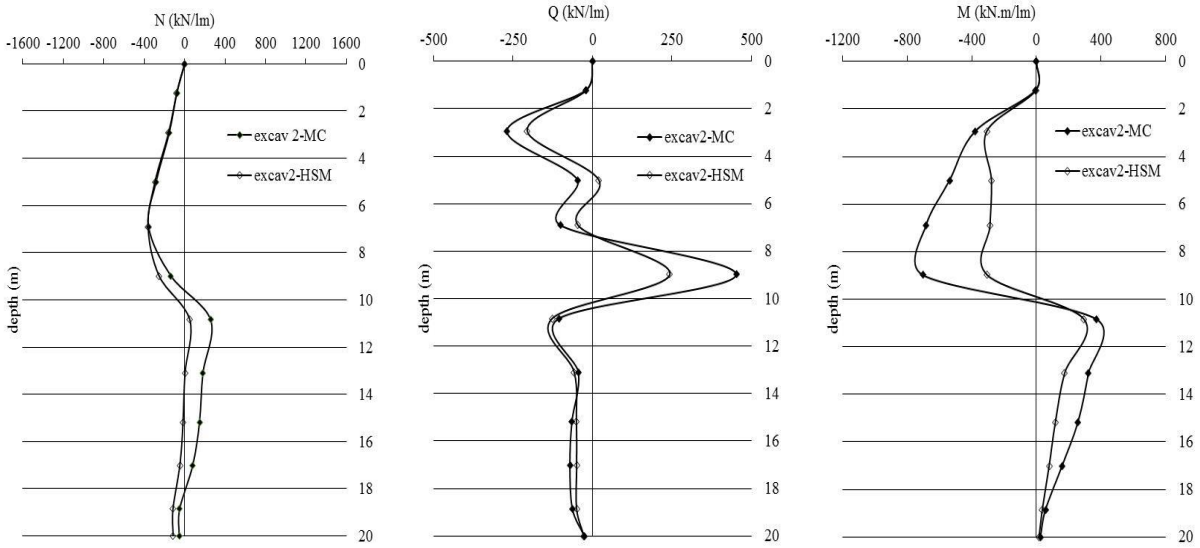

Figure 5.11 Variation of the normal force N, shear force Q, and bending moment M along the wall at the end of the second excavation phase.

Regarding the distribution of plastic zones, less failure points (Figure 5.12) are present when the hardening soil model is assumed; underneath the slab there are no failure points. Therefore, each type of constitutive law has led to specific soil and diaphragm wall mechanical response.

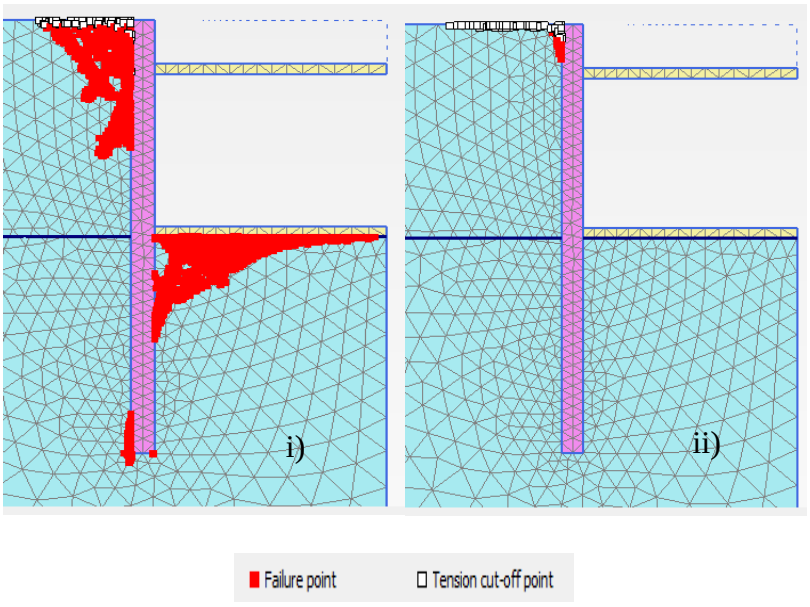

Figure 5.12 Distribution of the plastic zones in the soil for i) Mohr-Coulomb model ii) Hardening soil model.

Thereafter, the thermal solicitation TS2 is imposed in the diaphragm walls for five consecutive cycles. With the hardening soil model, the normal and shear forces and bending moments generated in the diaphragm wall are almost less than those obtained when Mohr-Coulomb is assumed. Even though the range of values for the variation of the normal and shear forces and bending moments are not the same, their profile of variation is almost the same. The influence of cyclic thermal loading is slightly detected especially during cooling phases; however the difference between the first and the last cycle can be considered negligible.

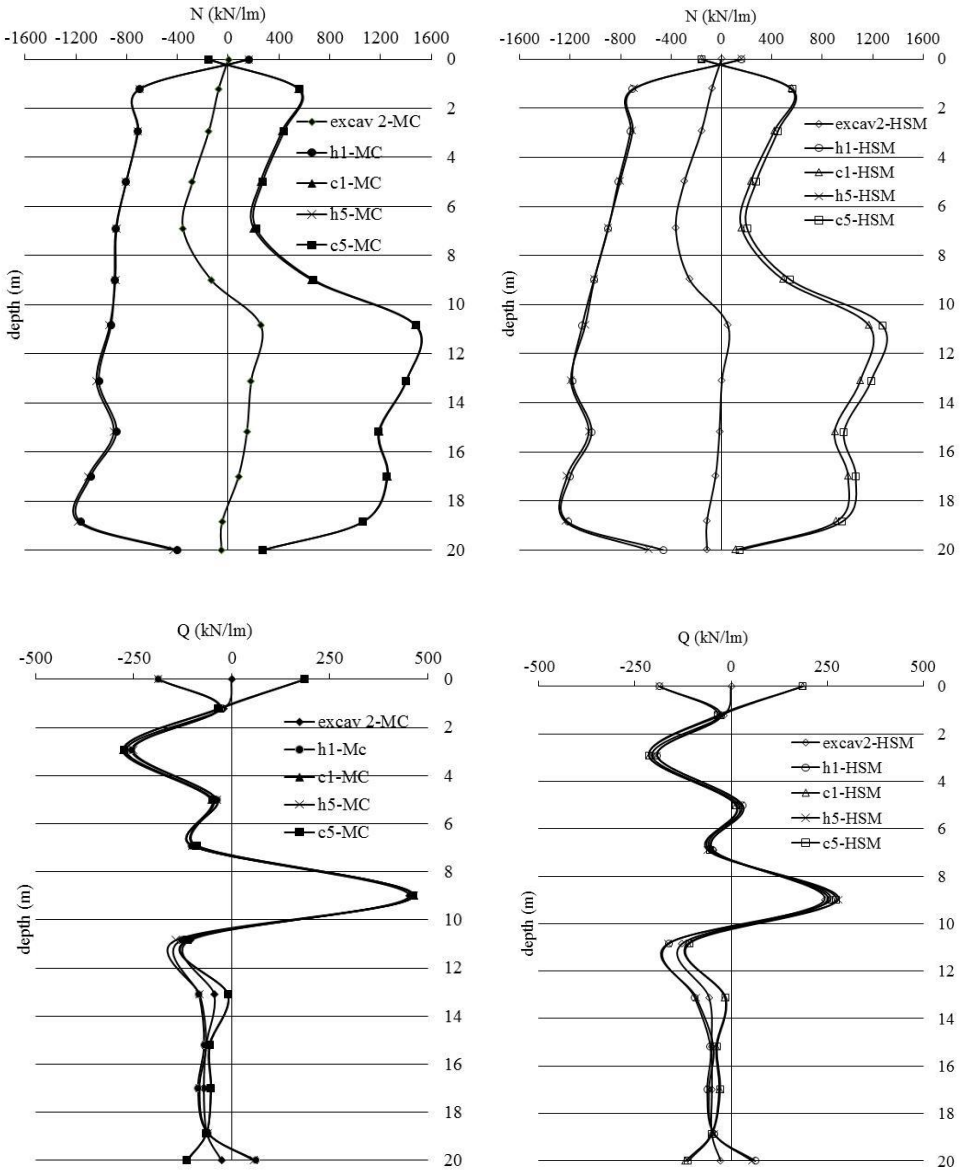

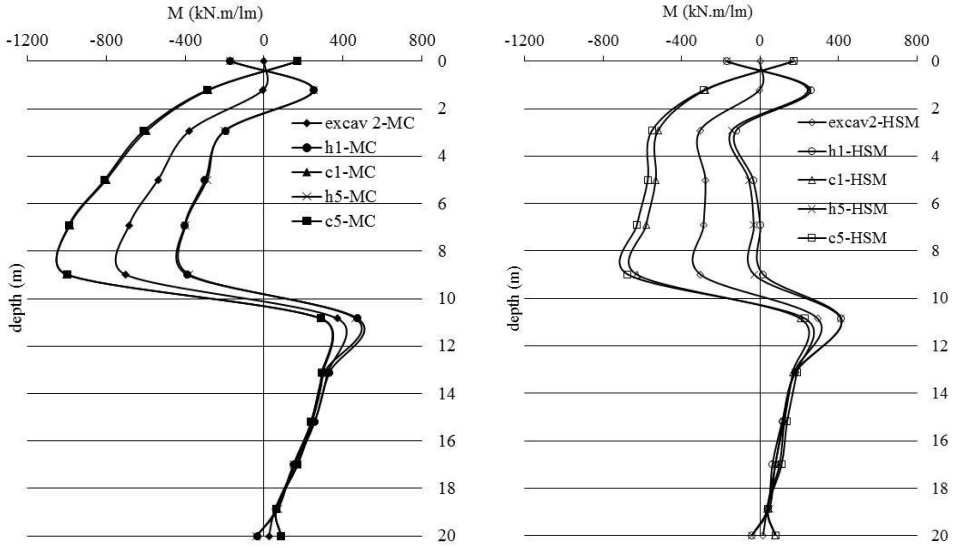

Figure 5.13 Variation of the normal and shear forces and bending moment for both constitutive laws.

Therefore, one can say that the impact of cyclic thermal loading is not pronounced even when the assumed soil model accounts for volumetric and shear hardening. Consequently, modelling one complete thermal cycle is sufficient to predict the thermo-mechanical response of the system.

5.7 Comparison between the studied cases

2D numerical models of energy diaphragm walls used for the construction of underground metro stations are conducted. Comparison between the different studied cases on two main levels derives the following conclusions:

- **Thermal load:** Regarding the order of the applied thermal load, it is found that the order of the thermal phases has almost a slight impact that can be neglected. On the other hand, for the type of the thermal loading, imposing continuous sinusoidal temperature has a slight influence on the mechanical behaviour of the energy walls compared to the case of applying constant temperature; lower axial forces and bending moment are obtained. This is related to the brutal temperature variations accompanied with the applied constant temperature.

- **Soil thermal and thermo-mechanical properties:** The soil thermal conductivity and its specific heat capacity appear to have no impact on the mechanical behaviour of the diaphragm wall. However, the soil thermal expansion coefficient leads to certain modifications in the distribution of the axial forces, and bending moment that reaches around 40% when the thermal expansion coefficient is doubled.

Regardless of the type of the thermal load or the soil thermal and thermo-mechanical properties, the following general observations can be noted:

- For all of the considered cases, at the strut and slab levels, there are remarkable variations of the normal and shear forces, and bending moment.
- Variations of the normal forces are more evident than those of the bending moment; confirming Sterpi et al. (2016) results.
- Along the embedment depth, the impact of the thermal loading diminishes. These results confirm also with those obtained by Sterpi et al. (2016) regarding the variation of the bending moment affected by thermal loading.

5.8 Recommendations

- The effect of cyclic thermal loading on the mechanical behaviour is not pronounced, thus modelling one thermal loading cycle for an energy diaphragm wall is sufficient to give a clear idea about its structural behaviour. Moreover, softening behaviour may develop at the interface, and then in this case its consequences should be verified.
- Imposing constant temperature uniformly along the wall length reduces the calculation time rather than imposing a sinusoidal variable temperature. Adding to this, imposing sinusoidal temperature does not allow configuring the influence of the applied thermal load, and thus clearly analyzing its impact.

- Special attention should be given to the in situ tests that allow the measurement of the soil thermal expansion coefficient as it proves to affect the structural performance of energy diaphragm walls.
- Regarding the structural design of the diaphragm walls and the choice of the assumed soil constitutive law, special attention should be paid regarding the characterization of the soil mechanical parameters in order to be able to simulate properly the soil behaviour and avoid problems caused by incorrect assumptions.

5.9 Conclusion

The use of energy diaphragm walls specifically for the construction of metro stations shows an increase nowadays and thus requires well defining all the aspects that are related to their mechanical behaviour under the impact of applied thermal loads. This chapter studies the mechanical behaviour of energy diaphragm walls affected by different types of thermal loading and various thermal and thermo-mechanical soil properties. Generally, all these different conditions and assumptions, their impact is not detrimental but requires to be considered at the design stage. Moreover, specifying the thermal expansion coefficient of the studied site requires special attention as it affects directly the structural behaviour of the energy diaphragm walls.

Conclusion and recommendations for further research

Conclusion

Geothermal structures mainly represented by piles and diaphragm walls are extensively being installed nowadays in several projects for they are needed as structural elements in addition to their role as sources of natural thermal energy.

This work deals with geothermal structures through two different manners. The first part is devoted to focus on the thermal performance of geothermal piles and diaphragm walls through representing two methods that could help design engineers in assessing the thermal performance of geothermal structures and therefore could facilitate the implementation of these structures.

The second part of the presented thesis deals with the mechanical behaviour of geothermal piles and diaphragm walls. Up to now, the design of geothermal structures is still ambiguous since it is not clear yet what type of thermal solicitation should be imposed into geothermal structures at the design stage. The conducted thesis tries to focus on these issues.

Main conclusions are divided into two parts:

Part I: related to the thermal performance of geothermal structures

- Two new approaches for the assessment of the allowable seasonally exchanged conductive and advective powers have been introduced.
- Both approaches are good tools to evaluate the sustainablility of geothermal structures and especially piles and diaphragm walls.

- The presence of groundwater flow has a positive impact on the enhancement of the allowable exchanged power between the geothermal structures and the surrounding soil.
- Thermally activating the whole diaphragm wall leads to produce higher thermal energy compared to the cases where only the embedment depth of the wall is thermally activated.
- The allowable exchanged power depends on the order of the applied thermal whether it starts by heating or cooling, and it relies on its type whether it is crenel or sinusoidal.
- Lower but more reasonable values for the exchanegd power are found when sinusoidal thermal load is imposed into geothermal structures.
- Two dimensional models of geothermal diaphragm walls give a general idea about the exchanged energy, however three dimensional models represent real cases and allow to take into consideration all the boundary conditions and thus guarantee the proper modelisation and the best design in return.

Part II: related to the thermo-mechanical behaviour of geothermal structures

- The type and order of the thermal load affects directly the mechanical behaviour of energy piles. For every specific case and according to its assumptions, modelling a certain number of thermal cycles is sufficient to capture the mechanical response of the geothermal pile.
- After two full thermal cycles, the impact of thermal load history disappears for both free and fixed pile head.
- For free head pile, the role of the rest phase can be neglected from a mechanical point of view; it has almost a slight influence on the global response of the energy pile. However, for a fully fixed pile head, the impact of the rest phase could not be ignored.
- Rapid stabilization of the induced thermal stresses is obtained directly after the first thermal cycle when sinusoidal thermal load is imposed into fixed head energy piles. The

stabilized values are equivalent to those generated during the first cycle due to crenel solicitations and imposed volumetric strains. However, for free head energy piles, three full thermal cycles with imposed sinusoidal solicitation are needed to stabilize the stresses, knowing that the stabilized values are equivalent to those obtained after the first cycle for the cases where crenel solicitation or volumetric strains are imposed.

- Sinusoial thermal sollicitation represents well real conditions, and avoid over-designing of the geothermal piles, and thus reduces the instalation costs.
- Transient calculation can be considered not necessary, but it enables to improve the design, especially to have a good assessment of additional axial force caused by the imposed thermal loads and to account for the impact of the thermal diffusion with time.
- Even though the considered soil constitutive law is simple and doesn't account for the cyclic degradations and creep, however, the mechanical behaviour of the geothermal piles with cyclic thermal loading is obvious.
- Soil thermal expansion coefficient influence the mechanical behaviour of geothermal piles, thus attention should be paid to the in-situ tests that allow measuring its value at the design stage.
- Modelling only one full thermal cycle is capable to reproduce the long-term mechanical response of energy diaphragm walls.
- Considering a constituive law for the soil that accounts for hardeing affects the structural behaviour of the diaphragm walls, and is considered as an economical solution.

Recommendations for further research

In the future, extensive studies should be done to clarify more about the thermal performance and the mechanical design of geothermal structures. Among the issues that require further study:

- Several numerical simulations based on real case studies capable to take into account different conditions in terms of climatic conditions, presence of ground water flow and its properties, various soil thermal and mechanical characteristics, and several conditions of toe and head fixities for the case of energy piles; all these simulations should be conducted. When all these conditions are well considered, then it would be easier to develop design charts for geothermal piles and diaphragm walls that could be used in any project for the preliminary design.
- The assessement and evaluation of the thermal performance of geothermal structures is a key indicator of their sustainability. Being capable to evaluate the thermal power that could be exchanged between geothermal structures and the surrounding soils is substantial for their design. Therefore, defining simple methods that could be employed for this task could be helpful.
- Modelling the soil-geothermal structure interface is indeed an important issue that requires to be studied further in details. Depending on the type of soil, whether it is cohesive or non-cohesive, the behaviour of the contact zones requires to be considered. The degradation at the contact zones may oblige using complex constitutive laws for these zones to properly design the soil response. Adding to this, the soil zones in contact with the geothermal structure may experience specific behaviour (such as freezing) and thus require special attention.
- The work should be extended to other types of energy geo-structures also, as they are being lately extensivley used such as tunnel linings. The research topic still encounters some major scientific obstacles regarding the thermal power and the thermo-mechanical behaviour of tunnels. Tunnels are fully embedded in soil at nearly constant depths, therefore they represent interseting material for research. In this context, it is important to examine if the tunneling excavation method and the grouting in the case of tunnel boring

machine method may affect the thermo-mechanical response of the whole system. It is expected that connections are mainly influenced by temperature variations rather than the linings, for this, detailed study needs to be carried regarding this point. Moreover, mechanically the initial stress level may influence the performance especially in the case of fully coupled thermo-hydro-mechanical analysis. Thus, attention should be paid concerning the behaviour of geothermal tunnels.

References

Abdeen Mustafa Omer. 2014. Soil Thermal Properties and the Effects of Groundwater on Closed Loops. *International Journal of Sustainable Energy and Environmental Research 3(1),* 34-52. .

Abuel-Naga H.M., Bergado D.T., Bouazza A., and Ramana G.V. 2007c. Volume change behaviour of saturated clays under drained heating conditions: experimental results and constitutive modeling. *Canadian Geotechnical Journal*, 2007c, Vol. 44.

Abuel-Naga H., Raouf M.I.N., Raouf A.M.I., and Nasser A.G. 2015. Energy piles: current state of knowledge and design challenges. *Enviromental geotechnics 2(4)*, 195-210.

Adam D., and Markiewicz R. 2009. Energy from earth-coupled structures, foundations, tunnels, and sewers. *Géotechnique* 59(3), 229-236.

Akrouch G.A., Sanchez M., and Briaud J-L. 2015. An experimental, analytical and numerical study on the thermal efficiency of energy piles in unsaturated soils. Computers and geotechnics 71(2016), 207-220.

Alrtimi A., Rouainia M., and Haigh S. 2016. Thermal conductivity of a sandy soil. *Applied Thermal Engineering* 106(2016), 551-560.

Amatya B.L., Soga K., Bourne-Webb P.J., Amis T., and Laloui L. 2012. Thermo-mechanical behaviour of energy piles. *Géotechnique* 59(3), 237-248.

Amis T., Robinson C.A.W., and Wong S. 2010. Integrating geothermal loops into the diaphragm walls of the Knightsbridge palace hotel project. Proceedings of the 11th DFI/EFFC international conference, London.

Arson C., Berns E., Akrouch G., Sanchez M., and Briaud J.-L. 2013. Heat Propagation around Geothermal Piles and Implications on Energy Balance. Materials and processes for energy: communicating current research and technological developments (A. Méndez-Vilas, Ed.).

Batini N., Rotta Loria A.F., Conti P., Testi D., Grassi W., and Laloui L. 2015. Energy and geotechnical behaviour of energy piles for different design solutions. *Applied Thermal Engineering* 86(2015), 199-213.

Bayandor S., Noorazed A., Mahboubi Ardakani A.R., and Delfan Azari M. 2014. Numerical analysis of thermo-mechanical behaviour of energy pile foundations. *Numerical methods in geotechnical engineering.*

Bazant Z. 1979. Methods of foundation engineering. Elsevier Science.

Bodas Freitas T.M., Cruz Silva F., Bourne-Webb P.J. 2013. The response of energy foundations under thermo-mechanical loading. Proceedings of the 18th international conference on soil mechanics and geotechnical engineering, Paris 2013.

Bouazza A., Adam D., Rao Singh M., and Ranjith PG. 2011. Direct Geothermal Energy from Geostructures. Australian Geothermal Energy Conference.

Bouazza, A., Laong, B., & Sigh, R. 2013. Soil effective thermal conductivity from energy pile thermal tests. *Coupled phenomena in environmental geotechnics*. London: CRC Press.

Bourne-Webb PJ, Amatya B., Soga K., Amis T., Davidson C., and Payne P. 2009. Energy Pile Test at Lamberth College, London : Geotechnical and Thermodynamic Aspects of Pile Response to Heat Cycles. *Géotechnique 59(3),* 237-248.

Bourne-Webb PJ, Amatya B, Soga K. 2013. A framework for understanding energy pile behaviour. *Proceeding of the Institution of Civil Engineers-Geotechnical Engineering 166(2),* 170-177.

Bourne-Webb P.J., Bodas Freitas T.M., and Freitas Assucao R.M. 2016a. Soil-pile thermal interactions in energy foundations. *Géotechnique,* vol. 66, issue 2, 167-171.

Bourne-Webb P.J., Bodas Freitas T.M., and da Costa Gonçalves R.A. 2016b. Thermal and mechanical aspects of the response of embedded retaining walls used as shallow geothermal heat exchangers. *Energy and Buildings* 125(2016), 130-141.

Brandl H. 2006. Energy Foundations and other thermo-active ground structures. *Géotechnique 56(2),* 81-122.

Cecinato F. & Loveridge F.A. 2015. Influences on the thermal efficiency of energy piles. *Energy* 82(2015), 1021-1033.

Cekerevac C. 2003. Thermal Effects on the Mechanical Behaviour of Saturated Clay. *Doctoral Thesis*, Lausanne, Switzerland.

Cervera C.P. 2013. Ground thermal modelling and analysis of energy pile foundations. Thesis.

Chiasson A.D., Rees S.J., and Spitler J.D. 2000. A preliminary assessment of the effects of groundwater flow on closed-loop ground-source heat pump systems. *ASHRAE Transactions.* 106(1): 380-393.

Choi J.C., Park J., and Lee S.R. 2012. Numerical evaluation of the effects of groundwater flow on borehole heat exchanger arrays. *Renewable Energy* 52(2013), 230-240.

Cornelio C., Di Donna A., and Barla M. 2016. Energy diaphragm walls for Turin metro. European Geothermal Congress 2016, Strasbourg, France, 9-24 Sept 2016.

Cui Y., and Zhu J. 2016. 3D transient heat transfer numerical analysis of multiple energy piles. *Energy and Buildings* 134(2017), 129-142.

Dawson A. 2008. Water in road structures movement, drainage and effects. *Book*, Geotechnical, geological and earthquake engineering, volume 5.

Diao N., Li Q., and Fang Z. 2004. Heat transfer in ground heat exchangers with groundwater advection. *International journal of thermal sciences* 43(2004), 1203-1211.

Di Donna A., Rotta Lorai A.F., and Laloui L. 2016a. Numerical study of the response of a group of energy piles under different combinations of thermo-mechanical loads. *Computers and Geotechnics* 72(2016), 126-142.

Di Donna A., Cecinato F., Loveridge F., and Barla M. 2016b. Energy performance of diaphragm walls used as heat exchangers. Proceedings of the Institute of Civil Engineers-Geotechnical Engineering, vol. 170, issue 3, 232-245.

Di Donna A. 2016. Energy walls for an underground car park. 25th European Young Geotechnical Engineers Conference.21st – 24th of June 2016, Sibiu, Romania.

Di Donna A., and Barla M. 2016. The role of ground conditions on energy tunnels' heat exchange. *Environmental Geotechnics* 3(4), 214-224.

Eslami H. 2014. Comportement thermo-hydromécanique des sols au voisinage des géo-structures énergétiques. *Doctoral Thesis*, Nancy, France.

Fleureau J.M. 1979. Influence d'un champ thermique ou électrique sur les phénomènes d'interaction solide-liquide dans les milieux poreux. Book, Paris, France.

French Recommendations, 2017. Recommandations pour la conception, le dimensionnement et la mise en oeuvre des géostructures thermiques, CFMS/ SYNTEC INGENIERIE/ SOFFONS-FNTP, Janvier 2017.

Fromentin A., Pahud D., Jaquier C., and Morath M. 1997. Recommandations pour la realization d'installations avec pieux échangeurs. Report 120.104. Office fédéral de l'énergie.

Gao, J., Zhang, X., Liu, J., Shan, Li K., & Yang, J. 2008. Thermal performance and ground temperature of vertical pile foundation heat exchangers: A case study. *Applied thermal engineering* 28: 2295-2304.

Gashti E.H.N., Uotinen V.M., and Kujala K. 2014. Numerical modelling of thermal regimes in steel energy pile foundations: A case study. *Energy and Buildings* 69(2014), 165-174.

Gashti E.H.N., Malaska M., and Kujala K. 2015. Analysis of thermo-active pile structures and their performance under groundwater flow conditions. *Energy and Buildings* 105(2015), 1-8.

Ghasemi-Fare O., and Basu P. 2013. A practical heat transfer model for geothermal piles.*Energy and Buildings* 66(2013), 470-479.

GI Energy 2017. https://www.gienergyus.com/blog/energy-foundations-energy-piles-talk-town/

GSHP association 2012. Thermal pile design, installation & materials standards. Issue 1.0, 1st October 2012.

Habert J. & Burlon S. 2015. Modelling thermoactive diaphragm walls. Second EAGE Workshop on Geomechanics and Energy, 13-15 October, Celle, Germany.

Habert J., El Mejahed M., and Bernard J.B. 2016. Lessons learned from mechanical monitoring of a thermoactive pile. Energy Geotechnics.1st International Conference on Energy Geotechnics, Kiel, Germany, 551-556.

Hamada Y., Saitoh H., Nakamura M., Kubota H., and Ochifuji K. 2007. Field performance of an energy pile system for space heating. *Energy and Buildings* 39(2007), 517-524.

Itasca 2005. FLAC3D Version 3.0. Theory and Background. Itasca Consulting group, Inc. Minnesota, USA.

Itasca 2012. FLAC3D Version 5.0. Theory and Background. Itasca Consulting group, Inc. Minnesota, USA.

Johansen O. 1975. Thermal conductivity of soils. Translated version of a thesis submitted in 1975.

Katsura T., Nakamura Y., Okawada T., Hori S., and Nagano K. 2009. Field test on heat extraction or injection performance of energy piles and its application. 11th international conference on energy storage, Effstock 2009.

Katzenbach R., Clauss F., Waberseck T., and Wagner I. 2008. Coupled numerical simulation of geothermal energy systems. *12th International conference of International Association for Computer Methods and Advances in Geomechanics* (IACMAG), 1-6 October, 2008, Goa, India.

Kersten, M. 1949. Thermal properties of soils. Minnesota, LII(21): 233 pages.

Laloui L., Nuth M., and Vulliet L. 2006. Experimental and numerical investigations of the behaviour of a heat exchanger pile. *International journal for numerical and analytical methods in geomechanics 30(8)*, 763-781.

Laloui L. and Di Donna A. 2011. Understanding the behaviour of energy geo-structures. *Proceedings of the Institution of Civil Engineers-Civil Engineering 164(4)*, 184-191.

Laloui L., Mimouni T., and Dupray F. 2013. Advances in the analysis of thermo-active foundations. *International symposium on Coupled Phenomena in environmental Geotechnics*, vol. 1, 85-102.

Lofthouse J., Simmons R.T., and Yonk R.M. 2016. Reliability of renewable energy: geothermal. Institute of Political Economy, Utah State University.

Loveridge F., and Powrie W. 2012. Pile heat exchangers: thermal behaviour and interactions. *Proceedings of the Institution of Civil Engineers, Geotechnical Engineering* 166(2013), 178-196.

Loveridge F., Amis T., and Powrie W. 2012. Energy pile performance and preventing ground freezing. The 2012 World Congress on *Advances in Civil, Environmental, and Materials Research (ACEM' 12)*, Seoul, Korea, August 26-30, 2012.

Loveridge F. 2012. The thermal performance of foundation piles used as heat exchangers in ground energy systems. *Doctoral thesis*, Faculty of Engineering and the Environment, University of Southampton, UK.

Lund J.W. and Boyd T.L. 2016. Direct utilization of geothermal energy 2015 worldwide review. *Geothermics*, vol. 60, 66-93.

Luo J., Zhao H., Gui S., Xiang W., Rohn J., and Blum P. 2016. Thermo-economic analysis of four different types of ground heat exchangers in energy piles. *Applied thermal engineering* 108(2016), 11-19.

Ma X., and Grabe J. 2010. Efficiency increase of soil heat exchangers due to groundwater flow and air injection wells. *Proceedings World Geothermal Congress*. Bali, Indonesia, 25-29 April 2010.

Maragna C., and Rachez X. 2015. Proceedings World Geothermal Congress. Melbourne, Australia, 19-25 April 2015.

Mukhopadhyay A.K., Neekhra S., and Zollinger D.G. 2007. Preliminary characterization of aggregate coefficient of thermal expansion and gradation for paving concrete. Texas transportation institute, Texas A&M University, technical report.

Ng C.W.W., Wang S.H., and Zhou C. 2016. Volume change behaviour of saturated sand under thermal cycles. Géotechnique Letters 6, 124-131.

NHBC (National House Building Council) 2010. Efficient design of piled foundations for low rise housing, design guide. NHBC Foundation, Milton Keynes, UK.

Nicholson D. P., Chen Q., Pillai A., and Chendorain M. 2013. Developments in thermal pile and thermal tunnel linings for city scale GSHP systems. Thirty-Eighth Workshop on Geothermal Reservoir Engineering, Stanford, California.

Ozudogru T.Y., Brettmann T., Olgun G., Martin II J.R., and Senol A. 2012. Thermal conductivity testing of energy piles: field testing and numerical modelling. GeoCongress, ASCE 2012.

Pahud D., & Hubbuch M. 2007. Measured thermal performances of the energy pile system of the dock midfield at Zurich airport. Proceedings European Geothermal Congress 2007, Germany.

Park H., Lee S-R., Yoon S., and Choi J-C. 2012. Evaluation of thermal response and performance of PHC energy pile: Field experiments and numerical simulation. *Applied Energy* 103(2012), 12-24.

P.A. CoE. Parliamentary Assembly. Council of Europe. 21 May 2010.

Raybach L. 2002. Status and prospects of geothermal heat pumps (GHP) in Europe and Worldwide; sustainability aspects of GHPs. International Summer School on Direct Application of Geothermal Energy.

Recordon E. 1993. Déformabilité des sols non saturés à diverses températures. *Revue Française de Géotechnique.* n° 65, pp 37-56.

Rotta Loria A.F., Gunawan A., Shi C., Laloui L., and W.W.Ng C. 2015. Numerical modelling of energy piles in saturated sand subjected to thermo-mechanical loads. *Geomechanics for energy and the environment* 1(2015), 1-15.

RT 2012. Réglementation thermique "Grenelle Environnement 2012", 6 Juillet 2010.

Rui F., Yiqiang J., Yang Y., Deng S., and Zuiliang M. 2007. A study on the performance of a geothermal heat exchanger under coupled heat conduction and groundwater advection. *Energy 32(11),* 2199-2209.

Rui Y. 2014. Finite element modelling of thermal piles and walls. Thesis, St Edmund's College.

Saggu R., and Chakraborty T. 2015. Cyclic thermo-mechanical analysis of energy piles in sand. *Geotech Geol Eng*. 2015(33), 321-342.

Sedano J.A.I., Evgin E., and Fu Z. 2011. A coupled analysis of heat and moisture transfer in soils. Proceedings of the 2011 COMSOL conference in Boston.

SIA. 2005. Utilisation de la chaleur du sol par des ouvrages de fondation et de soutènement en bèton, guide pour la conception, la réalisation et la maintenance. Documentation D0190-Swiss society of engineers and architects, Geneva, 100 pages.

Sigfusson, B. & Uihlein, A. 2015. 2014 JRC Geothermal energy status report: 64 pages.

Sterpi D., Coletto A., and Mauri L. 2016. Investigation on the behaviour of a thermo-active diaphragm wall by thermo-mechanical analyses. Geomechanics for Energy and the Environment 9(2017), 1-20.

Sterpi D., Angelotti A., Corti D., and Ramus M. 2014. Numerical analysis of heat transfer in thermo-active diaphragm walls. 8th European conference on numerical methods in geotechnical engineering, NUMGE 2014.

Sterpi D. & Angelotti A. 2013. Performance and Effects on the subsoil temperature of a thermo-active diaphragm wall. *International EAGE Workshop on Geomechanics and Energy* .

Sun M., Xia C., and Zhang G. 2013. Heat transfer model and design method for geothermal heat exchange tubes in diaphragm walls. *Energy and Buildings* 61(2013), 250-259.

Sundberg J. 1988. Thermal properties of soils and rocks. Book, Chalmers University of Technology.

Suryatriyastuti M.E. 2013. Numerical study of the thermo-active piles behaviour in cohesionless soils. *Doctoral thesis*. Lille, France.

Szymkiewicz F., Burlon S., Guirado C., Minatchy C., and Vinceslas G. 2015. Experimental study of heating-cooling cycles on the bearing capacity of CFA piles in sandy soils. *Problematic materials, environment, water and* energy 5(409).

Tang A.N., Pereira J.M., Hassen g., and Yavari N. 2013. Behaviour of Heat-Exchanger Piles from Physical Modeling. *Book Section*, Energy Geostructures.

Tolooiyan A., and Hemmingway P. 2012. A preliminary study of the effect of groundwater flow on the thermal front created by borehole heat exchangers. *International journal of low-carbon technologies.* 2014 (9), 284-295.

Tomlinson M., and Woodward J. 2008. Pile design and construction practice. Taylor and Francis. Fifth edition.

Van Meurs G.A.M. 1986. Seasonal heat storage in soil, department of applied physics, University of Technology Delft, Netherlans, *Thesis*.

VDI. Thermal use of the underground - Ground source heat pump systems. *Verein Deutscher Ingenieure* (VDI), Guideline 4640-2, (2001).

Xia C., Sun M., Zhang G., Xiao S., and Zou Y. 2012. Experimental study on geothermal heat exchangers buried in diaphragm walls. *Energy and Buildings 52*, 50-55.

Yavari N., Tang A.M., Pereira J.M., and Hassen G. 2016. Effect of temperature on the shear strength of soils and soil/structure interface. *Canadian Geotechnical Journal*, NRC Research Press, 53(7), 1186-1194.

Zarrella A., De Carli M., and Galgaro A. 2013. Thermal performance of two types of energy foundation pile: Helical pipe and triple U-tube. *Applied thermal engineering* 61(2013), 301-310.

Zhang W., Yang H., Lu L;, and Fang Z. 2015. Investigation on the heat transfer of energy piles with two-dimensional groundwater flow. *International journal of low-carbon technologies.* 2015(0), 1-8.